Production of a top pair with a pair of Higgs:
a multifaceted process

TOP-LHC France 2023
IPHC-Strasbourg

Aurore Savoy Navarro,

CEA-IRFU, University Paris-Saclay and CNRS/IN2P3

Outline

- Preamble
- The ttHH production process: from the SM to BSM/CHM
- From theory to experiment: Search for and study of the ttHH production process at LHC and beyond
- Concluding remarks and perspectives

Preamble

This presentation is based on:

=> Two published phenomenological works by:

- *Carlos Bautista*[1,2)], *Ricardo d'Elia Matheus*[1)], *Leonardo de Lima*[3)], *Eduardo Ponton*[1,2)], *Leonidas F. do Prado*[1,4)], *Aurore Savoy Navarro*[4,4')] *(next slide)*
  - *1) Institute of Theoretical Physics, IFT, at the University Estadual of Sao Paulo, UNESP, Sao Paulo, BR*
  - *2) International Center for Theoretical Physics, South American Institute for Fundamental Research ICTP-SAIFR, Sao Paulo, BR*
  - *3) Universidade Tecnologica Federal do Parana, Toledo, BR.*
  - *4) CEA-IRFU, University Paris Saclay and 4') CNRS-IN2P3*
- *Carlos Bautista*[1,2)], *Ricardo d'Elia Matheus*[1)], *Leonardo de Lima*[3)], *ASN*[4,4')] *(See [next +1] slide)*

=> One published experimental work by CMS, thanks to the dedicated work by:

- *Mehmet Ozgur Sahin*[4)], *Aurore Savoy-Navarro*[4,4')], *Sezen Sekmen*[5)], *Gamze Sokmen*[6)] *(See [next + 2] slide)*
  - *5) Kyungpook National University, KNU, KR*
  - *6) Middle East Technical University, ODTÜ METU, TR*

=> And ongoing experimental collaboration carried on within CMS (not yet published) => not presented here.

Leonidas F. do Prado[1, 4)], Mehmet Ozgur Sahin[4)], Aurore Savoy-Navarro[4,4')], Sezen Sekmen[5)], Gamze Sokmen[6)],
Maxwell Chertok and Wei Wei (UC-Davis, USA)

Preamble: *From the interest on the VLF impact on ttH production and Yt to ttH & ttHH* *Phenomenology studies with CHM at present and future pp colliders, and experimental ttHH study*

- On Fall 2015 with Ricardo (IFT-UNESP) and Eduardo (IFT &ICTP-SAIFR), we launched Phenomenology/Theoretical project to look for VLF hypothesis impact on the ttH production and the Top-Higgs Yukawa coupling, for an application to the study of tttH process with LHC data.

  This study was performed on purpose with simple SM extensions.

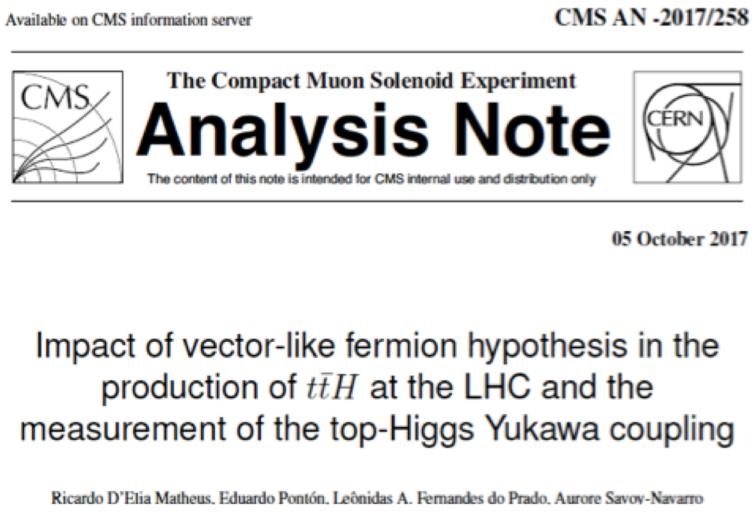

Available on CMS information server

CMS AN -2017/258

The Compact Muon Solenoid Experiment

Analysis Note

The content of this note is intended for CMS internal use and distribution only

05 October 2017

Impact of vector-like fermion hypothesis in the production of $t\bar{t}H$ at the LHC and the measurement of the top-Higgs Yukawa coupling

Ricardo D'Elia Matheus, Eduardo Pontón, Leônidas A. Fernandes do Prado, Aurore Savoy-Navarro

- End 2017 we moved to MCHM with ttH and ttHH within dedicated theoretical studies and phenomenology simulated scenarios for LHC to HE-LHC (=> HL-LHC/HE-LHC YR).

  The strong case of ttHH was raised in our work.

- Fall 2018 we launched with Leonidas ***the first experimental ttHH production study at LHC*** while pursuing in parallel the phenomenology related studies, joined by Leonardo and Carlos.

JHEP03(2021)049 and related previous work (YR-CERN)

Higgs Physics at HL-LHC and HE-LHC, CERN Yellow Report


arXiv:1902.00134v2 [hep-ph] 19 Mar 2019

CERN-LPCC-2018-04
March 20, 2019

Higgs Physics
at the HL-LHC and HE-LHC

Report from Working Group 2 on the Physics of the HL-LHC, and Perspectives at the HE-LHC

Conveners:
M. Cepeda[1,2], S. Gori[3], P. Ilten[4], M. Kado[5,6,7], F. Riva[8]

Contributors:
R. Abdul Khalek[9,10], A. Aboubrahim[11], J. Alimena[12], S. Alioli[13,13], A. Alves[14], C. Asawatangtrakuldee[15], A. Azatov[16,17], P. Azzi[18], S. Bailey[19], S. Banerjee[20], E.L. Barberio[21], D. Barducci[16], G. Barone[22], M. Bauer[20], C. Bautista[23], P. Bechtle[24], K. Becker[25], A. Benaglia[26], M. Bengala[27], N. Berger[28], C. Bertella[29], A. Bethani[30], A. Betti[24], A. Biekotter[31], F. Bishara[15], D. Bloch[32], P. Bokan[33], O. Bondu[34], M. Bonvini[6], L. Borgonovi[35,36], M. Borsato[37], S. Boselli[38], S. Braibant-Giacomelli[35,36], G. Buchalla[39], L. Cadamuro[40], C. Caillol[41], A. Calandri[42,43], A. Calderon Tazon[44], J.M. Campbell[45], F. Caola[20], M. Capozi[46], M. Carena[45,47], C.M. Carloni Calame[48], A. Carmona[49], E. Carquin[50], A. Carvalho Antunes De Oliveira[51], A. Castaneda Hernandez[52], O. Cata[53], A. Celis[54], A. Cerri[55], F. Cerutti[56,57], G.S. Chahal[58,20], A. Chakraborty[59], G. Chaudhary[60], X. Chen[61], A.S. Chisholm[1,4], R. Contino[62], A.J. Costa[27], R. Covarelli[63,64], N. Craig[65], D. Curtin[66], L. D'Eramo[67], N.P. Dang[68], P. Das[69], S. Dawson[22], O.A. De Aguiar Francisco[1], J. de Blas[70,18], S. De Curtis[71], N. De Filippis[72,73], H. De la Torre[74], L. de Lima[75], A. De Wit[15], C. Delaere[34], M. Delcourt[34], M. Delmastro[28], S. Demers[76], N. Dev[77], R. Di Nardo[78], S. Di Vita[79], S. Dildick[80], L.A.F. do Prado[81,23], M. Donadelli[82], D. Du[83], G. Durieux[84,15], M. Dührssen[1], O. Eberhardt[85], K. El Morabit[86], J. Elias-Miro[1], J. Ellis[87,51,1], C. Englert[88], R. Essig[89], S. Falke[28], M. Farina[89], A. Ferrari[90], A. Ferroglia[91], M.C.N. Fiolhais[92], M. Flechl[93], S. Folgueras[94], E. Fontanesi[35,36], P. Francavilla[67,95], R. Franceschini[96,97], R. Frederix[98], S. Frixione[99], G. Gómez-Ceballos[100], A. Gabrielli[56,57], S. Gadatsch[1], M. Gallinaro[27], A. Gandrakota[101], J. Gao[102], F.M. Garay Walls[103], T. Gehrmann[61], Y. Gershtein[101], T. Ghosh[104], A. Gilbert[1], R. Glein[105], E.W.N. Glover[20], R. Gomez-Ambrosio[20], R. Gonçalo[27], D. Gonçalves[106], M. Gorbahn[107], E. Gouveia[27], M. Gouzevitch[108], P. Govoni[26,13], M. Grazzini[61], B. Greenberg[101], K. Grimm[109], A.V. Gritsan[110], A. Grohsjean[15], C. Grojean[15], J. Gu[111], R. Gugel[25], R.S. Gupta[20], C.B. Gwilliam[112], S. Höche[113], M. Haacke[103], Y. Haddad[58], U. Haisch[46], G.N. Hamity[114], T. Han[106], L.A. Harland-Lang[19], R. Harnik[45], S. Heinemeyer[44,115], G. Heinrich[46], B. Henning[8], V. Hirschi[43], K. Hoepfner[116], J.M. Hogan[117,118], S. Homiller[119,22], Y. Huang[120], A. Huss[1], S. Jézéquel[28], Sa. Jain[69], S.P. Jones[1], K. Köneke[25], J. Kalinowski[121], J.F. Kamenik[122,123], M. Kaplan[100], A. Karlberg[61], M. Kaur[60], P. Keicher[86], M. Kerner[61], A. Khanov[124], J. Kieseler[1], J.H. Kim[125], M. Kim[126], T. Klijnsma[43], F. Kling[127], M. Klute[100], J.R. Komaragiri[128], K. Kong[125], J. Kozaczuk[129], P Kozow[121], C. Krause[45], S. Lai[33], J. Langford[58], B. Le[21], L. Lechner[93], W.A. Leight[130], K.J.C. Leney[131], T. Lenz[24], C-Q. Li[132], H. Li[83], Q. Li[133], S. Liebler[134], J. Lindert[20], D. Liu[135], J. Liu[136], Y. Liu[137], Z. Liu[138,45], D. Lombardo[8], A. Long[139], K. Long[41], I. Low[140,135], G. Luisoni[46], L.L. Ma[83], A.-M. Magnan[58], D. Majumder[125], A. Malinauskas[19], F. Maltoni[141], M.L. Mangano[1], G. Marchiori[67,67], A.C. Marini[100], A. Martin[77], S. Marzani[142,99], A. Massironi[1], K.T. Matchev[40,143], R.D. Matheus[23], K. Mazumdar[69], J. Mazzitelli[61], A.E. Mcdougall[21], P. Meade[119], P. Meridiani[6], A.B. Meyer[15], E. Michielin[18], P. Milenovic[1,144], V. Milosevic[58], K. Mimasu[141], B. Mistlberger[145], M. Mlynarikova[146], M. Mondragon[147], P.F. Monni[1], G. Montagna[148,48], F. Monti[26,13], M. Moreno Llacer[1], A. Mueck[149], P.C. Muiño[27], C. Murphy[150], W.J.

Impact of Minimal Composite Higgs on the ttH, ttHH, processes at LHC.

Ricardo D'Elia Matheus[1], Eduardo Pontón[1,2], Leonardo de Lima[5],
Leônidas A. Fernandes do Prado[1,3]*, Aurore Savoy-Navarro[4], Carlos Bautista[1]

1-Instituto de Física Teórica (IFT-UNESP), Sao Paulo (Brazil)
2- ICTP South American Institute for Fundamental Research, São Paulo (Brazil)
3- SPRACE-UNESP, Sao Paulo (Brazil)
4- CNRS/IN2P3-University Paris-Diderot, Paris (France)
5- Universidade Federal da Fronteira Sul UFFS, Paraná State (Brazil)

**Supported by Science Without Borders program/CAPES for UNESP-SPRACE & FAPESP (2015/26624-6)*

WORKSHOP on the PHYSICS of the HL-LHC & PERSPECTIVES at HE-LHC
CERN, June 18-20, 2018
(WG2 HIGGS Working Group)

Probing the Top – Higgs Sector with composite Higgs Models at Present and Future Hadron Colliders

Eduardo Pontón[1,2], Ricardo D'Elia Matheus[1], Aurore Savoy-Navarro[4] ,
Leonardo de Lima[3], Leônidas A. Fernandes do Prado[1,4], Carlos Bautista[1,2]

1 - Instituto de Física Teórica (IFT-UNESP), Sao Paulo (Brazil)
2 - ICTP South American Institute for Fundamental Research, São Paulo (Brazil)
3 - Universidade Tecnológica Federal do Paraná, Toledo (Brazil)
4 - IRFU-CEA, Université Paris-Saclay and CNRS - IN2P3 (France)

4th FCC Physics and Experiments Workshop
CERN, November 10 - 13, 2020

This work explores the $t\bar{t}h$ and $t\bar{t}hh$ processes as important probes to explore the top-Higgs sector using two simple Composite Higgs realizations with the aim to provide sets of representative points with detailed experimental outcomes relevant at the HL-LHC and Future Hadron Colliders.

Published on arXiv: 2008.13026 and submitted to JHEP

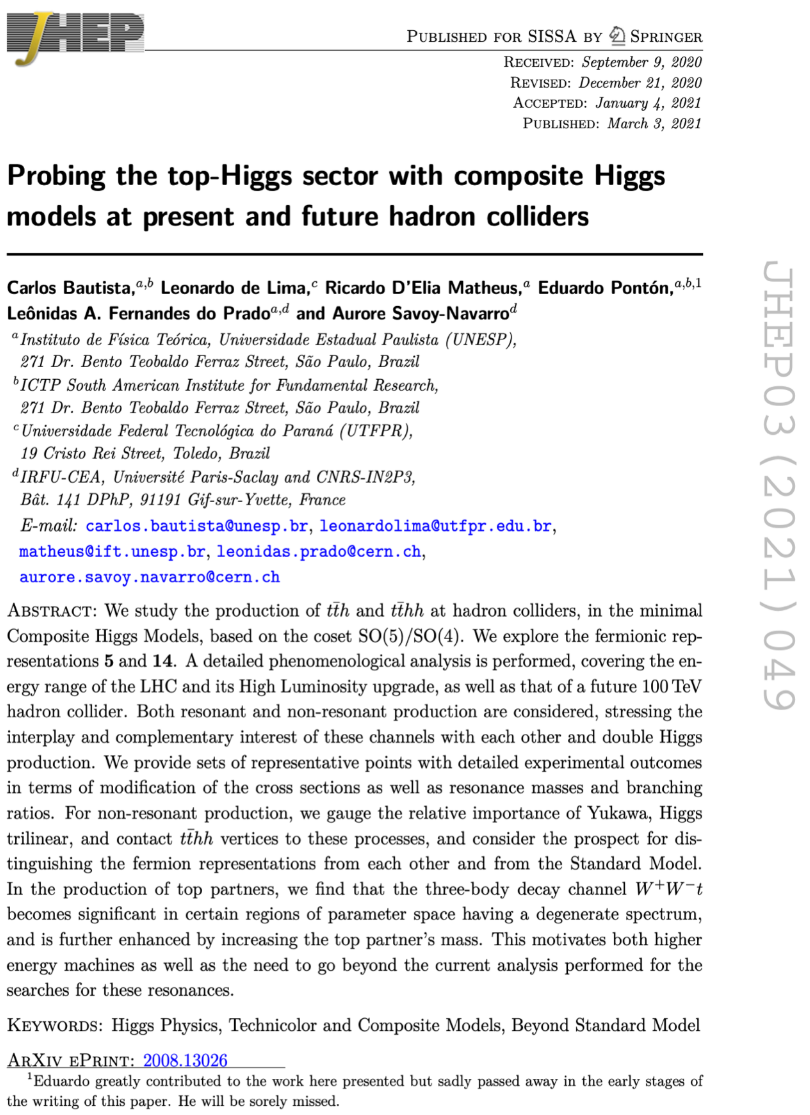
JHEP03(2021)049

Published for SISSA by Springer
Received: *September 9, 2020*
Revised: *December 21, 2020*
Accepted: *January 4, 2021*
Published: *March 3, 2021*

Probing the top-Higgs sector with composite Higgs models at present and future hadron colliders

Carlos Bautista,[a,b] Leonardo de Lima,[c] Ricardo D'Elia Matheus,[a] Eduardo Pontón,[a,b,1] Leônidas A. Fernandes do Prado[a,d] and Aurore Savoy-Navarro[d]

[a] *Instituto de Física Teórica, Universidade Estadual Paulista (UNESP),*
271 Dr. Bento Teobaldo Ferraz Street, São Paulo, Brazil
[b] *ICTP South American Institute for Fundamental Research,*
271 Dr. Bento Teobaldo Ferraz Street, São Paulo, Brazil
[c] *Universidade Federal Tecnológica do Paraná (UTFPR),*
19 Cristo Rei Street, Toledo, Brazil
[d] *IRFU-CEA, Université Paris-Saclay and CNRS-IN2P3,*
Bât. 141 DPhP, 91191 Gif-sur-Yvette, France
E-mail: carlos.bautista@unesp.br, leonardolima@utfpr.edu.br,
matheus@ift.unesp.br, leonidas.prado@cern.ch,
aurore.savoy.navarro@cern.ch

Abstract: We study the production of $t\bar{t}h$ and $t\bar{t}hh$ at hadron colliders, in the minimal Composite Higgs Models, based on the coset SO(5)/SO(4). We explore the fermionic representations **5** and **14**. A detailed phenomenological analysis is performed, covering the energy range of the LHC and its High Luminosity upgrade, as well as that of a future 100 TeV hadron collider. Both resonant and non-resonant production are considered, stressing the interplay and complementary interest of these channels with each other and double Higgs production. We provide sets of representative points with detailed experimental outcomes in terms of modification of the cross sections as well as resonance masses and branching ratios. For non-resonant production, we gauge the relative importance of Yukawa, Higgs trilinear, and contact $t\bar{t}hh$ vertices to these processes, and consider the prospect for distinguishing the fermion representations from each other and from the Standard Model. In the production of top partners, we find that the three-body decay channel W^+W^-t becomes significant in certain regions of parameter space having a degenerate spectrum, and is further enhanced by increasing the top partner's mass. This motivates both higher energy machines as well as the need to go beyond the current analysis performed for the searches for these resonances.

Keywords: Higgs Physics, Technicolor and Composite Models, Beyond Standard Model

ArXiv ePrint: 2008.13026

---

[1] Eduardo greatly contributed to the work here presented but sadly passed away in the early stages of the writing of this paper. He will be sorely missed.

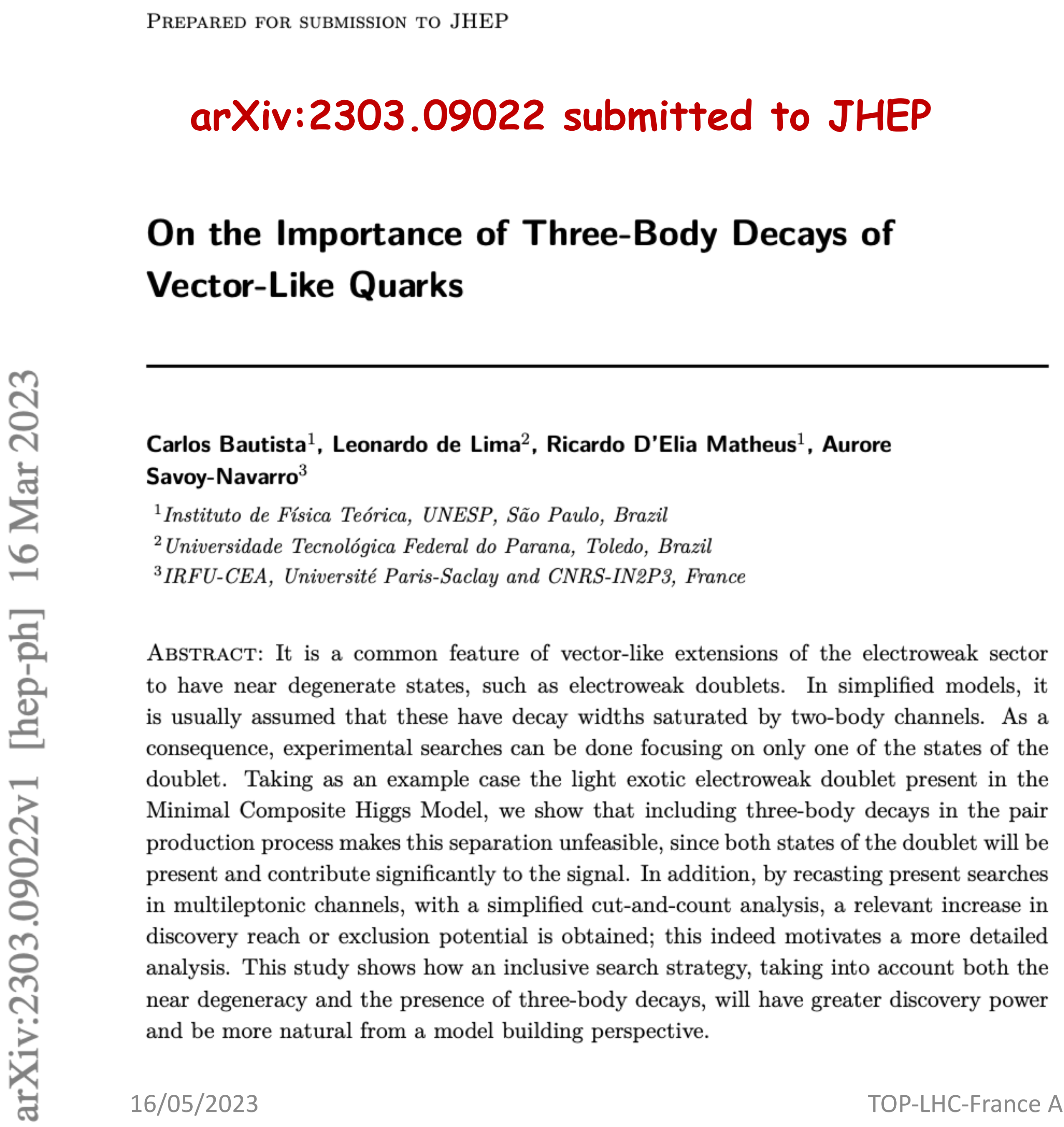

Prepared for submission to JHEP

arXiv:2303.09022 submitted to JHEP

On the Importance of Three-Body Decays of Vector-Like Quarks

Carlos Bautista[1], **Leonardo de Lima**[2], **Ricardo D'Elia Matheus**[1], **Aurore Savoy-Navarro**[3]

[1] *Instituto de Física Teórica, UNESP, São Paulo, Brazil*
[2] *Universidade Tecnológica Federal do Parana, Toledo, Brazil*
[3] *IRFU-CEA, Université Paris-Saclay and CNRS-IN2P3, France*

Abstract: It is a common feature of vector-like extensions of the electroweak sector to have near degenerate states, such as electroweak doublets. In simplified models, it is usually assumed that these have decay widths saturated by two-body channels. As a consequence, experimental searches can be done focusing on only one of the states of the doublet. Taking as an example case the light exotic electroweak doublet present in the Minimal Composite Higgs Model, we show that including three-body decays in the pair production process makes this separation unfeasible, since both states of the doublet will be present and contribute significantly to the signal. In addition, by recasting present searches in multileptonic channels, with a simplified cut-and-count analysis, a relevant increase in discovery reach or exclusion potential is obtained; this indeed motivates a more detailed analysis. This study shows how an inclusive search strategy, taking into account both the near degeneracy and the presence of three-body decays, will have greater discovery power and be more natural from a model building perspective.

arXiv:2303.09022v1 [hep-ph] 16 Mar 2023

March 2022

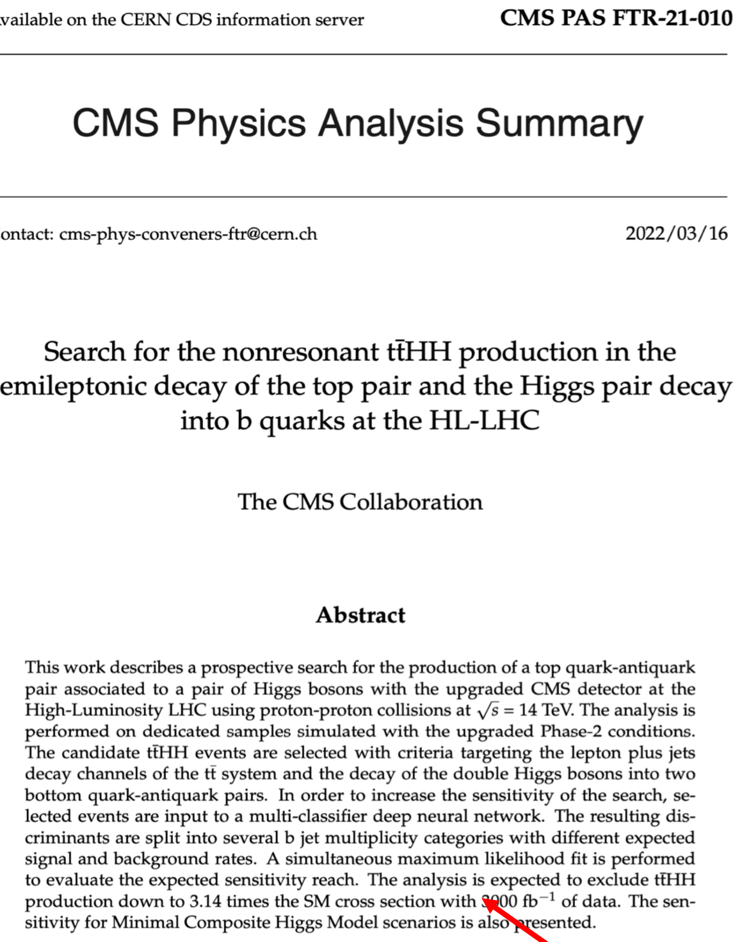

vailable on the CERN CDS information server **CMS PAS FTR-21-010**

CMS Physics Analysis Summary

ontact: cms-phys-conveners-ftr@cern.ch 2022/03/16

Search for the nonresonant $t\bar{t}HH$ production in the emileptonic decay of the top pair and the Higgs pair decay into b quarks at the HL-LHC

The CMS Collaboration

Abstract

This work describes a prospective search for the production of a top quark-antiquark pair associated to a pair of Higgs bosons with the upgraded CMS detector at the High-Luminosity LHC using proton-proton collisions at $\sqrt{s} = 14$ TeV. The analysis is performed on dedicated samples simulated with the upgraded Phase-2 conditions. The candidate $t\bar{t}HH$ events are selected with criteria targeting the lepton plus jets decay channels of the $t\bar{t}$ system and the decay of the double Higgs bosons into two bottom quark-antiquark pairs. In order to increase the sensitivity of the search, selected events are input to a multi-classifier deep neural network. The resulting discriminants are split into several b jet multiplicity categories with different expected signal and background rates. A simultaneous maximum likelihood fit is performed to evaluate the expected sensitivity reach. The analysis is expected to exclude $t\bar{t}HH$ production down to 3.14 times the SM cross section with 3000 fb^{-1} of data. The sensitivity for Minimal Composite Higgs Model scenarios is also presented.

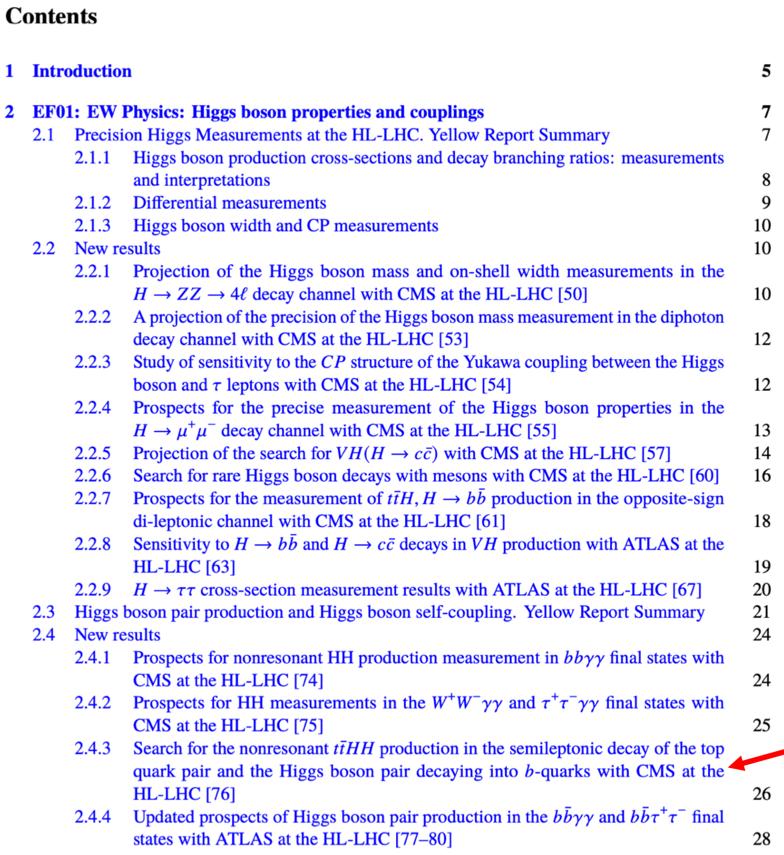

Contents

1 Introduction 5
2 EF01: EW Physics: Higgs boson properties and couplings 7
2.1 Precision Higgs Measurements at the HL-LHC. Yellow Report Summary 7
2.1.1 Higgs boson production cross-sections and decay branching ratios: measurements and interpretations 8
2.1.2 Differential measurements 9
2.1.3 Higgs boson width and CP measurements 10
2.2 New results 10
2.2.1 Projection of the Higgs boson mass and on-shell width measurements in the $H \rightarrow ZZ \rightarrow 4\ell$ decay channel with CMS at the HL-LHC [50] 10
2.2.2 A projection of the precision of the Higgs boson mass measurement in the diphoton decay channel with CMS at the HL-LHC [53] 12
2.2.3 Study of sensitivity to the CP structure of the Yukawa coupling between the Higgs boson and τ leptons with CMS at the HL-LHC [54] 12
2.2.4 Prospects for the precise measurement of the Higgs boson properties in the $H \rightarrow \mu^+\mu^-$ decay channel with CMS at the HL-LHC [55] 13
2.2.5 Projection of the search for $VH(H \rightarrow c\bar{c})$ with CMS at the HL-LHC [57] 14
2.2.6 Search for rare Higgs boson decays with mesons with CMS at the HL-LHC [60] 16
2.2.7 Prospects for the measurement of $t\bar{t}H, H \rightarrow b\bar{b}$ production in the opposite-sign di-leptonic channel with CMS at the HL-LHC [61] 18
2.2.8 Sensitivity to $H \rightarrow b\bar{b}$ and $H \rightarrow c\bar{c}$ decays in VH production with ATLAS at the HL-LHC [63] 19
2.2.9 $H \rightarrow \tau\tau$ cross-section measurement results with ATLAS at the HL-LHC [67] 20
2.3 Higgs boson pair production and Higgs boson self-coupling. Yellow Report Summary 21
2.4 New results 24
2.4.1 Prospects for nonresonant HH production measurement in $bb\gamma\gamma$ final states with CMS at the HL-LHC [74] 24
2.4.2 Prospects for HH measurements in the $W^+W^-\gamma\gamma$ and $\tau^+\tau^-\gamma\gamma$ final states with CMS at the HL-LHC [75] 25
2.4.3 Search for the nonresonant $t\bar{t}HH$ production in the semileptonic decay of the top quark pair and the Higgs pair decaying into b-quarks with CMS at the HL-LHC [76] 26
2.4.4 Updated prospects of Higgs boson pair production in the $b\bar{b}\gamma\gamma$ and $b\bar{b}\tau^+\tau^-$ final states with ATLAS at the HL-LHC [77–80] 28

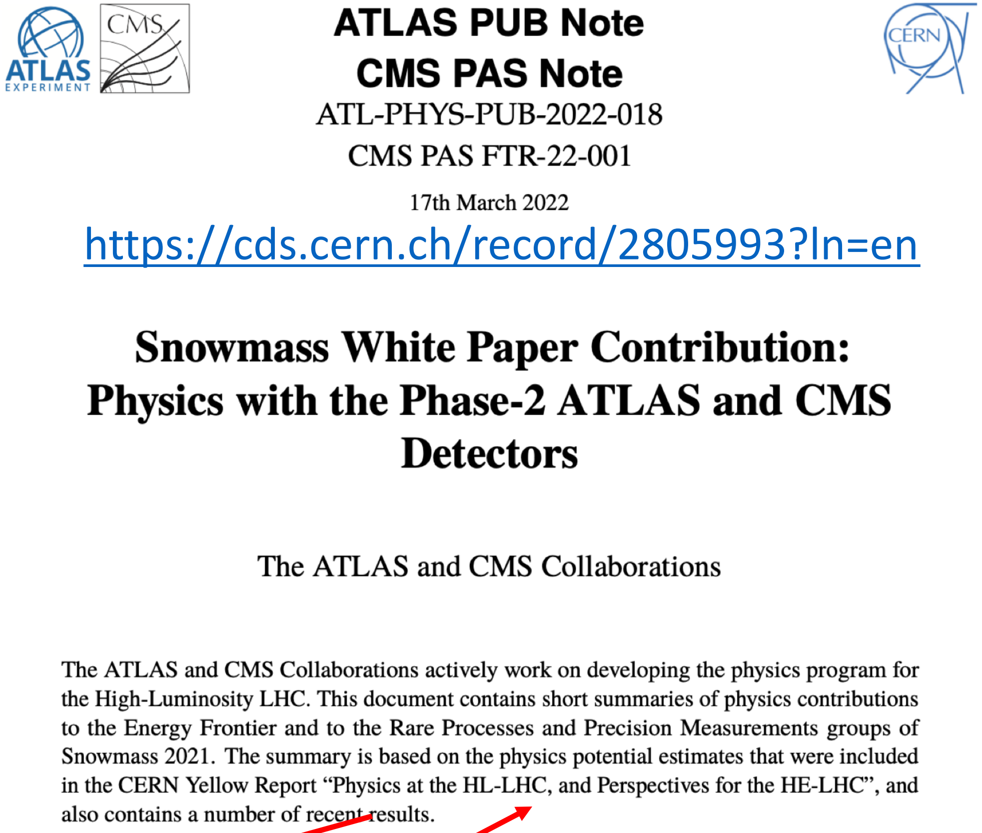

ATLAS PUB Note
CMS PAS Note
ATL-PHYS-PUB-2022-018
CMS PAS FTR-22-001

17th March 2022

https://cds.cern.ch/record/2805993?ln=en

Snowmass White Paper Contribution: Physics with the Phase-2 ATLAS and CMS Detectors

The ATLAS and CMS Collaborations

The ATLAS and CMS Collaborations actively work on developing the physics program for the High-Luminosity LHC. This document contains short summaries of physics contributions to the Energy Frontier and to the Rare Processes and Precision Measurements groups of Snowmass 2021. The summary is based on the physics potential estimates that were included in the CERN Yellow Report "Physics at the HL-LHC, and Perspectives for the HE-LHC", and also contains a number of recent results.

White paper

CMS-Publications of the ttHH study for Snowmass 2022

The ttHH production process: from the SM to BSM/CHM

The many di-Higgs production mechanisms in the SM.

Gluon-gluon fusion (ggF)

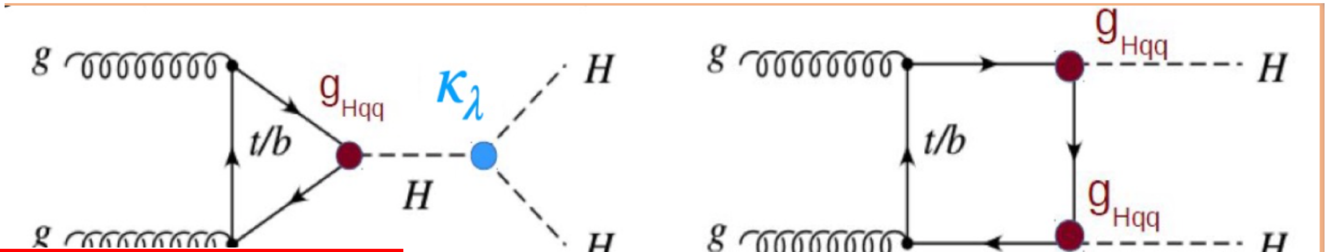

Top pair associated production/ Di-Higgs bremsstrahlung off top quarks ($t\bar{t}$HH)

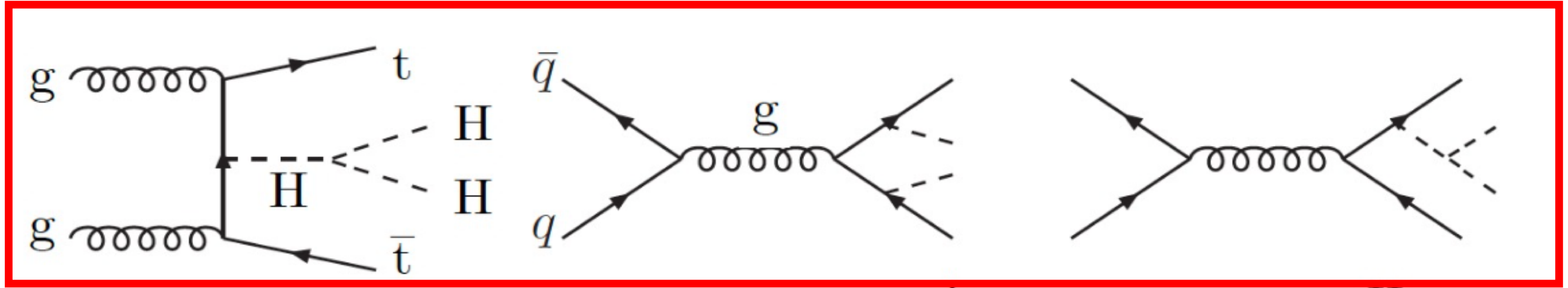

Di-Higgs bremsstrahlung/Vector Boson associated production

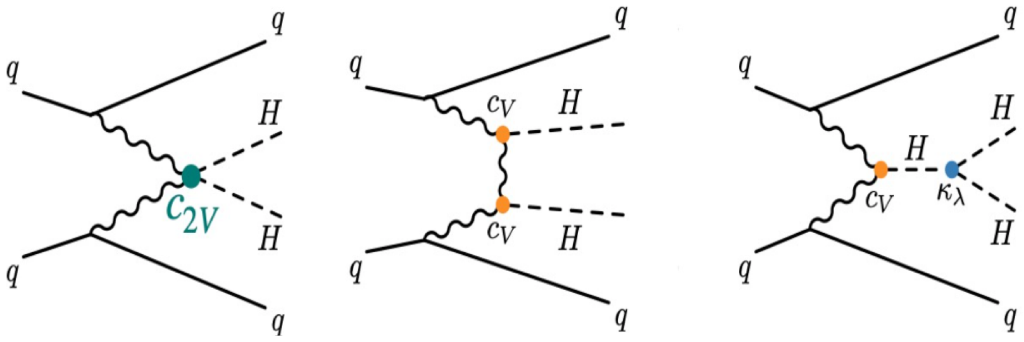

Vector Boson Fusion (VBF)

Single top quark associated production

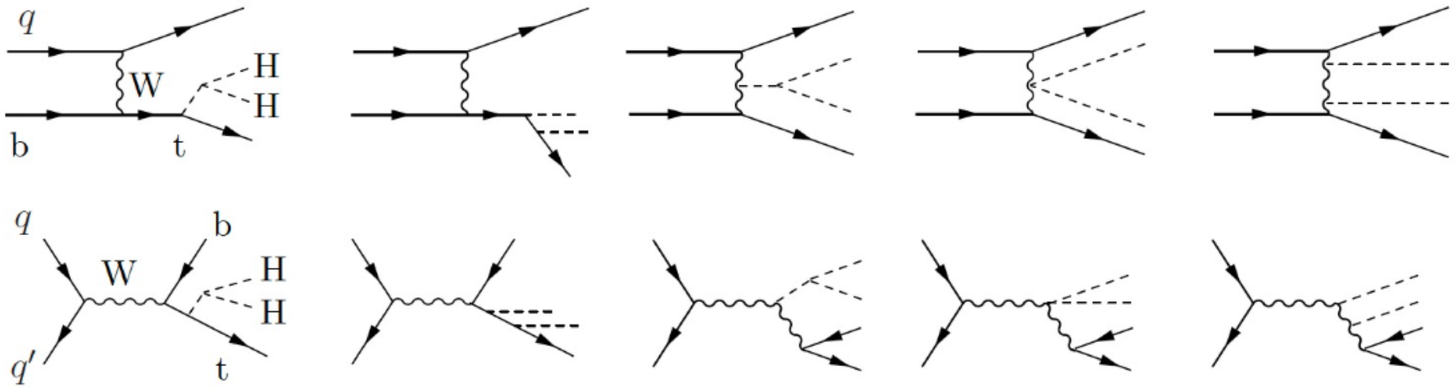

The ttHH production in the SM CASE

The ttHH production in SM is interesting per se, with LHC as a unique playground from now & till end of HL-LHC

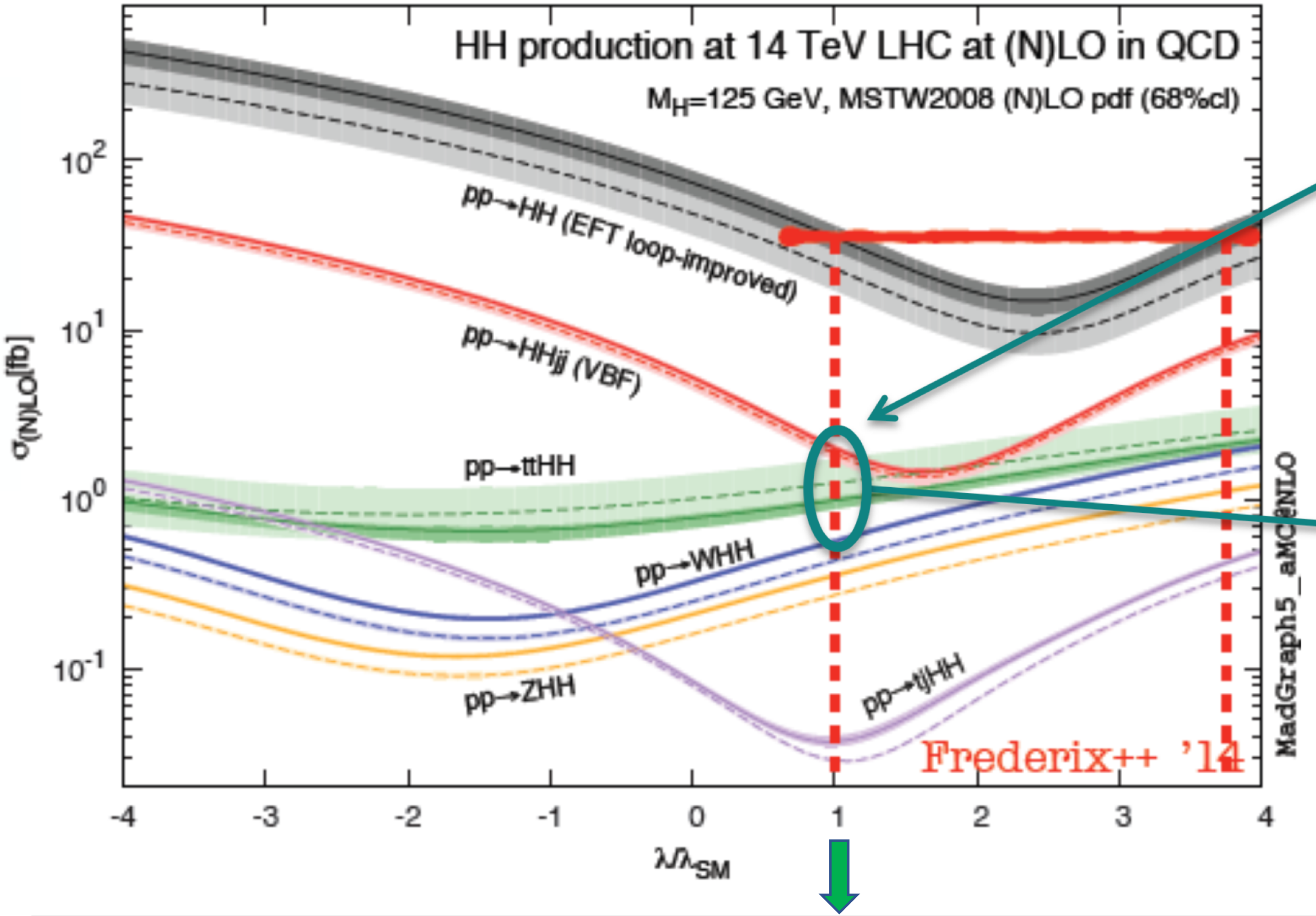

Processes at the few fb level involving double Higgs.

Accessing a new region in the exploration of the Higgs sector: interplay between HH, VBF(HH), ttHH

At 13 TeV: σ(tthh) = 0.775 fb (NLO QCD)*
σ(hh) = 31.05 fb (NNLO)
σ(VBFhh)=1.7fb (NLO)

*(*D. De Florian et al., arXiv 1610.07922)*

At 14 TeV: σ(tthh) = 0.948 fb (NLO QCD)

ZHH	WHH	VBF HH	ttHH	tjHH	ttH
$0.359^{+1.9\%}_{-1.3\%} \pm 1.7\%$ fb	$0.573^{+2.0\%}_{-1.4\%} \pm 1.9\%$ fb	$1.95^{+1.1\%}_{-1.5\%} \pm 2.0\%$ fb	$0.948^{+3.9\%}_{-13.5\%} \pm 3.2\%$ fb	$0.0383^{+5.2\%}_{-3.3\%} \pm 4.7\%$ fb	$612^{+6.0\%}_{-9.2\%} \pm 3.5\%$ fb

Evolution of production cross-sections with E_{cm} (from: LHCHXSWG-2019-005)

Total production cross sections for Higgs pairs within SM via gluon fusion, VBF, double Higgs-strahlung and double Higgs bremsstrahlung off top quarks. PDF4LHC15 parton densities have been used with scale choices according Table here below. The size of the bands shows the total uncertainties originating from the scale dependence and the PDF+αs uncertainties.

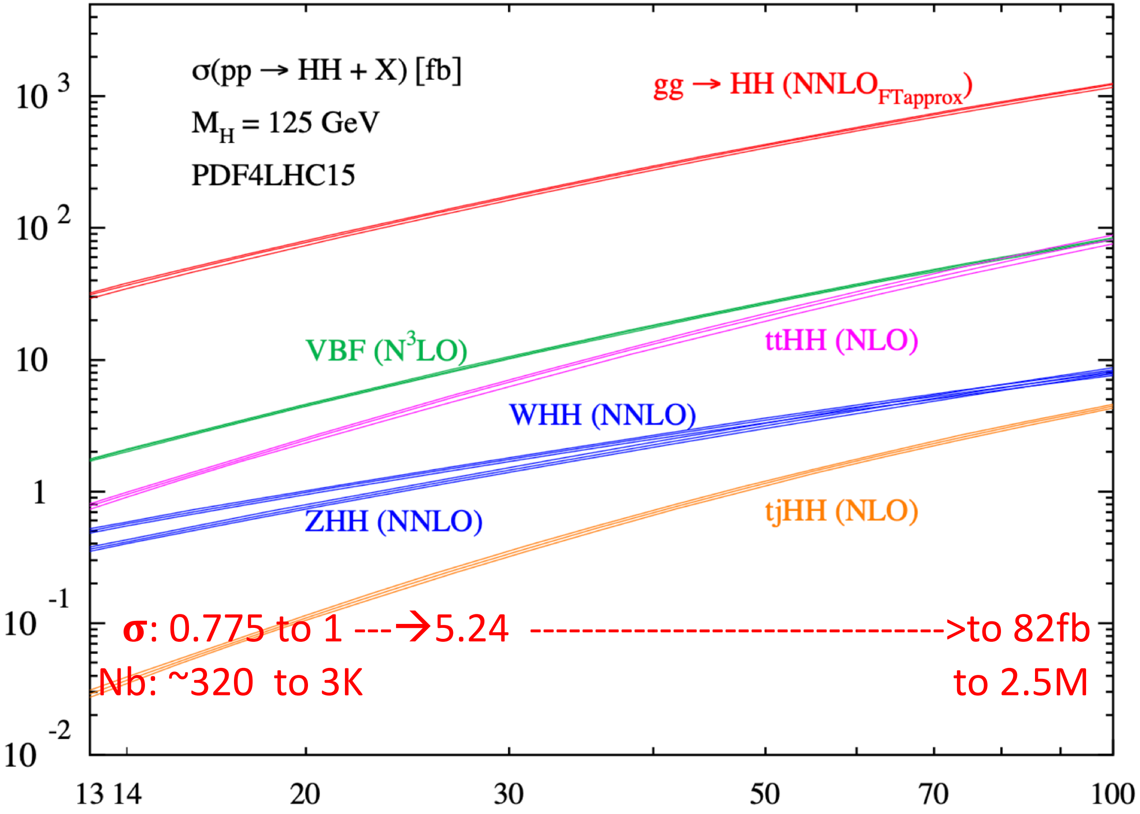

σ: 0.775 to 1 ---→5.24 ------------------------------->to 82fb

Nb: ~320 to 3K to 2.5M

$\sqrt{s}$	13 TeV	14 TeV	27 TeV	100 TeV
ggF HH	$31.05^{+2.2\%}_{-5.0\%} \pm 3.0\%$	$36.69^{+2.1\%}_{-4.9\%} \pm 3.0\%$	$139.9^{+1.3\%}_{-3.9\%} \pm 2.5\%$	$1224^{+0.9\%}_{-3.2\%} \pm 2.4\%$
VBF HH	$1.73^{+0.03\%}_{-0.04\%} \pm 2.1\%$	$2.05^{+0.03\%}_{-0.04\%} \pm 2.1\%$	$8.40^{+0.11\%}_{-0.04\%} \pm 2.1\%$	$82.8^{+0.13\%}_{-0.04\%} \pm 2.1\%$
ZHH	$0.363^{+3.4\%}_{-2.7\%} \pm 1.9\%$	$0.415^{+3.5\%}_{-2.7\%} \pm 1.8\%$	$1.23^{+4.1\%}_{-3.3\%} \pm 1.5\%$	$8.23^{+5.9\%}_{-4.6\%} \pm 1.7\%$
W^+HH	$0.329^{+0.32\%}_{-0.41\%} \pm 2.2\%$	$0.369^{+0.33\%}_{-0.39\%} \pm 2.1\%$	$0.941^{+0.52\%}_{-0.53\%} \pm 1.8\%$	$4.70^{+0.90\%}_{-0.96\%} \pm 1.8\%$
W^-HH	$0.173^{+1.2\%}_{-1.3\%} \pm 2.8\%$	$0.198^{+1.2\%}_{-1.3\%} \pm 2.7\%$	$0.568^{+1.9\%}_{-2.0\%} \pm 2.1\%$	$3.30^{+3.5\%}_{-4.3\%} \pm 1.9\%$
$t\bar{t}HH$	$0.775^{+1.5\%}_{-4.3\%} \pm 3.2\%$	$0.949^{+1.7\%}_{-4.5\%} \pm 3.1\%$	$5.24^{+2.9\%}_{-6.4\%} \pm 2.5\%$	$82.1^{+7.9\%}_{-7.4\%} \pm 1.6\%$
$tjHH$	$0.0289^{+5.5\%}_{-3.6\%} \pm 4.7\%$	$0.0367^{+4.2\%}_{-1.8\%} \pm 4.6\%$	$0.254^{+3.8\%}_{-2.8\%} \pm 3.6\%$	$4.44^{+2.2\%}_{-2.8\%} \pm 2.4\%$

FYI: tttt production cross-section 14/13~1.3; 13/27~12.6

Renormalization and factorisation scales set to $m_{HH}/2$ for gluon fusion, to the individual virtualities $Q_{1,2} = \sqrt{-q^2_{1,2}}$ of the t-channel vector-bosons for VBF (with a lower cut of 1 GeV), to m_{HHV} (*V* =*W*,*Z*) for *HHV* production, to $m_{tt}/2$ or ttHH and $m_{HH}/2$ for tjHH production. They were varied up and down by a factor of 2 to obtain the scale uncertainties, indicated as superscript/subscript. PDF4LHC15 parton distributions used to obtain the results, and corresponding αs +PDF uncertainties. The cross sections for *t j HH* involve both top and anti-top production.

ttHH: STUDY OF COUPLINGS IN THE TOP HIGGS SECTOR

The interplay between HH, VBF(HH), ttH and ttHH vs *Couplings, here only at LO only & within SM*

(But negative interference => only 50% left at LO)

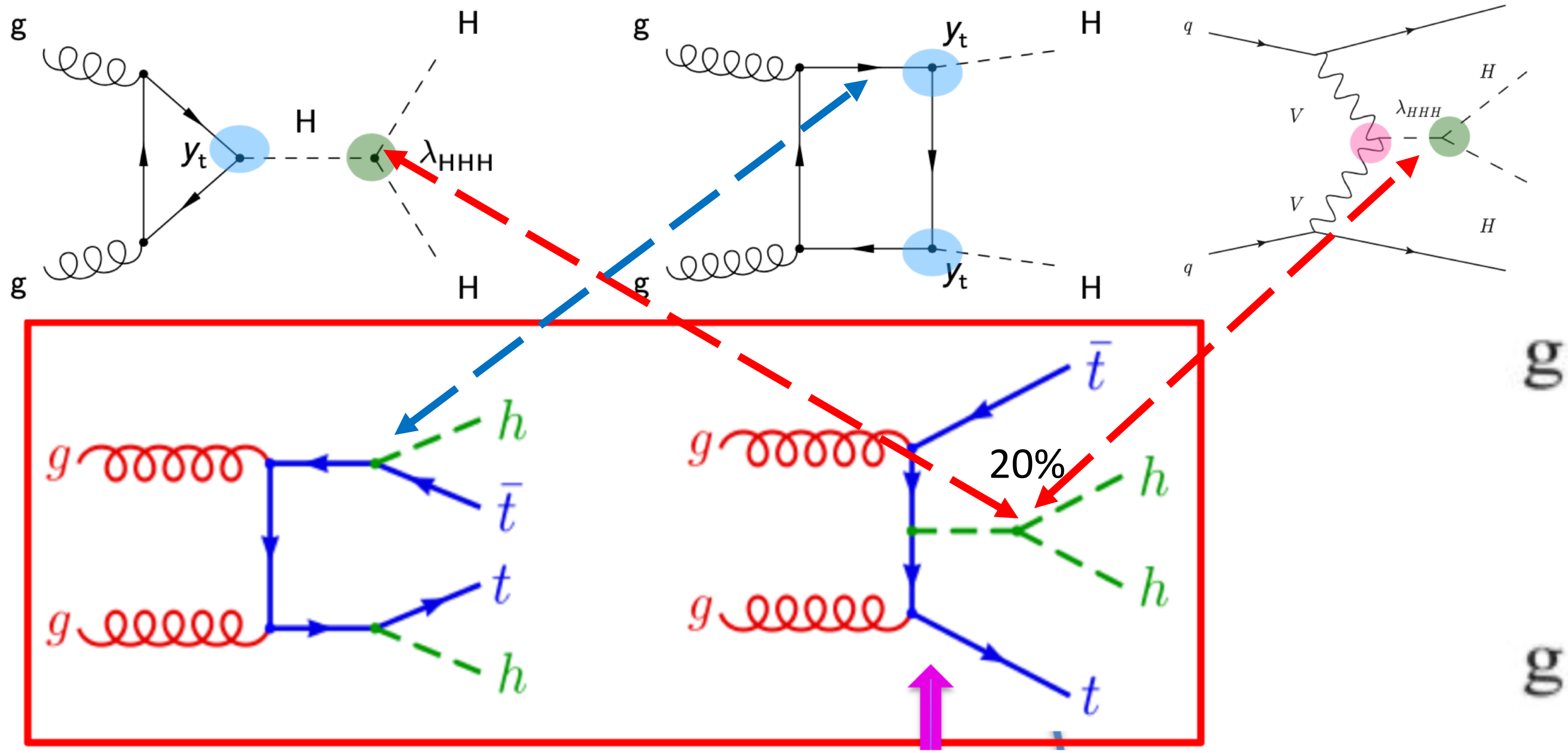

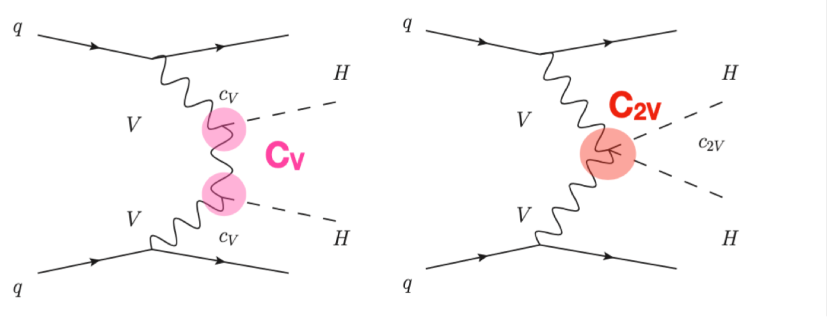

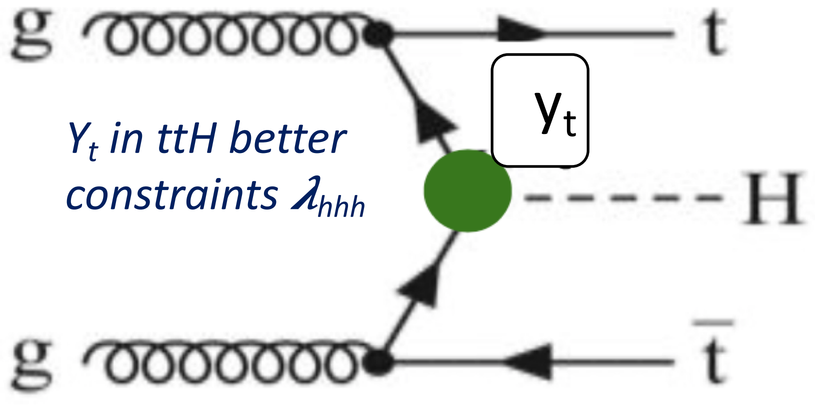

Y_t in ttH better constraints λ_{hhh}

Unlike ttH which gives access to only Yukawa top-Higgs coupling, ttHH gives access to both the top-Higgs Yukawa and the triple Higgs couplings, like the HH process, but without negative interference term.

HEFT operators modifying the ttHH production

$$\sigma(k_\lambda , k_t , c_2) = k_t^4 \sigma_a + k_\lambda^2 \; k_t^2 \sigma_b + c_2^2 \; \sigma_c + k_t^3 k_\lambda \, \sigma i_{ab} + k_t^2 c_2 \, \sigma i_{ac} + k_\lambda k_t c_2 \, \sigma i_{bc}$$

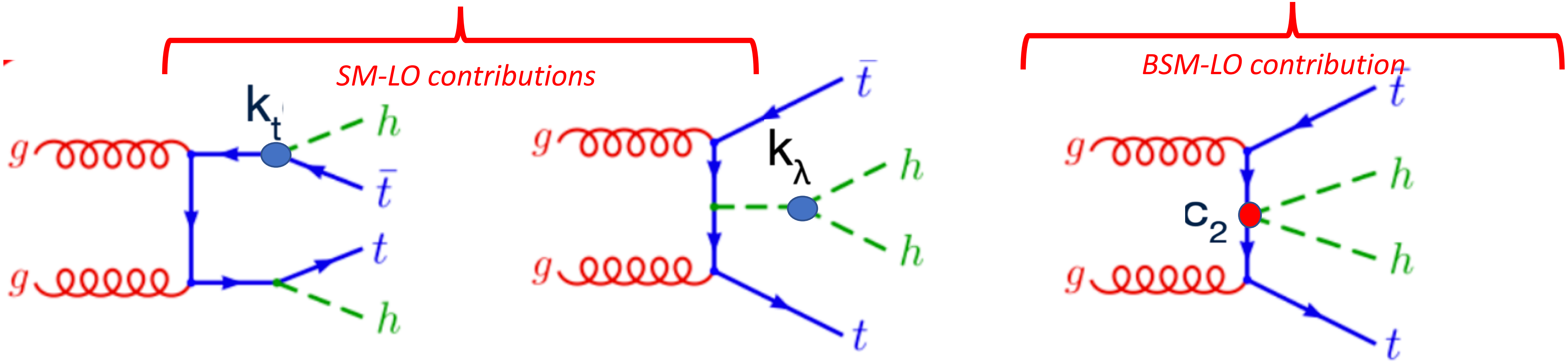

Similar non-resonant contributions in Composite Higgs Models

BSM case:the ttHH production at LO in MCHM

ttHH production processes common to SM & MCHM

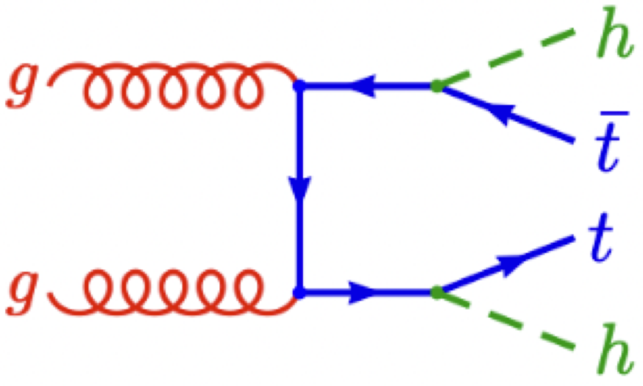

Yukawa vertex (~80%)

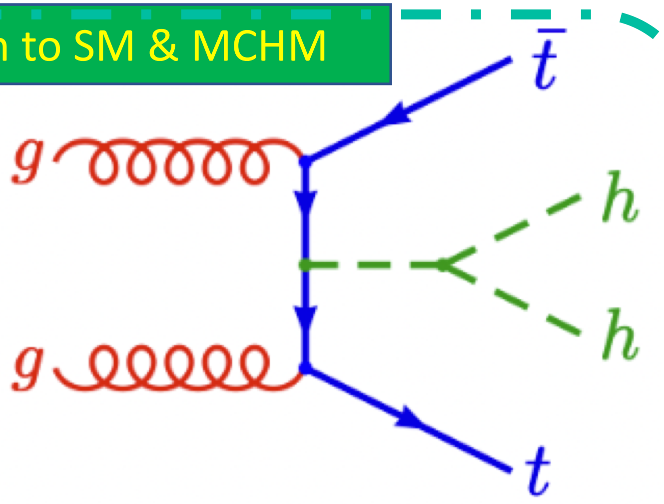

Higgs trilinear self-coupling (20%/**15%**)

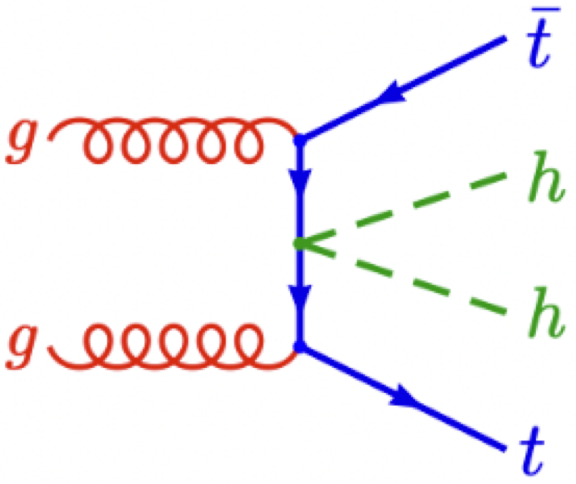

Double Higgs Yukawa vertex(~5%)

AND

QCD pair production of heavy top partners with their top-Higgs decay

In red: processes specific to MCHM

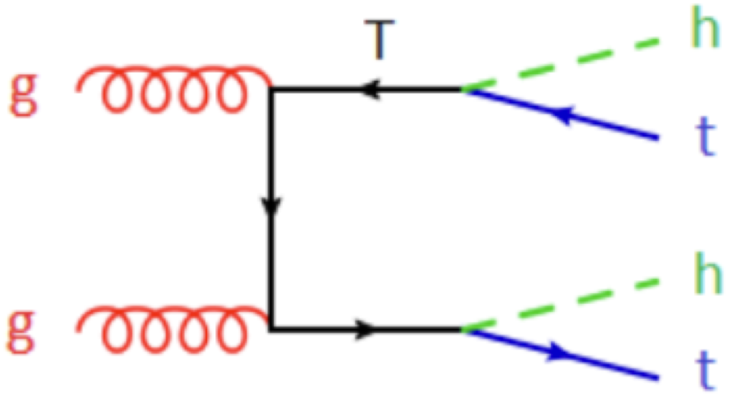

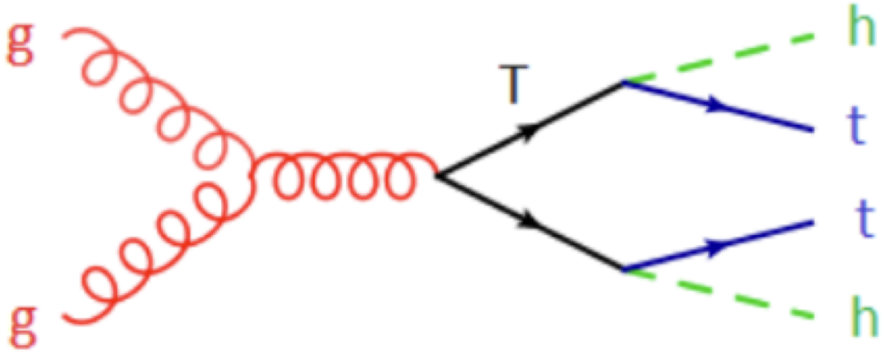

***ttHH:** the resonant part => search for VLQ (≥ simple extension of SM)*

NON RESONANT PRODUCTION PROCESS at LO:

SM-LO contributions

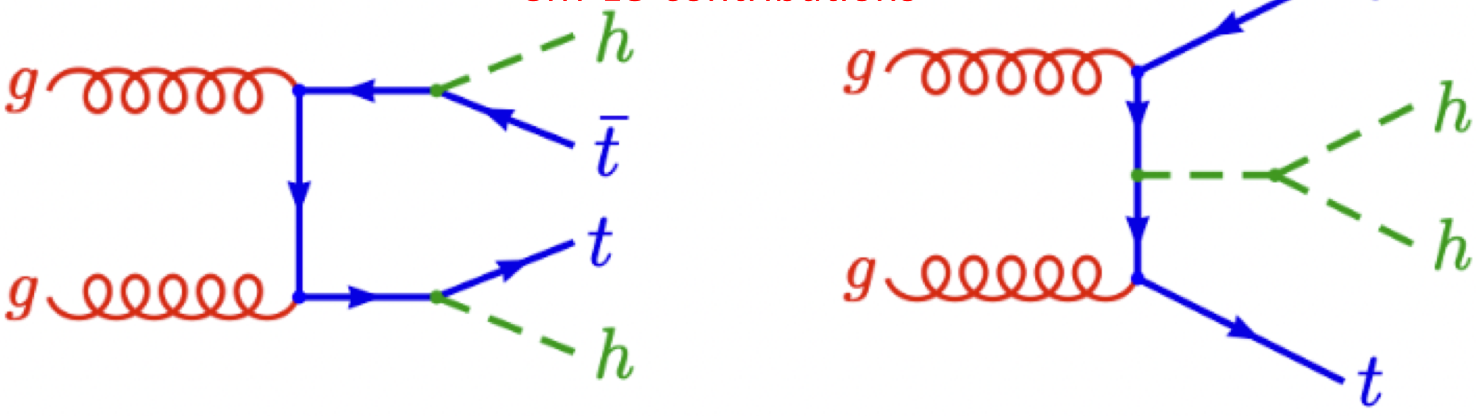

BSM-LO contribution

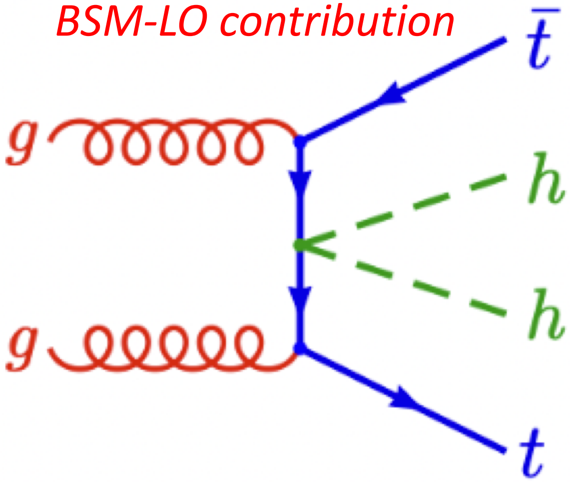

RESONANT PRODUCTION PROCESS at LO:

QCD pair production of heavy top partners with their top-Higgs decay

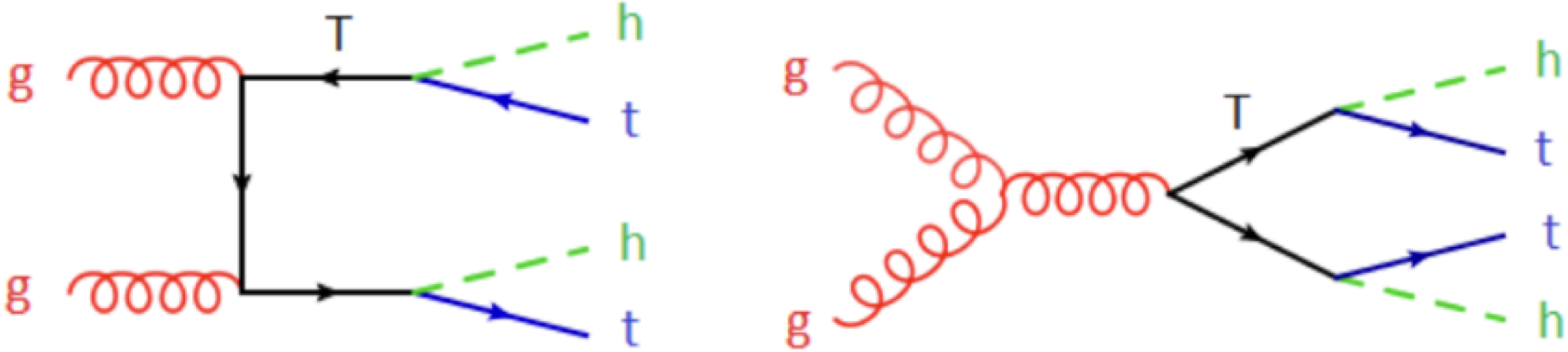

Study of the ttH and ttHH processes within the Minimal Composite Higgs

Based on:
1) Probing the top-Higgs sector with Composite Higgs Models at present and future hadron colliders (JHEP(2021), 049
2) On the importance of 3-body decays of VLQs (arXiv 2023.09022, submitted JHEP, May 9)
(and published ATLAS, CMS searches for heavy VLQ resonances at LHC)

N.B. Due to time constraints we here review only some of the points studied in the two pheno papers, which are of specific interests in the present reported experimental studies. Thus points related to couplings measurement and link with EFT are not presented here.

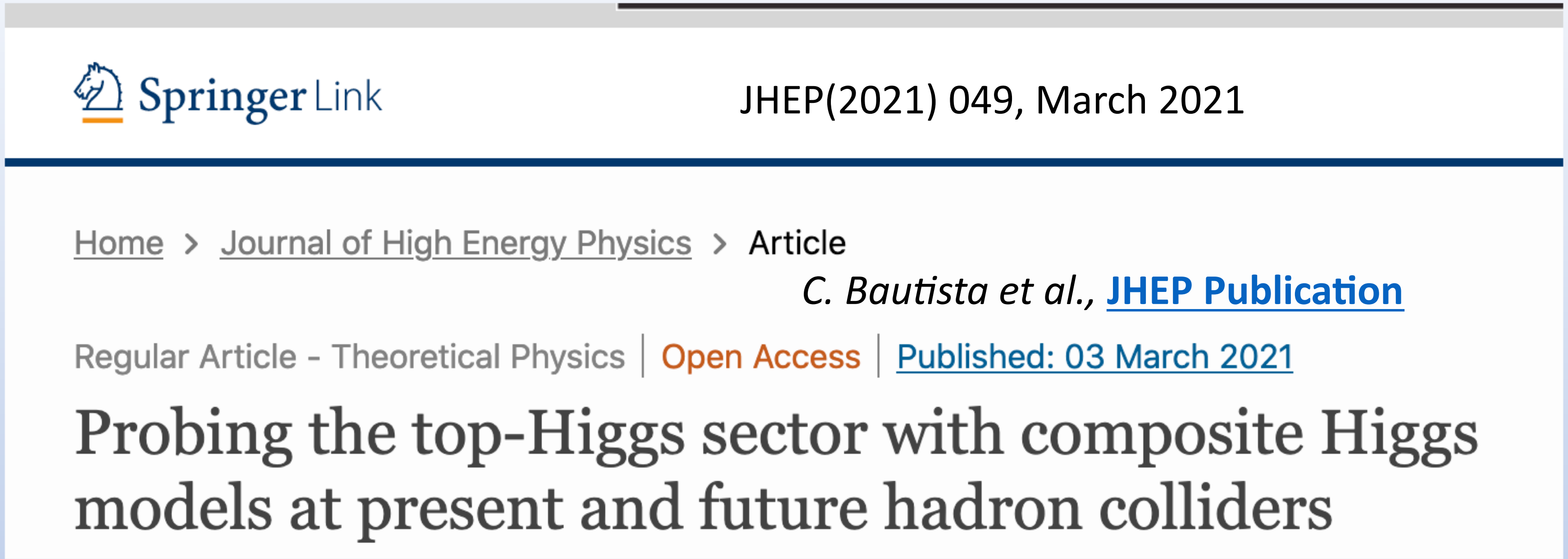

JHEP(2021) 049, March 2021

Home > Journal of High Energy Physics > Article

C. Bautista et al., **JHEP Publication**

Regular Article - Theoretical Physics | Open Access | Published: 03 March 2021

Probing the top-Higgs sector with composite Higgs models at present and future hadron colliders

- Study of tth & tthh production processes in the context of CHM
- Can be probed by precision measurements of couplings + resonance searches.
- We concentrate on the fermion sector and its interplay with the Higgs boson. This depends on the composite resonances associated with the top quark.

The Minimal Composite Higgs

- Higgs is a pNGB (pseudo Nambu Goldstone Boson) of SO(5)/SO(4)
- Potential is generated by SM interactions with strong sector.

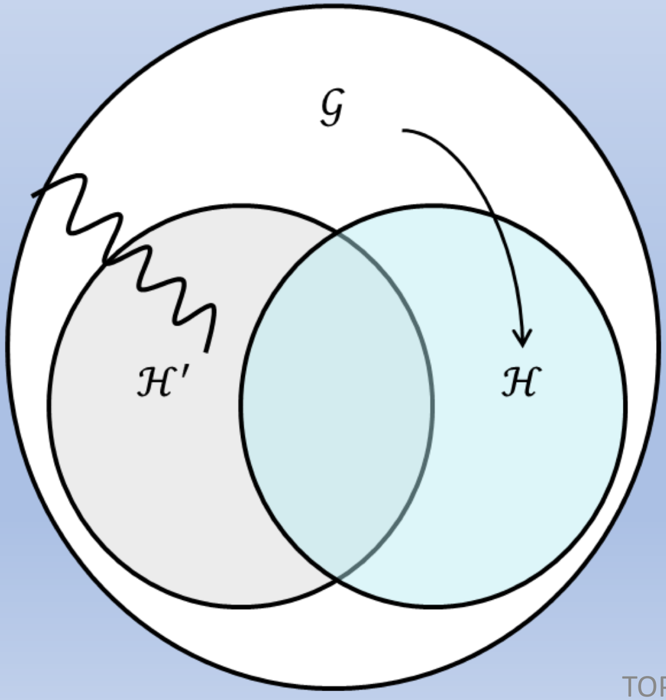

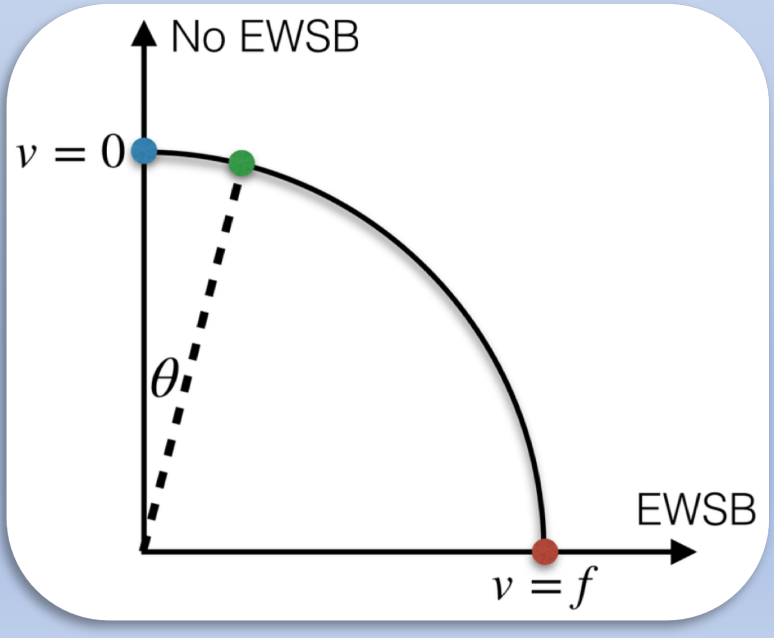

The Minimal Composite Higgs

- Many extensions possible: non-minimal breaking, neutral naturalness, UV completion....
- Here we focus on the top sector resonances in the smallest (custodial) SO(5) irreps: **5** and **14**
- Fermion masses arise from linear mixing with resonances “partial compositness”
- Resonances fall into irreductible representations (irreps.) of SO(4), with distinct phenomenology

Fermionic Representations

- Under SO(4), **5** = **4** ⊕ **1**

$$\Psi_4 \sim (\underbrace{X_{5/3}, X_{2/3}}_{Y=7/6}, \underbrace{T, B}_{Y=1/6})$$

$$\Psi_1 \sim \underbrace{\tilde{T}}_{Y=2/6}\,,$$

$$\begin{aligned}\mathcal{L}^{\mathbf{5}}_{\text{mix}} &= f\,\overline{Q}^{\mathbf{5}}_L U\left[y_{L4}\Psi_{\mathbf{4}} + y_{L1}\Psi_{\mathbf{1}}\right] + \text{h.c.}\\ &+ f\,\overline{T}^{\mathbf{5}}_R U\left[y_{R4}\Psi_{\mathbf{4}} + y_{R1}\Psi_{\mathbf{1}}\right] + \text{h.c.}\end{aligned}$$

$$\Longrightarrow$$

$$\begin{aligned}M_{T_{2/3}} &= \sqrt{M_1^2 + y_R^2 f^2},\\ &\quad M_4, \quad \sqrt{M_4^2 + y_L^2 f^2}\\ M_B &= \sqrt{M_4^2 + y_L^2 f^2}\\ M_{X_{5/3}} &= M_4\end{aligned}$$

Fermionic Representations

- Under SO(4), **14** = **9** ⊕ **4** ⊕ **1**

$$\Psi_{\mathbf{9}} \quad \sim \quad (\underbrace{U_{8/3}, U_{5/3}, U_{2/3}}_{Y=5/3}, \underbrace{V_{5/3}, V_{2/3}, V_{-1/3}}_{Y=2/3}, \underbrace{F_{2/3}, F_{-1/3}, F_{-4/3}}_{Y=-1/3})$$

$$\begin{aligned}\mathcal{L}^{\mathbf{14}}_{\text{mix}} &= f\,\mathrm{Tr}\left[U^{\intercal}\overline{Q}^{\mathbf{14}}_{L}U\left(y_{L9}\Psi_{\mathbf{9}} + y_{L4}\Psi_{\mathbf{4}} + y_{L1}\Psi_{\mathbf{1}}\right)\right] + \text{h.c.}\\ &\quad + f\,\mathrm{Tr}\left[U^{\intercal}\overline{T}^{\mathbf{14}}_{R}U\left(y_{R9}\Psi_{\mathbf{9}} + y_{R4}\Psi_{\mathbf{4}} + y_{R1}\Psi_{\mathbf{1}}\right)\right] + \text{h.c.}\end{aligned}$$

Standard Model Couplings

- SM couplings are modified by functions of $\xi = v^2/f^2$ and also by resonance mixings.
- Couplings entering tth and tthh:

$$\mathcal{L}_h = \frac{1}{2}\partial_\mu h \partial^\mu h - \frac{1}{2} m_h^2 h^2 - \kappa_\lambda \lambda_{\text{SM}} v h^3 - \frac{m_t}{v}\left(v + \kappa_t h + \frac{c_2}{v} hh\right)\left(\bar{t}_L t_R + \text{h.c.}\right)$$
$$+ \frac{1}{4}\frac{\alpha_s}{3\pi v}\left(c_g h - \frac{c_{2g}}{2v} hh\right) G^{\mu\nu} G_{\mu\nu}$$

SM limit: κ = 1, c = 0

The top Yukawa

- Below resonances:

$$\kappa_t^{5} = 1 - \frac{3}{2}\xi \qquad \kappa_t^{14} = 1 - 4\xi$$

→ **Suppressed**

- Except, if $M_1 \sim M_4$ or $M_9 \ll M_{1,4}$

$$\kappa_t^{14} = 3$$

→ **Enhanced!**

Higgs Coupling Modifications in CHM

- Top-Yukawa coupling is of central interest here. SM couplings are modified by functions of $\xi = \frac{v^2}{f^2}$ & by resonance mixings.
- Compositeness gives rise to top-Yukawa couplings (y_L,y_R)
- In MCHM, tth coupling modified as:

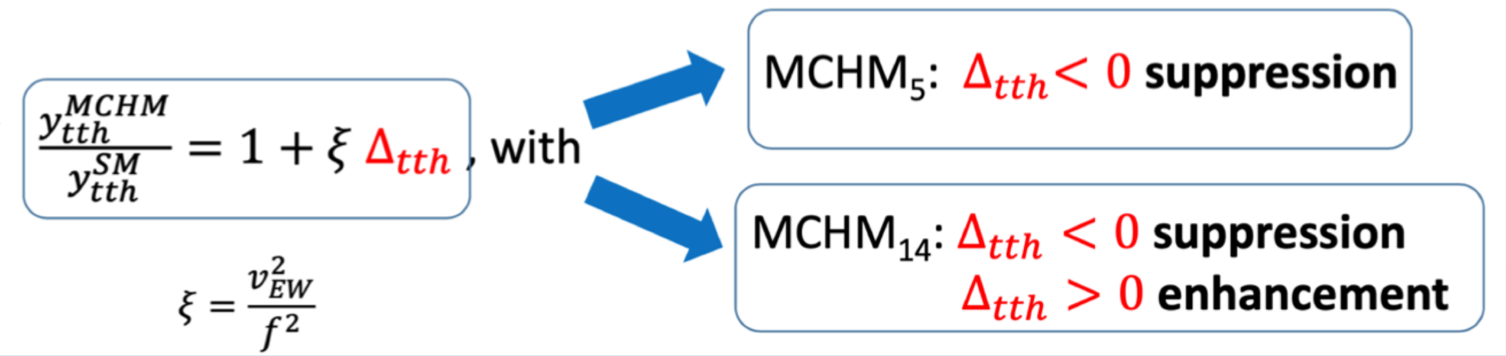

$$\frac{y_{tth}^{MCHM}}{y_{tth}^{SM}} = 1 + \xi\, \Delta_{tth}$$, with

$$\xi = \frac{v_{EW}^2}{f^2}$$

MCHM$_5$: $\Delta_{tth} < 0$ **suppression**

MCHM$_{14}$: $\Delta_{tth} < 0$ **suppression**
$\Delta_{tth} > 0$ **enhancement**

- Higgs sector non-linearities

  generate new vertices such as tthh

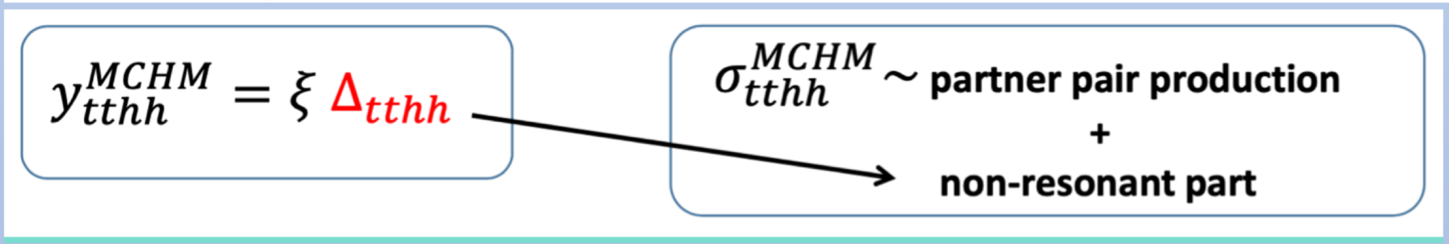

$$y_{tthh}^{MCHM} = \xi\, \Delta_{tthh}$$

$\sigma_{tthh}^{MCHM} \sim$ **partner pair production**
+
non-resonant part

- Top-Higgs Yukawa coupling through mixing with singlet, 4-plet &nonet resonances (green squares represent mixing)

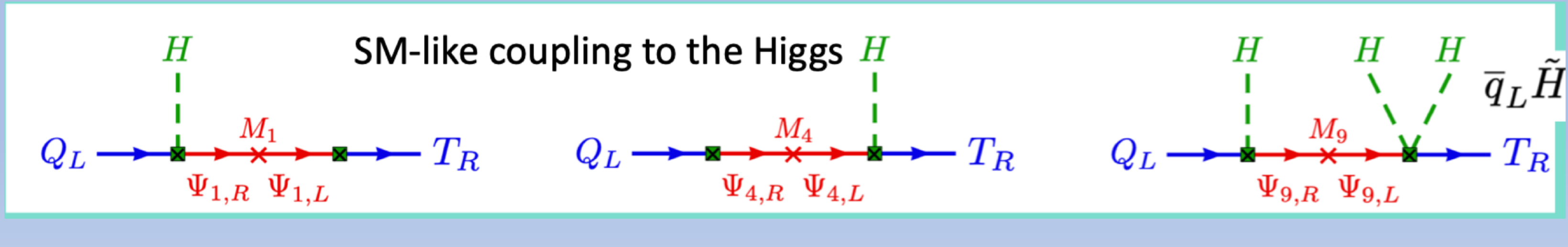
SM-like coupling to the Higgs

$\bar{q}_L \tilde{H} t_R H^\dagger H$, non SM-like, cubic non renormalizable coupling

The thh & $\bar{t}thh$ processes in MCHM

- Complementary better to say in “interplay with” to HH (gluon fusion and VBF)
- μ(ttH): all modifications enter only through y_t

$$\boxed{\sigma_{\text{MCHM}}(t\bar{t}h) = \left(\frac{y_t}{y_t^{\text{SM}}}\right)^2 \sigma_{\text{SM}}(t\bar{t}h)}$$

NO Modification on Kinematic distributions ONLY on TOTAL RATE

- While the ttHH) process is described by
  - Sum of Resonant + <u>Non Resonant contributions</u> controlled by:

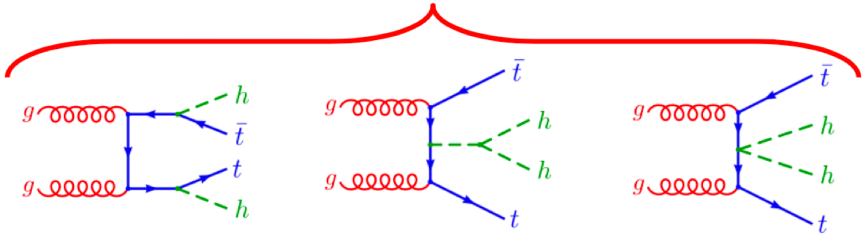

Yukawa vertex

Trilinear Self Coupling

“Double Higgs” Yukawa vertex

Non Resonant (NR) production can dominate if resonances are heavy

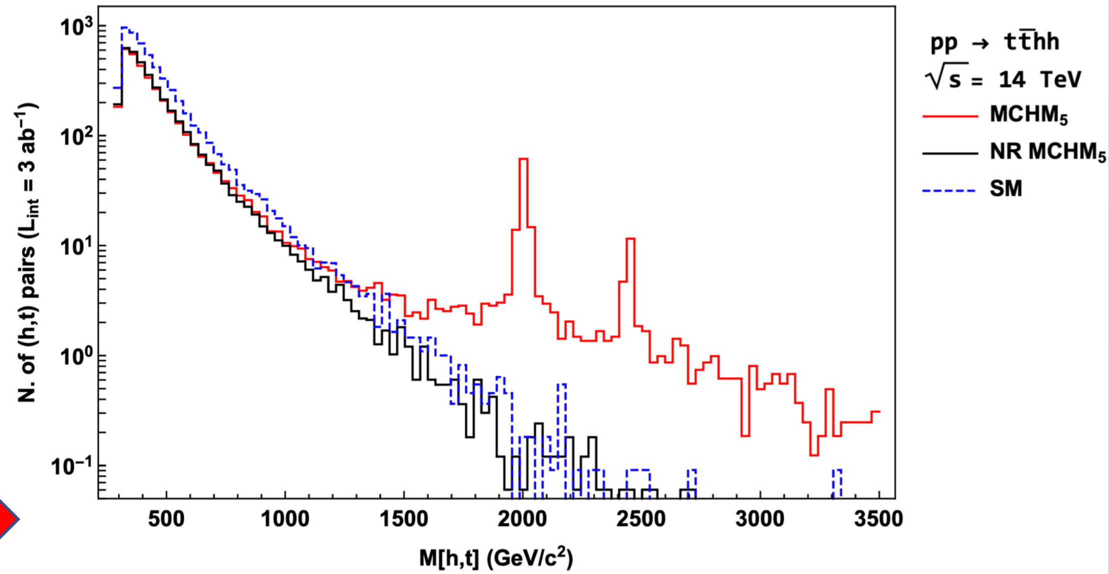

- Dominated by top yukawa, h^3 ~ 15% & a few % for hht
- But resonances impact kinematic distributions (see HL-LHC experimental study)

Pheno analysis in MCHM 5 and 14 parameter spaces:

- Top sector is controlled by: Mi, y_{Li} , y_{Ri} and c_L, c_R (MCHM5) or c_4, c_9 c_{T9} (MCHM$_{14}$)
- Phase redefinition & impose CP conservation in strong sector => 3 (5) physical signs for **5 (14)**
- Terms controlled by the "c" couplings modify cross sections, decays BR and widths but generally do not affect the shape of distributions. They can be encoded in a K- factor.
- We end up with

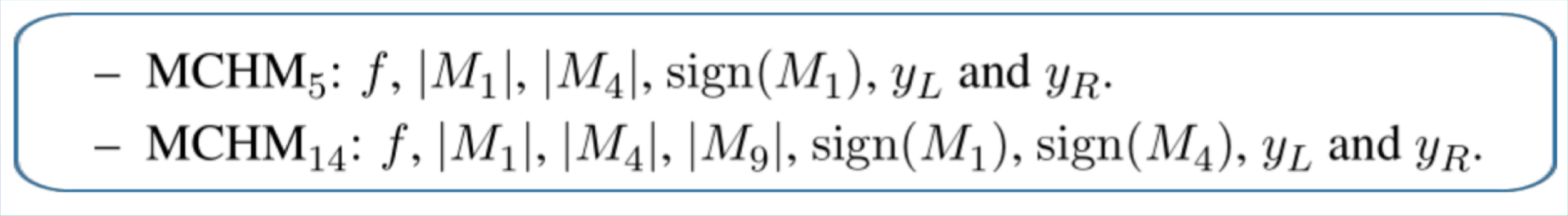

– MCHM$_5$: f, $|M_1|$, $|M_4|$, sign(M_1), y_L and y_R.
– MCHM$_{14}$: f, $|M_1|$, $|M_4|$, $|M_9|$, sign(M_1), sign(M_4), y_L and y_R.

- We fixed y_R by m_{top}=150 GeV.

(Approximate running mass near the resonance scale, intended to capture the main running effect on the couplings. The pole mass of 173 GeV is used in the kinematics.)

- We obtain the unitary transformations and use them to extract the Higgs couplings.

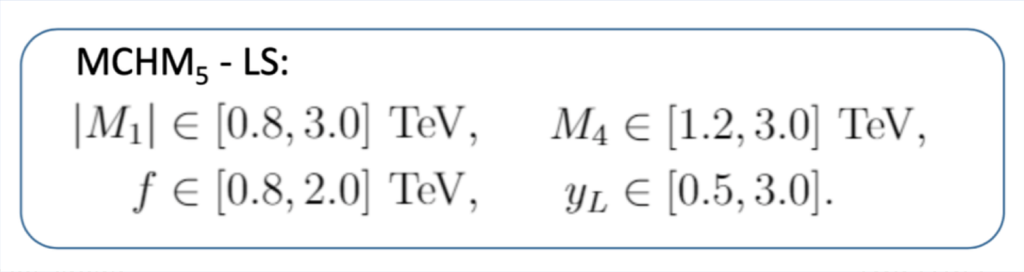

MCHM$_5$ - LS:

$$|M_1| \in [0.8, 3.0]\ \text{TeV}, \quad M_4 \in [1.2, 3.0]\ \text{TeV},$$
$$f \in [0.8, 2.0]\ \text{TeV}, \quad y_L \in [0.5, 3.0].$$

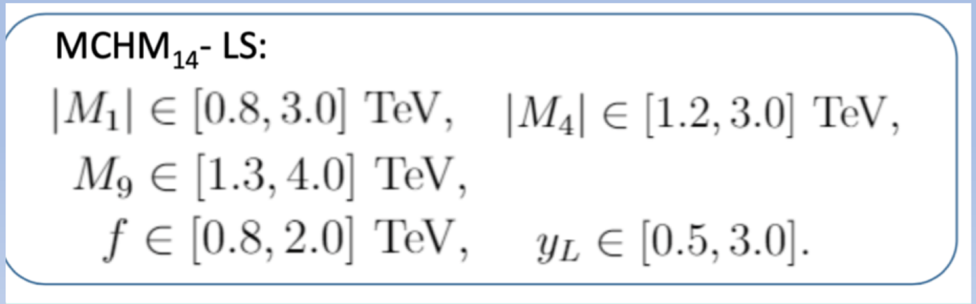

MCHM$_{14}$- LS:

$$|M_1| \in [0.8, 3.0]\ \text{TeV}, \quad |M_4| \in [1.2, 3.0]\ \text{TeV},$$
$$M_9 \in [1.3, 4.0]\ \text{TeV},$$
$$f \in [0.8, 2.0]\ \text{TeV}, \quad y_L \in [0.5, 3.0].$$

The top Yukawa in MCHM 5 and 14 parameter space

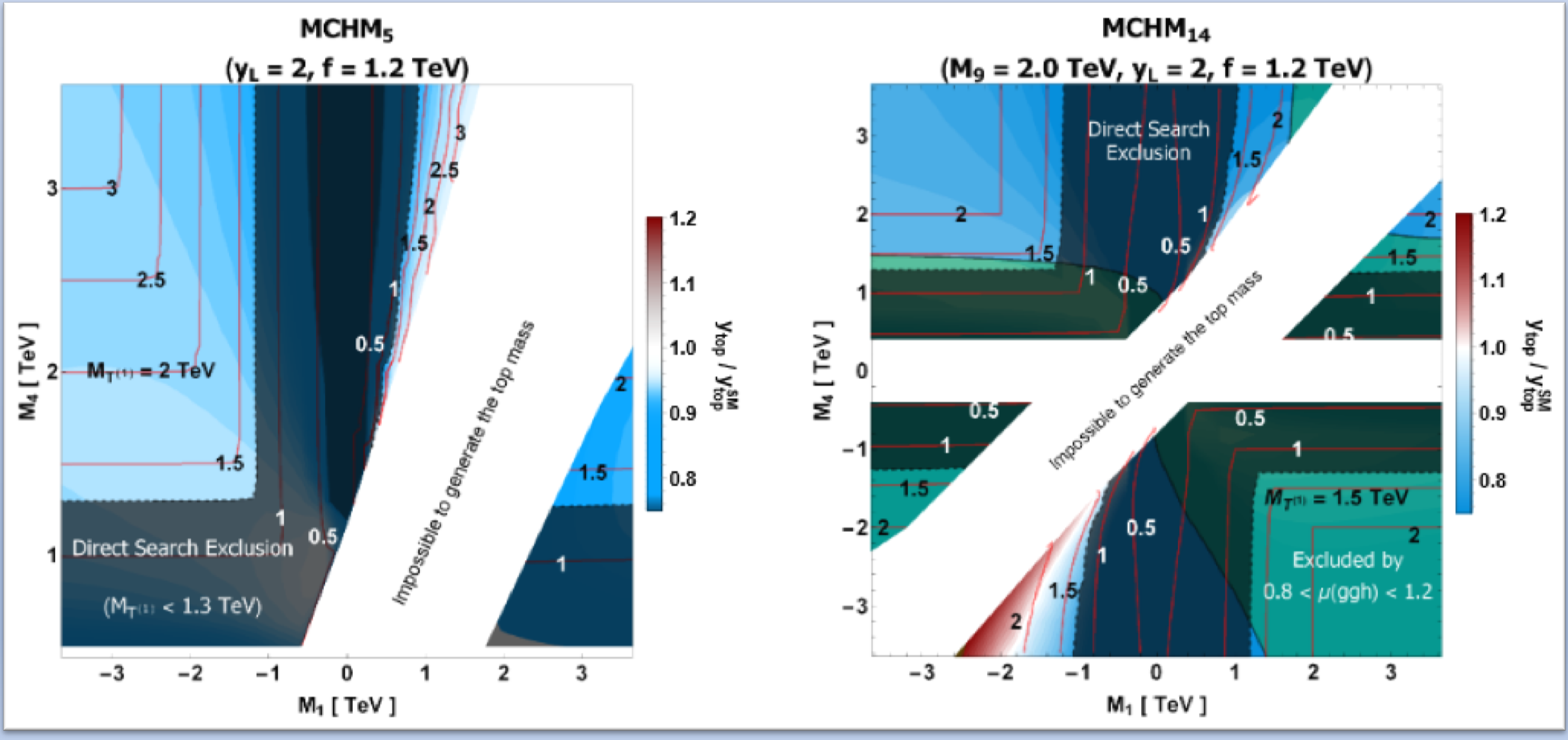

Parameter space scan

- Multidimensional parameter space
- How to identify representative points in a scan?
- Bin by bin clustering (A.Carvalho et. al JHEP 04 (2016) 126):

$$TS_{ab} = -2 \sum_{i=1}^{N_{bins}} \left[log(n_{(i,a)}!) + log(n_{(i,b)}!) - 2log\left(\frac{n_{(i,a)} + n_{(i,b)}}{2}! \right) \right]$$

- $TS_{ab} \geq 0$, measures closeness of a and b.
- Iteratively merge points with smallest TS_{ab}.
- Stop when a "reasonable number" of clusters is achieved.

Some clusters from the MCHM$_5$ scan

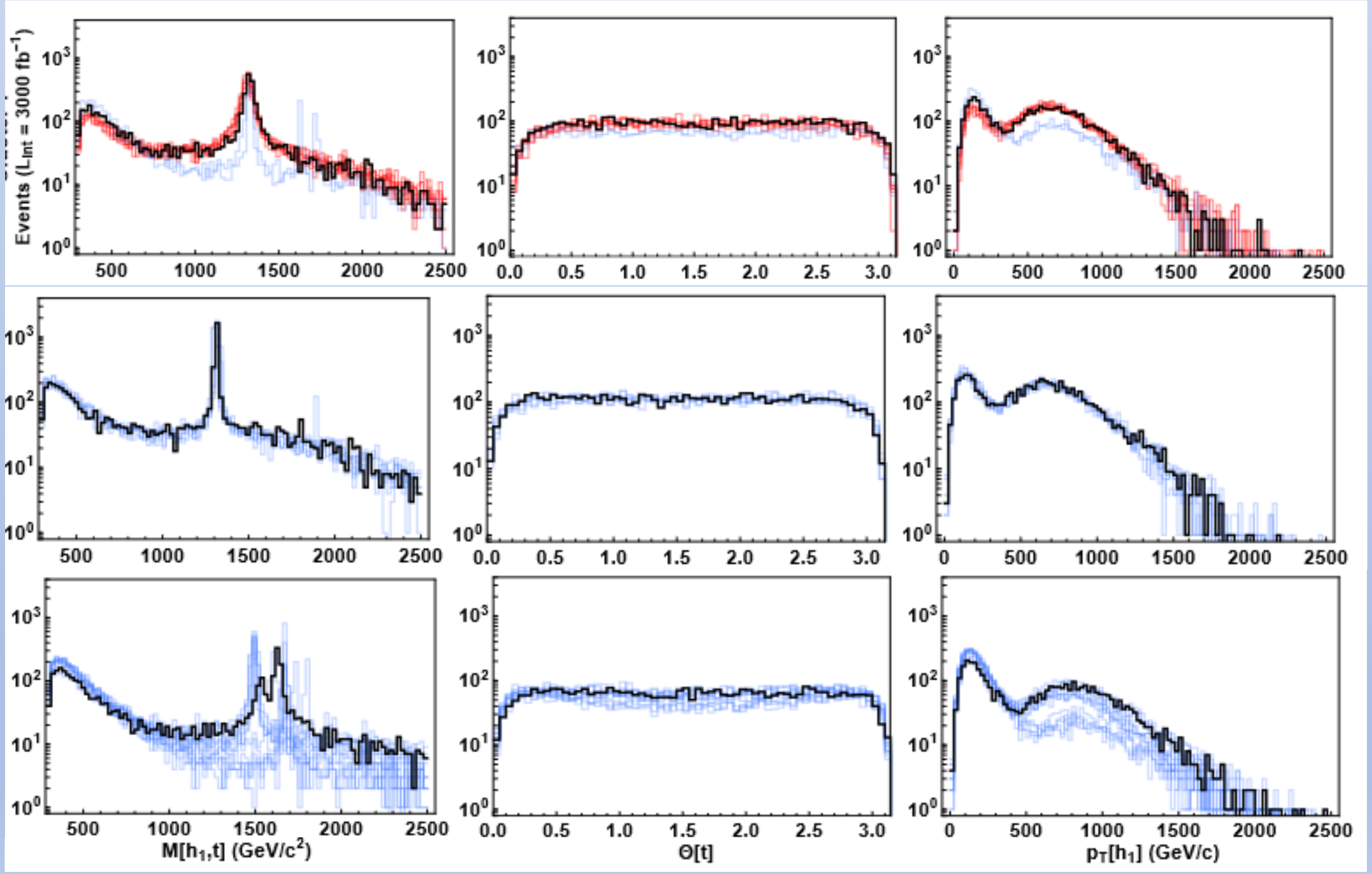

- Red and blue: 1st and 2nd quadrants of MCHM$_5$

Some clusters from the MCHM$_5$ scan

- Allows one to see new qualitative features in the parameter space
- 1st quadrant points have generally wider resonances
- In hindsight, expected from the relation

$$m_t \sim y_L y_R |M_4 - M_1|$$

Benchmarks points MCHM$_5$ in Low Scale region (LHC & HL-LHC)

Pheno analysis: Feynrules->UFOfiles->Madgraph->(ready for “fast simu” =Delphes, or full simu)

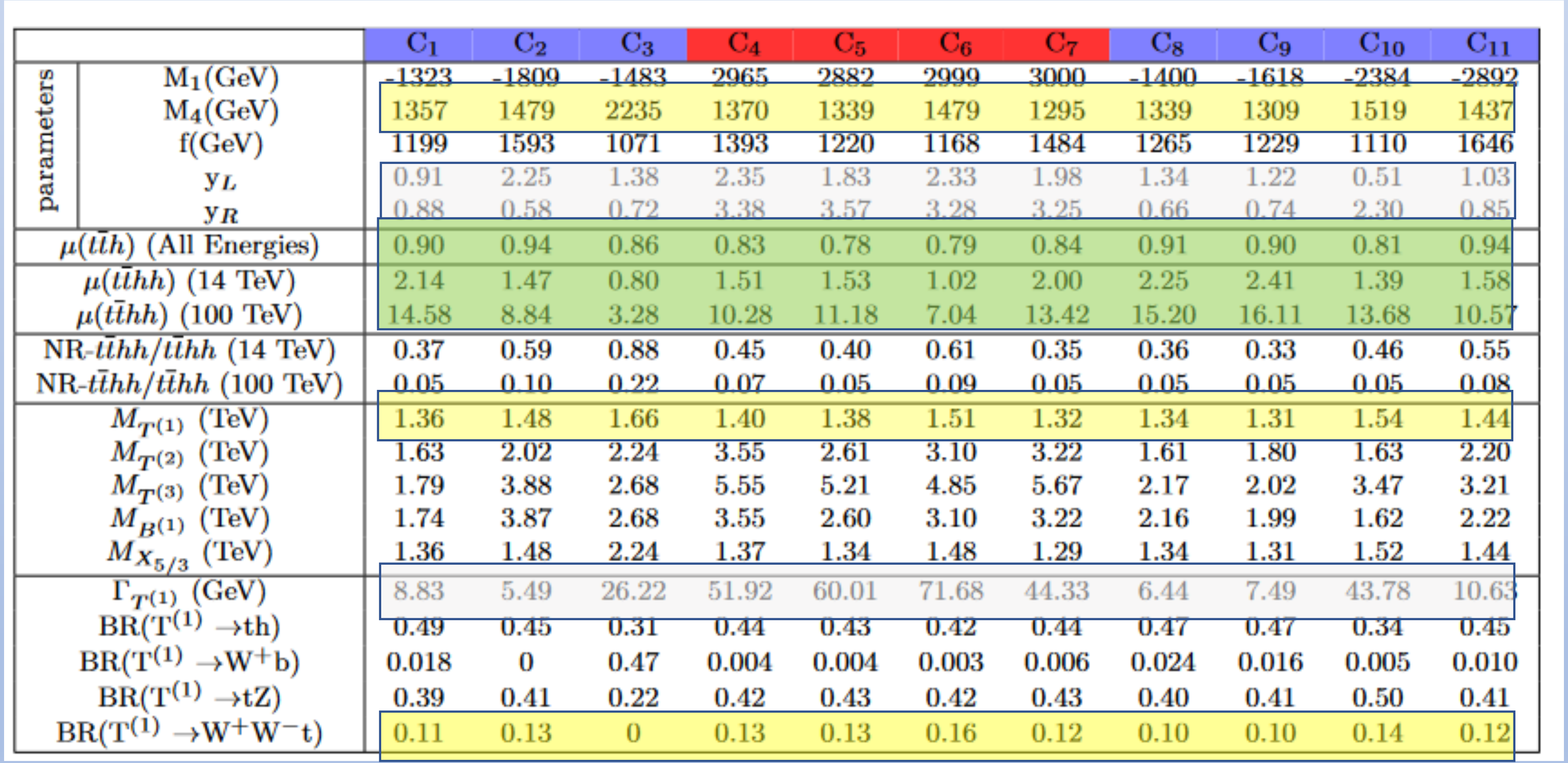

		C$_1$	C$_2$	C$_3$	C$_4$	C$_5$	C$_6$	C$_7$	C$_8$	C$_9$	C$_{10}$	C$_{11}$
parameters	M$_1$(GeV)	-1323	-1809	-1483	2965	2882	2999	3000	-1400	-1618	-2384	-2892
	M$_4$(GeV)	1357	1479	2235	1370	1339	1479	1295	1339	1309	1519	1437
	f(GeV)	1199	1593	1071	1393	1220	1168	1484	1265	1229	1110	1646
	y_L	0.91	2.25	1.38	2.35	1.83	2.33	1.98	1.34	1.22	0.51	1.03
	y_R	0.88	0.58	0.72	3.38	3.57	3.28	3.25	0.66	0.74	2.30	0.85
$\mu(t\bar{t}h)$ (All Energies)		0.90	0.94	0.86	0.83	0.78	0.79	0.84	0.91	0.90	0.81	0.94
$\mu(t\bar{t}hh)$ (14 TeV)		2.14	1.47	0.80	1.51	1.53	1.02	2.00	2.25	2.41	1.39	1.58
$\mu(t\bar{t}hh)$ (100 TeV)		14.58	8.84	3.28	10.28	11.18	7.04	13.42	15.20	16.11	13.68	10.57
NR-$t\bar{t}hh/t\bar{t}hh$ (14 TeV)		0.37	0.59	0.88	0.45	0.40	0.61	0.35	0.36	0.33	0.46	0.55
NR-$t\bar{t}hh/t\bar{t}hh$ (100 TeV)		0.05	0.10	0.22	0.07	0.05	0.09	0.05	0.05	0.05	0.05	0.08
$M_{T^{(1)}}$ (TeV)		1.36	1.48	1.66	1.40	1.38	1.51	1.32	1.34	1.31	1.54	1.44
$M_{T^{(2)}}$ (TeV)		1.63	2.02	2.24	3.55	2.61	3.10	3.22	1.61	1.80	1.63	2.20
$M_{T^{(3)}}$ (TeV)		1.79	3.88	2.68	5.55	5.21	4.85	5.67	2.17	2.02	3.47	3.21
$M_{B^{(1)}}$ (TeV)		1.74	3.87	2.68	3.55	2.60	3.10	3.22	2.16	1.99	1.62	2.22
$M_{X_{5/3}}$ (TeV)		1.36	1.48	2.24	1.37	1.34	1.48	1.29	1.34	1.31	1.52	1.44
$\Gamma_{T^{(1)}}$ (GeV)		8.83	5.49	26.22	51.92	60.01	71.68	44.33	6.44	7.49	43.78	10.63
BR(T$^{(1)}$ →th)		0.49	0.45	0.31	0.44	0.43	0.42	0.44	0.47	0.47	0.34	0.45
BR(T$^{(1)}$ →W$^+$b)		0.018	0	0.47	0.004	0.004	0.003	0.006	0.024	0.016	0.005	0.010
BR(T$^{(1)}$ →tZ)		0.39	0.41	0.22	0.42	0.43	0.42	0.43	0.40	0.41	0.50	0.41
BR(T$^{(1)}$ →W$^+$W$^-$t)		0.11	0.13	0	0.13	0.13	0.16	0.12	0.10	0.10	0.14	0.12

Red and blue: 1st and 2nd quadrants of M$_1$-M$_4$ space

Benchmarks points MCHM_{14} , low scale region (LHC HL-LHC)

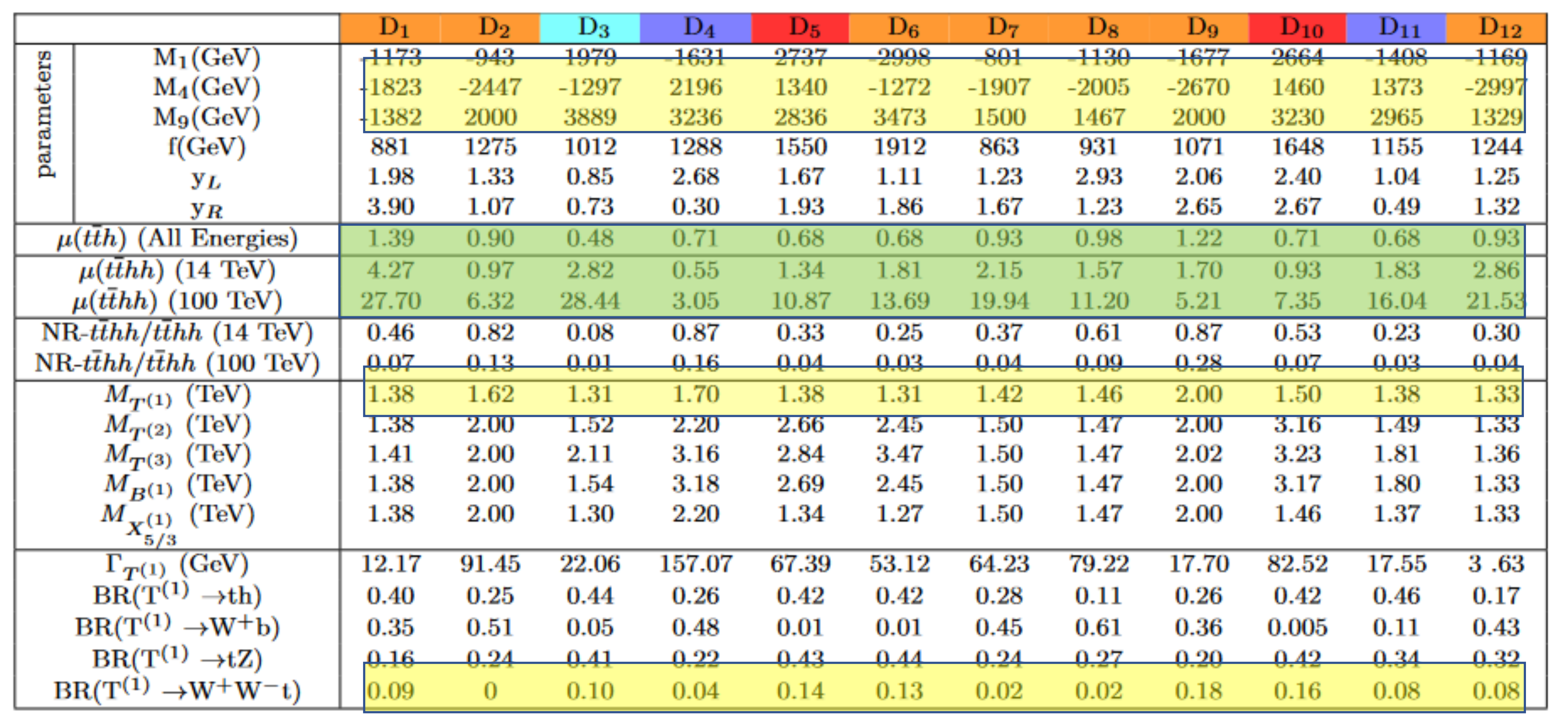

		D_1	D_2	D_3	D_4	D_5	D_6	D_7	D_8	D_9	D_{10}	D_{11}	D_{12}
parameters	M_1(GeV)	-1173	-943	1979	-1631	2737	-2998	-801	-1130	-1677	2664	-1408	-1169
	M_4(GeV)	-1823	-2447	-1297	2196	1340	-1272	-1907	-2005	-2670	1460	1373	-2997
	M_9(GeV)	-1382	2000	3889	3236	2836	3473	1500	1467	2000	3230	2965	1329
	f(GeV)	881	1275	1012	1288	1550	1912	863	931	1071	1648	1155	1244
	y_L	1.98	1.33	0.85	2.68	1.67	1.11	1.23	2.93	2.06	2.40	1.04	1.25
	y_R	3.90	1.07	0.73	0.30	1.93	1.86	1.67	1.23	2.65	2.67	0.49	1.32
$\mu(t\bar{t}h)$ (All Energies)		1.39	0.90	0.48	0.71	0.68	0.68	0.93	0.98	1.22	0.71	0.68	0.93
$\mu(t\bar{t}hh)$ (14 TeV)		4.27	0.97	2.82	0.55	1.34	1.81	2.15	1.57	1.70	0.93	1.83	2.86
$\mu(t\bar{t}hh)$ (100 TeV)		27.70	6.32	28.44	3.05	10.87	13.69	19.94	11.20	5.21	7.35	16.04	21.53
NR-$t\bar{t}hh/t\bar{t}hh$ (14 TeV)		0.46	0.82	0.08	0.87	0.33	0.25	0.37	0.61	0.87	0.53	0.23	0.30
NR-$t\bar{t}hh/t\bar{t}hh$ (100 TeV)		0.07	0.13	0.01	0.16	0.04	0.03	0.04	0.09	0.28	0.07	0.03	0.04
$M_{T^{(1)}}$ (TeV)		1.38	1.62	1.31	1.70	1.38	1.31	1.42	1.46	2.00	1.50	1.38	1.33
$M_{T^{(2)}}$ (TeV)		1.38	2.00	1.52	2.20	2.66	2.45	1.50	1.47	2.00	3.16	1.49	1.33
$M_{T^{(3)}}$ (TeV)		1.41	2.00	2.11	3.16	2.84	3.47	1.50	1.47	2.02	3.23	1.81	1.36
$M_{B^{(1)}}$ (TeV)		1.38	2.00	1.54	3.18	2.69	2.45	1.50	1.47	2.00	3.17	1.80	1.33
$M_{X_{5/3}^{(1)}}$ (TeV)		1.38	2.00	1.30	2.20	1.34	1.27	1.50	1.47	2.00	1.46	1.37	1.33
$\Gamma_{T^{(1)}}$ (GeV)		12.17	91.45	22.06	157.07	67.39	53.12	64.23	79.22	17.70	82.52	17.55	3 .63
BR($T^{(1)} \to th$)		0.40	0.25	0.44	0.26	0.42	0.42	0.28	0.11	0.26	0.42	0.46	0.17
BR($T^{(1)} \to W^+b$)		0.35	0.51	0.05	0.48	0.01	0.01	0.45	0.61	0.36	0.005	0.11	0.43
BR($T^{(1)} \to tZ$)		0.16	0.24	0.41	0.22	0.43	0.44	0.24	0.27	0.20	0.42	0.34	0.32
BR($T^{(1)} \to W^+W^-t$)		0.09	0	0.10	0.04	0.14	0.13	0.02	0.02	0.18	0.16	0.08	0.08

Red and orange: 1^{st} and 3^{nd} quadrants of M_1-M_4 space

Blue and cyan: 2^{st} and 4^{nd} quadrants

Three body decays in MCHM5

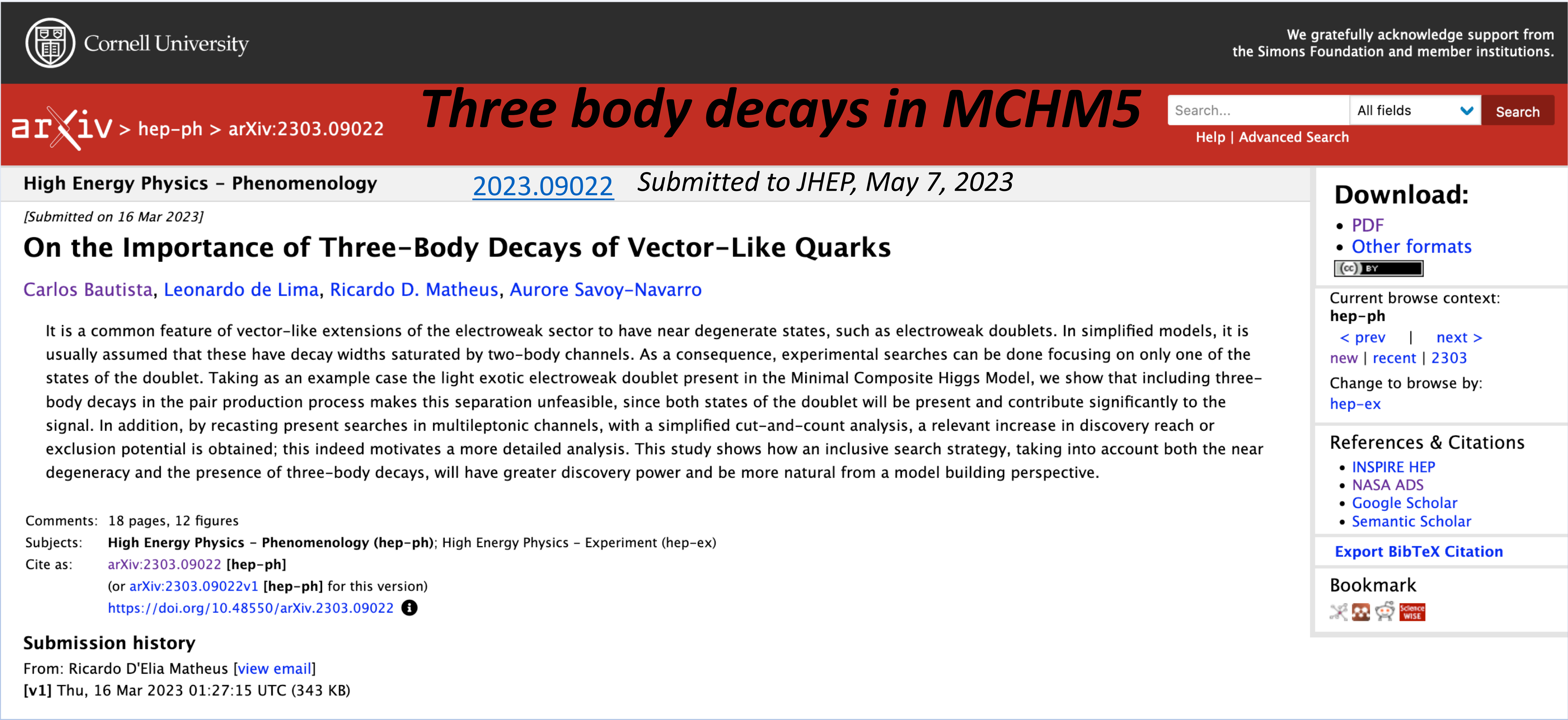

High Energy Physics – Phenomenology

2023.09022 *Submitted to JHEP, May 7, 2023*

[Submitted on 16 Mar 2023]

On the Importance of Three-Body Decays of Vector-Like Quarks

Carlos Bautista, Leonardo de Lima, Ricardo D. Matheus, Aurore Savoy-Navarro

It is a common feature of vector-like extensions of the electroweak sector to have near degenerate states, such as electroweak doublets. In simplified models, it is usually assumed that these have decay widths saturated by two-body channels. As a consequence, experimental searches can be done focusing on only one of the states of the doublet. Taking as an example case the light exotic electroweak doublet present in the Minimal Composite Higgs Model, we show that including three-body decays in the pair production process makes this separation unfeasible, since both states of the doublet will be present and contribute significantly to the signal. In addition, by recasting present searches in multileptonic channels, with a simplified cut-and-count analysis, a relevant increase in discovery reach or exclusion potential is obtained; this indeed motivates a more detailed analysis. This study shows how an inclusive search strategy, taking into account both the near degeneracy and the presence of three-body decays, will have greater discovery power and be more natural from a model building perspective.

Comments:	18 pages, 12 figures
Subjects:	**High Energy Physics – Phenomenology (hep-ph)**; High Energy Physics – Experiment (hep-ex)
Cite as:	arXiv:2303.09022 **[hep-ph]**
	(or arXiv:2303.09022v1 **[hep-ph]** for this version)
	https://doi.org/10.48550/arXiv.2303.09022

Submission history

From: Ricardo D'Elia Matheus [view email]
[v1] Thu, 16 Mar 2023 01:27:15 UTC (343 KB)

Download:
- PDF
- Other formats

Current browse context:
hep-ph
< prev | next >
new | recent | 2303
Change to browse by:
hep-ex

References & Citations
- INSPIRE HEP
- NASA ADS
- Google Scholar
- Semantic Scholar

Export BibTeX Citation

Bookmark

=> Back to the VLF resonances from which all started ...

Experimental “model independent” VLQ searches

Usually assumed:

- Only one VLQ contributing to the chosen signal. Other BSM resonances are much heavier, absent or decay into different final states
- Separate searches carried out for T and $X_{5/3}$
- Decay width is saturated by a few 2-body decay modes of the VLQs.

$$X_{5/3} \to tW, \qquad T \to Wb, tZ, th$$

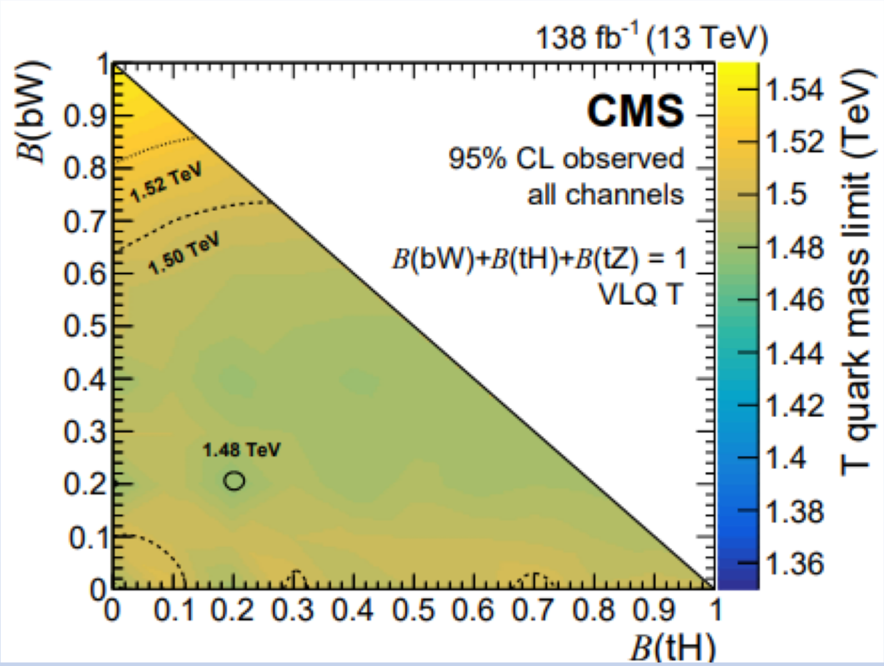

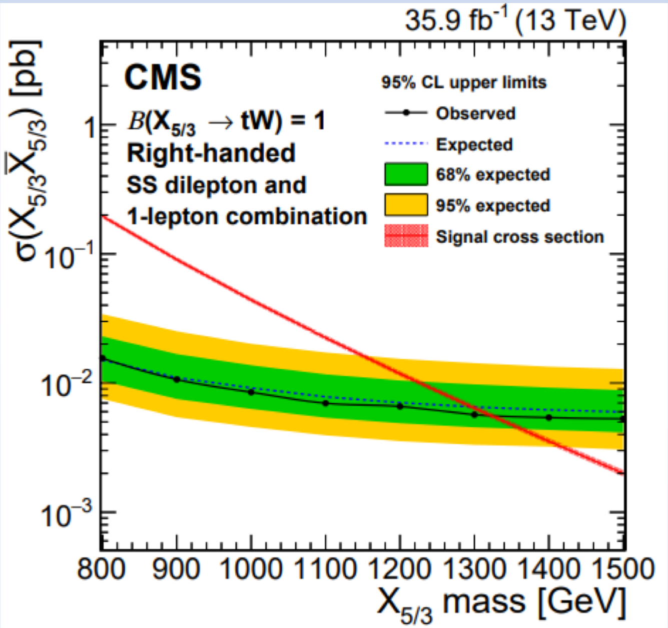

CMS Collab.. JHEP, vol. 03, p. 082, 2019.

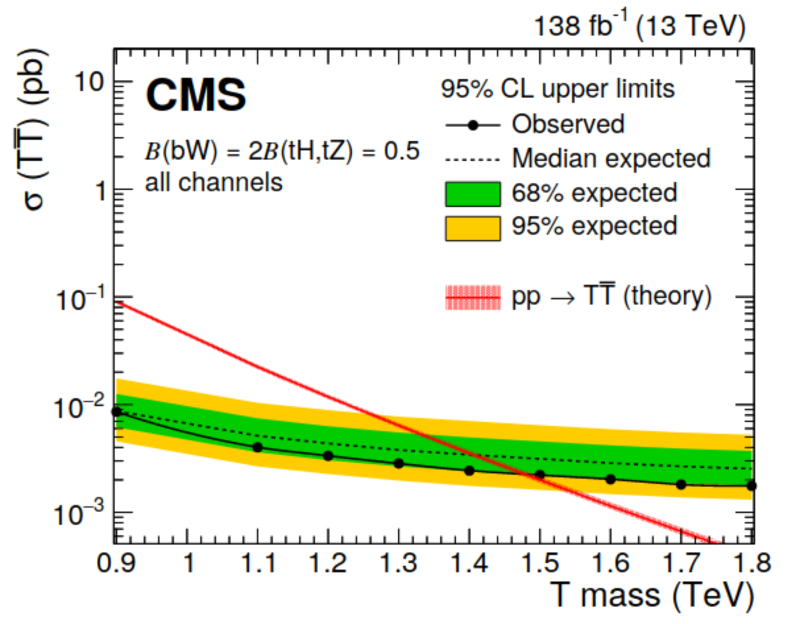

CMS Collab. CMS-B2G-20-011, CERN-EP-2022-175.

MCHM5: The lightest top partner can be singlet or 4plet like.

The physical states after diagonalization are:

$$T_L^{(1)} = U_{L,1} t_L + U_{L,2} T_L + U_{L,3} X_{2/3L} + U_{L,4} \tilde{T}_L$$

$$T_R^{(1)} = U_{R,1} t_R + U_{R,2} T_R + U_{R,3} X_{2/3R} + U_{R,4} \tilde{T}_R$$

With: L, R chiralities; $U_{L,R}$ =corresponding Unitary rotations to mass basis

To measure singlet & fourplet contributions, define:

$$\sin^2\theta = \frac{\eta_L^F + \eta_R^F}{2} \qquad \cos^2\theta = \frac{\eta_L^S + \eta_R^S}{2},$$

with

$$\eta^F_{L(R)} = U^2_{L(R),2} + U^2_{L(R),3}$$

$$\eta^S_{L(R)} = U^2_{L(R),1} + U^2_{L(R),4}$$

η^F η^S = respt the 4plet and singlet contributions for each L,R chirality

*Θ angle characterizes nature of $T^{(1)}$ **Θ** =0 (singlet) = $\pi/2$(4plet)*

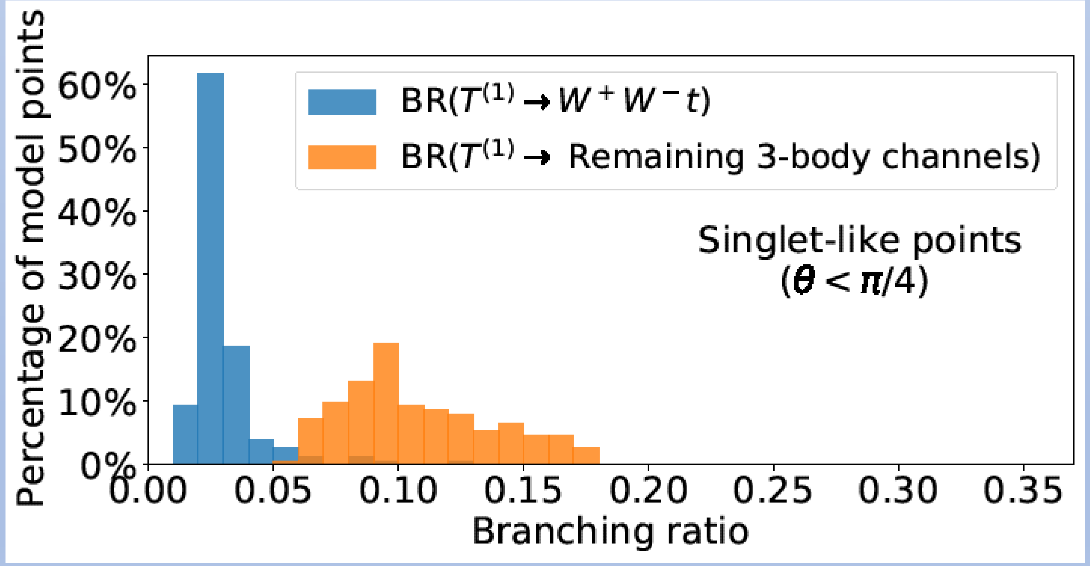

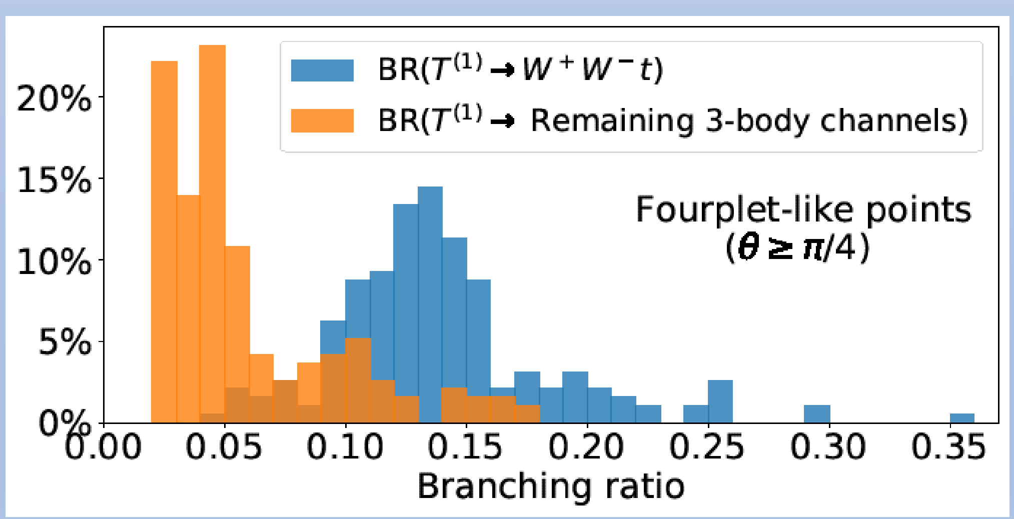

→ **For fourplet-like points, 3-body decay branching ratios are sizable**

Three body decays in MCHM$_5$ of lighest VLQ states

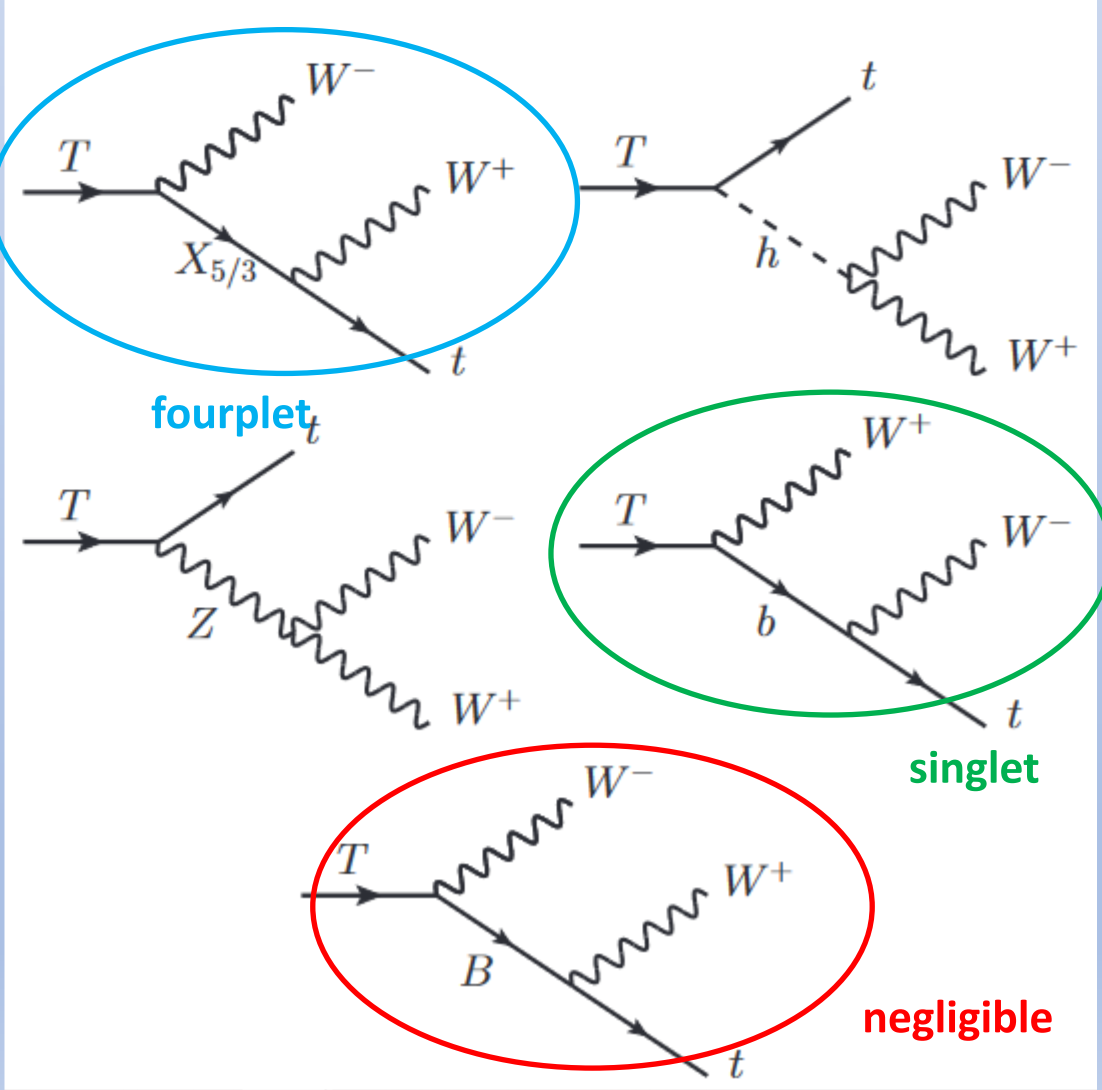

4plet-like T$^{(1)}$: bigger BR(T->3-body) with prevailing T $^{(1)}$ → W +W –t .
The singlet-like case is just the opposite.
=> MOTIVATES focus on 4-plet case.

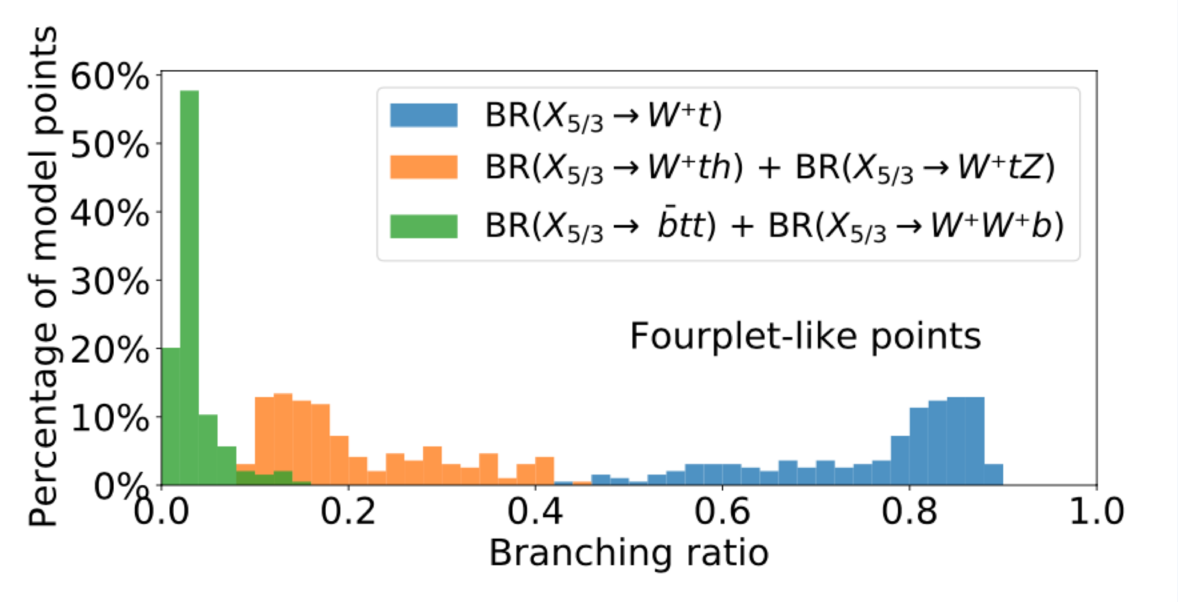

The 4plet-like scenario also more interesting for X$_{5/3}$
One of the lightest states and near degenerate with T$^{(1)}$
with splitting caused by EWK effects and smaller than mW .
=> only allowed 2-body decay is X$_{5/3}$ → W$^+$ t.

Effect on T partner pair production

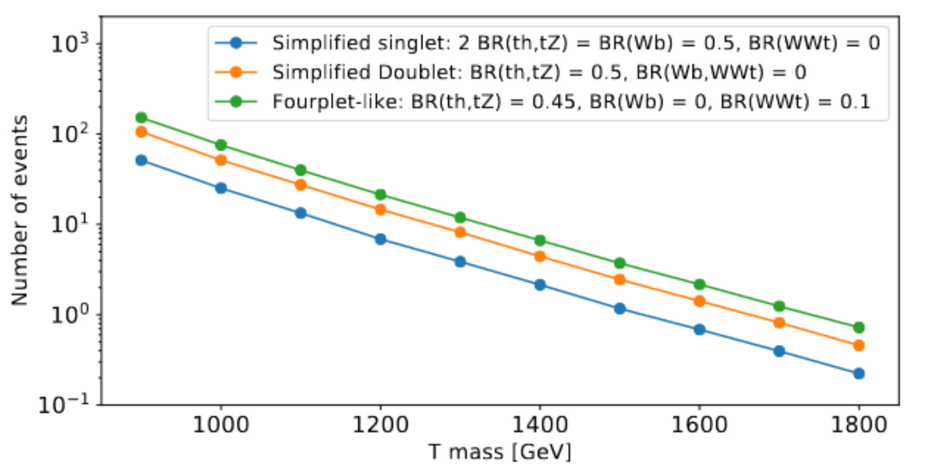

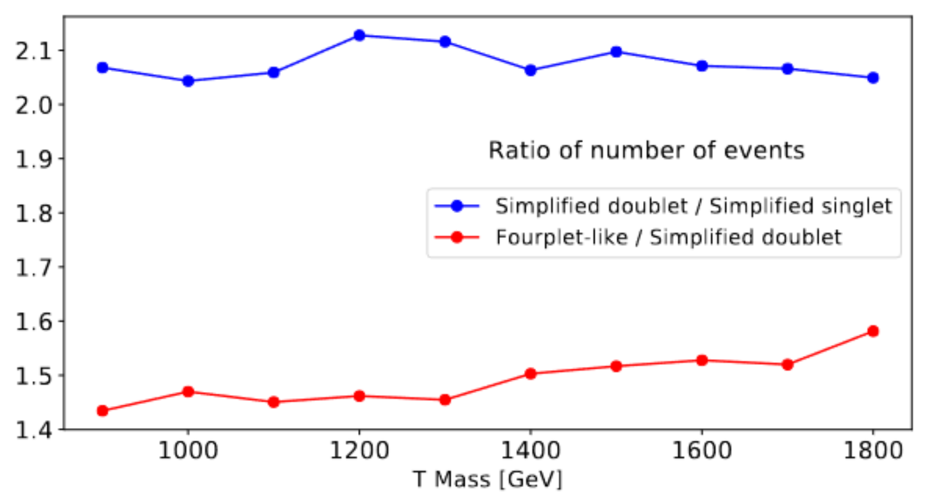

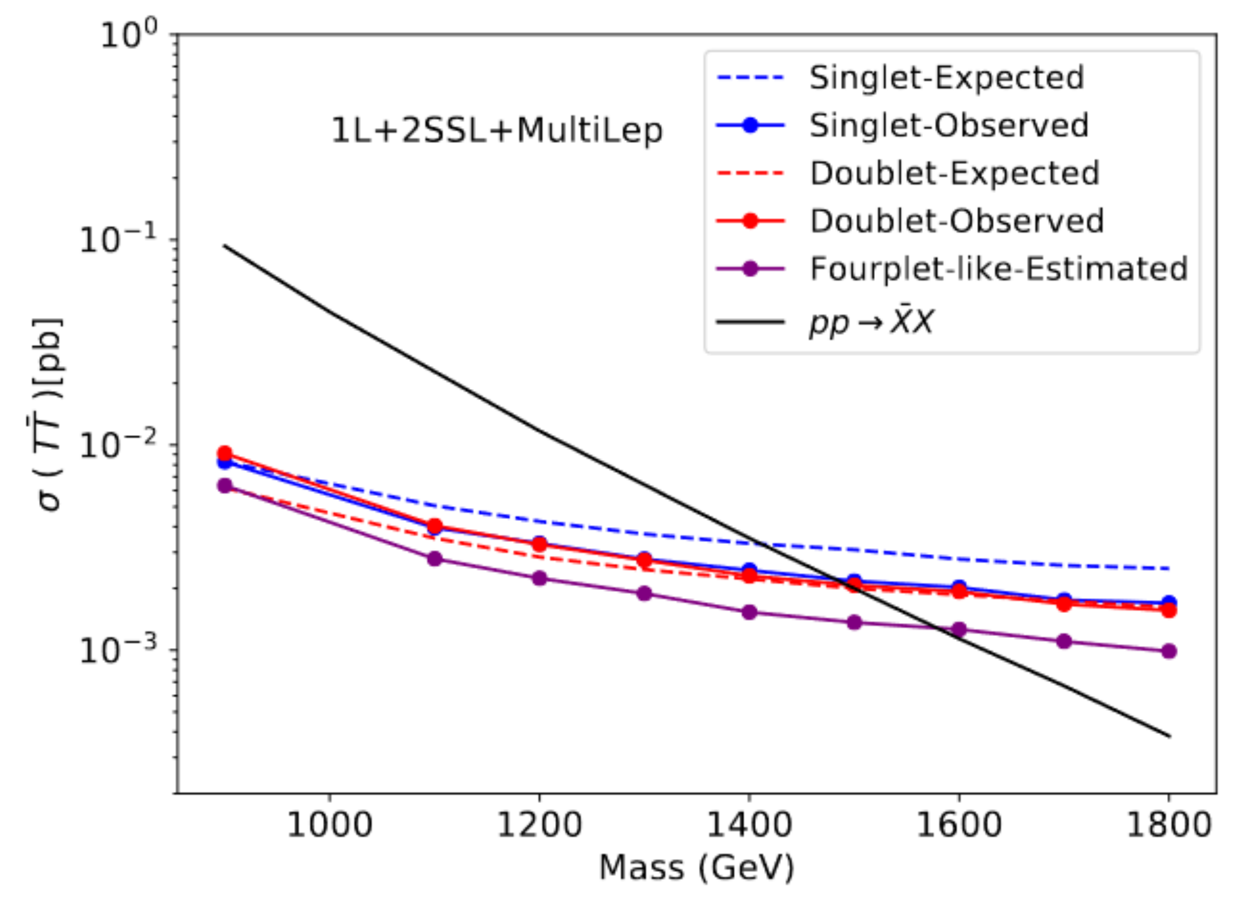

- A naive rescaling of existing searches shows an improved exclusion by roughly 100 GeV.
- This motivates analysis including the 3-body channels

Search for vector-like resonances in the presence of 3-body decay

- **MCHM5** with a 4plet-like $T^{(1)}$ = simplest scenario in a complete model providing 2 light VLQs
- **Key characteristic** of a model with a **4plet-like $T^{(1)}$= degeneracy in mass with $X_{5/3}$**

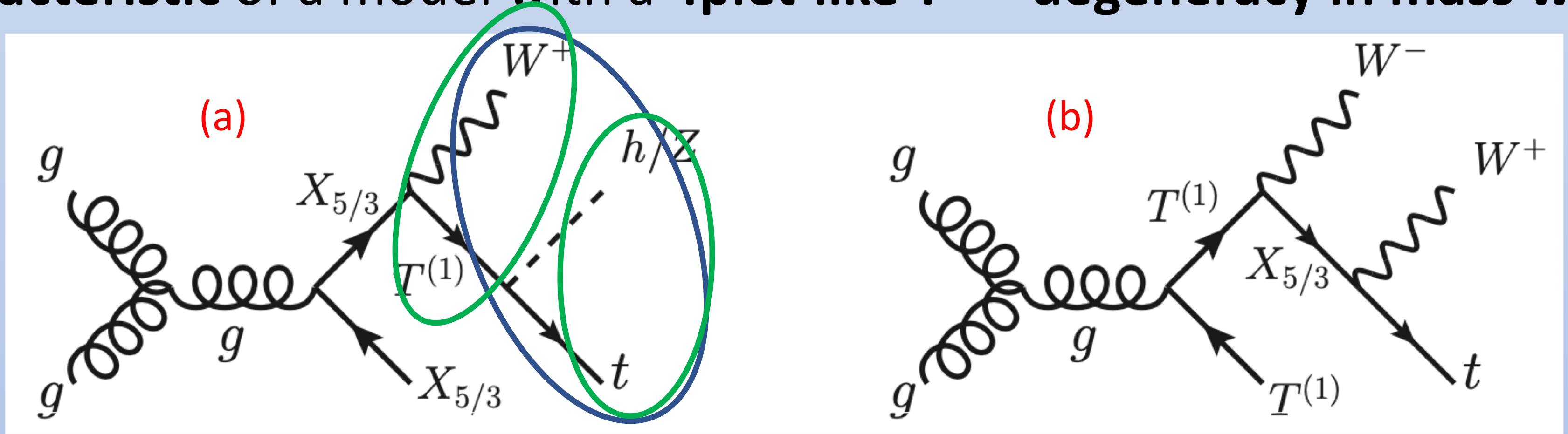

- Due to their **degenerate masses, $X_{5/3}$ and $T^{(1)}$** cannot be simultanously on-shell in a,b-diagrams
  - diagram (a) generates either production of an on-shell $X_{5/3}$, followed by its 3-body decay (blue ellipse)
  - or $X_{5/3}$ mediated production of on-shell $T^{(1)}$+W, followed by 2-body decay of $T^{(1)}$ -> tZ (2 green ellipses)
- Key point: *Same final states for these 2 situations: WtZ Wt*
- Analogous situation occurs in diagram (b), with the roles of $T^{(1)}$ and $X_{5/3}$ reversed.

Near degenerate states: off+on shell contributions

These two contributions can mix in kinematic variables

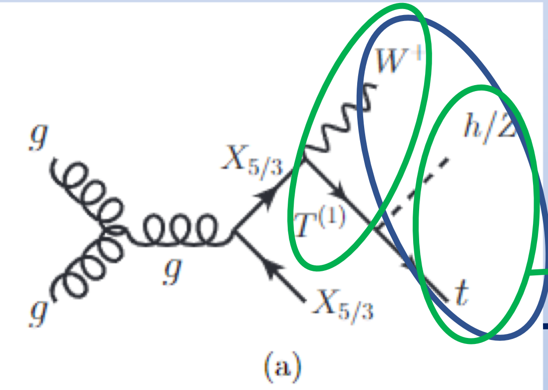

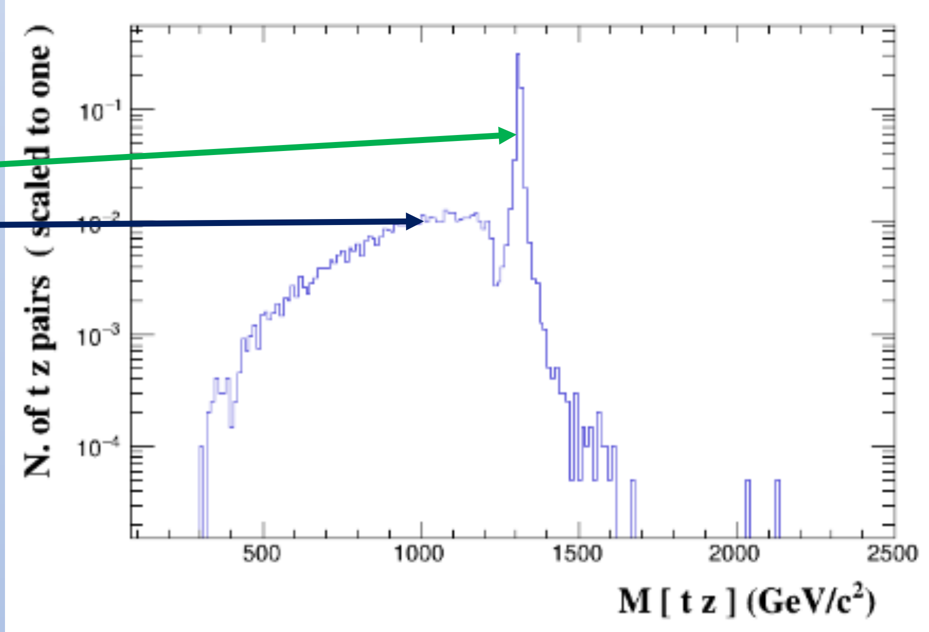

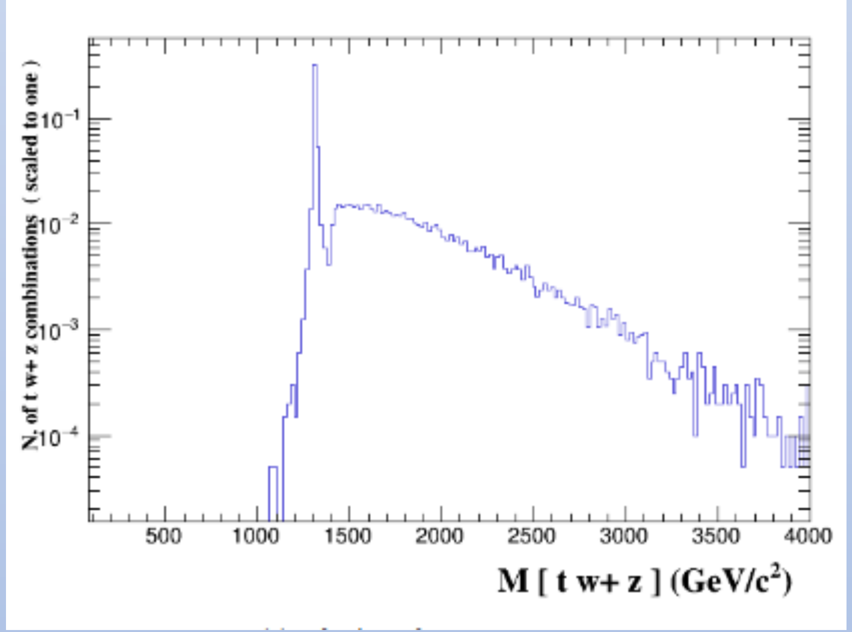

Invariant mass for (a) for
the benchmark point chosen
as show case

1) i) peak at 1.3 TeV generated by decays of on-shell $T^{(1)}$
   ii) the bump in the region M[t,Z] ~1.3 TeV generated by 3-body decays of on-shell $X_{5/3}$ (which force $T^{(1)}$ off-shell)
2) Same applies M[W +, t, Z], with a peak from on-shell $X_{5/3}$ sitting on top of a off-shell $X_{5/3}$ bump.

NB : this is general feature of mass degeneracy & presence of 3-body decays, in any model as long as the involved coupling constants are sizeable. In MCHM5 this is guaranteed because $T^{(1)}$ and $X_{5/3}$ are coming from the same multiplet .

=> Difficult to disentangle between $T^{(1)}$ and $X_{5/3}$ signals=> TURN IT as an ADVANTAGE with INCLUSIVE SEARCH

Inclusive search with contributions of pair production **of both** $\boldsymbol{T^{(1)}}$ & $\boldsymbol{X_{5/3}}$ to the same signals

$XX \to (Wth)Wt, XX \to (WtZ)Wt$, $\mathrm{TT} \to (WWt)th, TT \to (WWt)tZ.$

- With t → Wb and $\mathrm{h(Z)} \to$ b b, the signature is $4W4$b.
- Multileptonic search channels (2SSL + 3L)

Madgraph (LO) → Pythia → Delphes (HL-LHC card)

1. "Objects definition" (labelled as "no cuts" in Tables):
   Leptons: isolation variable (I) < 0.1,
   $p_T > 30$ GeV, $|\eta| < 3$
   Jets: reconstruction using AKT4
   $p_T > 30$ GeV, $|\eta| < 3$
2. $\mathrm{N_b} \geq 3$: As signal contains 4 b and most background don't.
3. $H_T^{lep} > 1.6$ TeV: High transverse momentum in signal from heavy particles decay.
4. Etmiss > 100 GeV or > 150 GeV: to ensure we are excluding rarer background contributions.

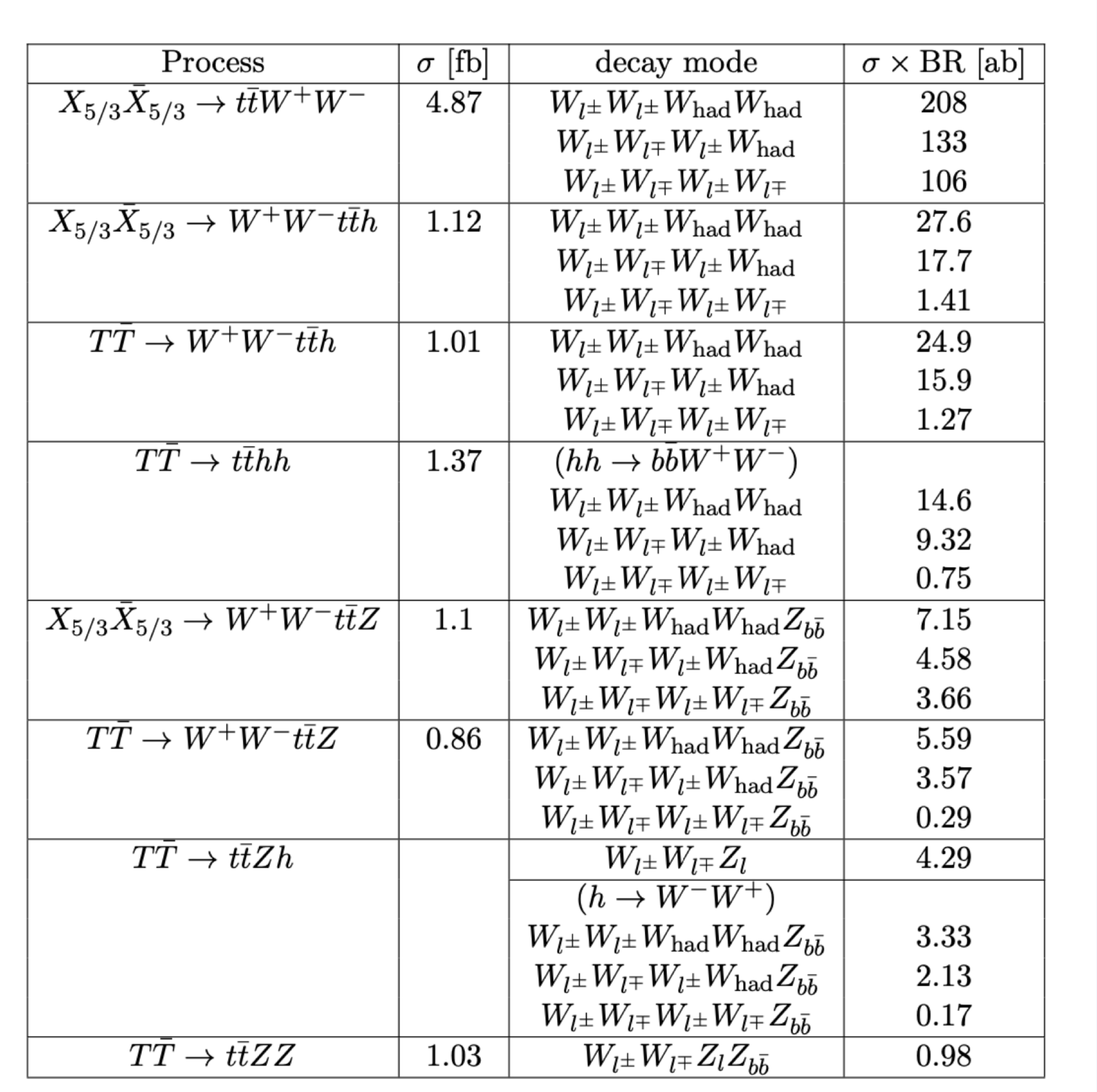

Process	σ [fb]	decay mode	$\sigma \times$ BR [ab]
$X_{5/3}\bar{X}_{5/3} \to t\bar{t}W^+W^-$	4.87	$W_{l\pm}W_{l\pm}W_{\text{had}}W_{\text{had}}$	208
		$W_{l\pm}W_{l\mp}W_{l\pm}W_{\text{had}}$	133
		$W_{l\pm}W_{l\mp}W_{l\pm}W_{l\mp}$	106
$X_{5/3}\bar{X}_{5/3} \to W^+W^-t\bar{t}h$	1.12	$W_{l\pm}W_{l\pm}W_{\text{had}}W_{\text{had}}$	27.6
		$W_{l\pm}W_{l\mp}W_{l\pm}W_{\text{had}}$	17.7
		$W_{l\pm}W_{l\mp}W_{l\pm}W_{l\mp}$	1.41
$T\bar{T} \to W^+W^-t\bar{t}h$	1.01	$W_{l\pm}W_{l\pm}W_{\text{had}}W_{\text{had}}$	24.9
		$W_{l\pm}W_{l\mp}W_{l\pm}W_{\text{had}}$	15.9
		$W_{l\pm}W_{l\mp}W_{l\pm}W_{l\mp}$	1.27
$T\bar{T} \to t\bar{t}hh$	1.37	$(hh \to b\bar{b}W^+W^-)$	
		$W_{l\pm}W_{l\pm}W_{\text{had}}W_{\text{had}}$	14.6
		$W_{l\pm}W_{l\mp}W_{l\pm}W_{\text{had}}$	9.32
		$W_{l\pm}W_{l\mp}W_{l\pm}W_{l\mp}$	0.75
$X_{5/3}\bar{X}_{5/3} \to W^+W^-t\bar{t}Z$	1.1	$W_{l\pm}W_{l\pm}W_{\text{had}}W_{\text{had}}Z_{b\bar{b}}$	7.15
		$W_{l\pm}W_{l\mp}W_{l\pm}W_{\text{had}}Z_{b\bar{b}}$	4.58
		$W_{l\pm}W_{l\mp}W_{l\pm}W_{l\mp}Z_{b\bar{b}}$	3.66
$T\bar{T} \to W^+W^-t\bar{t}Z$	0.86	$W_{l\pm}W_{l\pm}W_{\text{had}}W_{\text{had}}Z_{b\bar{b}}$	5.59
		$W_{l\pm}W_{l\mp}W_{l\pm}W_{\text{had}}Z_{b\bar{b}}$	3.57
		$W_{l\pm}W_{l\mp}W_{l\pm}W_{l\mp}Z_{b\bar{b}}$	0.29
$T\bar{T} \to t\bar{t}Zh$		$W_{l\pm}W_{l\mp}Z_l$	4.29
		$(h \to W^-W^+)$	
		$W_{l\pm}W_{l\pm}W_{\text{had}}W_{\text{had}}Z_{b\bar{b}}$	3.33
		$W_{l\pm}W_{l\mp}W_{l\pm}W_{\text{had}}Z_{b\bar{b}}$	2.13
		$W_{l\pm}W_{l\mp}W_{l\pm}W_{l\mp}Z_{b\bar{b}}$	0.17
$T\bar{T} \to t\bar{t}ZZ$	1.03	$W_{l\pm}W_{l\mp}Z_lZ_{b\bar{b}}$	0.98

Signal processes for C9 in 2SSL search at LO, √s = 14 TeV
T = $\mathrm{T^1}$, $\mathrm{T^2}$ or $\mathrm{T^3}$

RESULTS

Most important backgrounds wrt 2SSL, 3L or 2SSL+3L

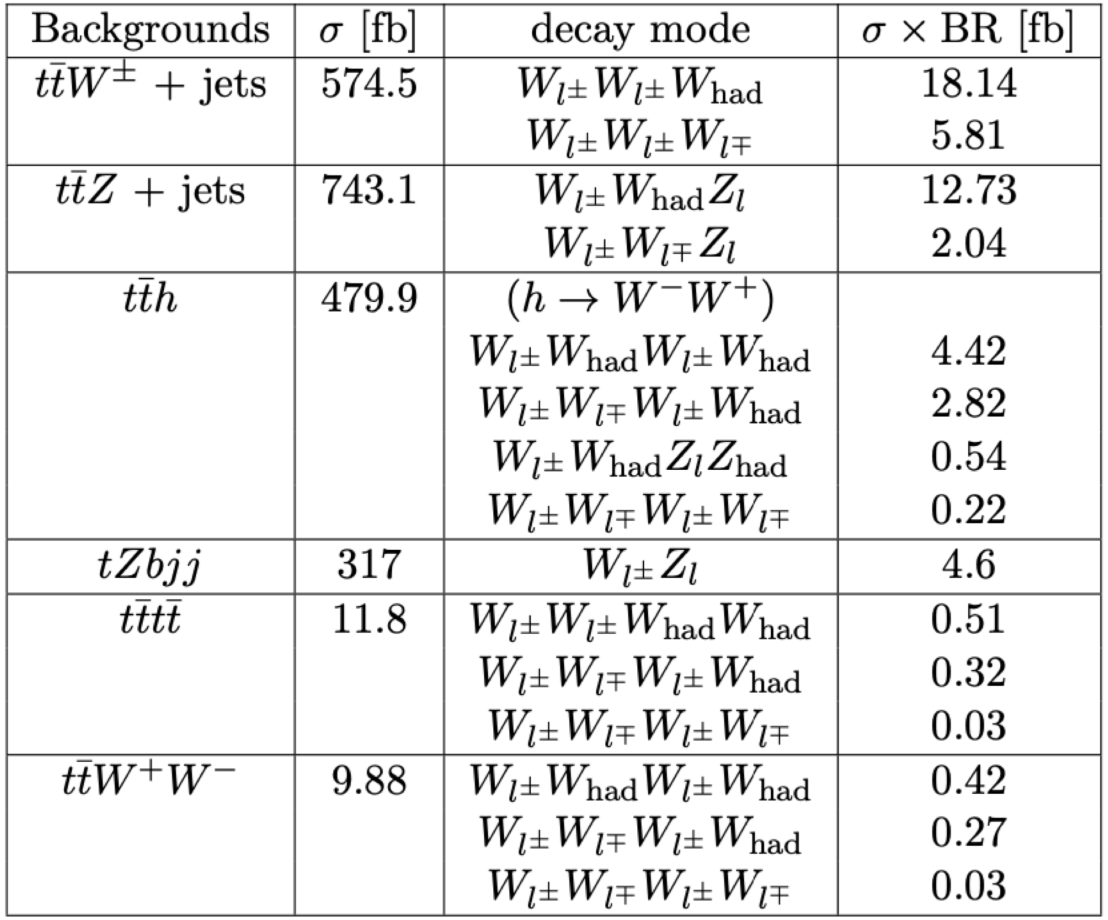

Backgrounds	σ [fb]	decay mode	$\sigma \times$ BR [fb]
$t\bar{t}W^{\pm}$ + jets	574.5	$W_{l^\pm} W_{l^\pm} W_{\text{had}}$	18.14
		$W_{l^\pm} W_{l^\pm} W_{l^\mp}$	5.81
$t\bar{t}Z$ + jets	743.1	$W_{l^\pm} W_{\text{had}} Z_l$	12.73
		$W_{l^\pm} W_{l^\mp} Z_l$	2.04
$t\bar{t}h$	479.9	$(h \to W^- W^+)$	
		$W_{l^\pm} W_{\text{had}} W_{l^\pm} W_{\text{had}}$	4.42
		$W_{l^\pm} W_{l^\mp} W_{l^\pm} W_{\text{had}}$	2.82
		$W_{l^\pm} W_{\text{had}} Z_l Z_{\text{had}}$	0.54
		$W_{l^\pm} W_{l^\mp} W_{l^\pm} W_{l^\mp}$	0.22
$tZbjj$	317	$W_{l^\pm} Z_l$	4.6
$t\bar{t}t\bar{t}$	11.8	$W_{l^\pm} W_{l^\pm} W_{\text{had}} W_{\text{had}}$	0.51
		$W_{l^\pm} W_{l^\mp} W_{l^\pm} W_{\text{had}}$	0.32
		$W_{l^\pm} W_{l^\mp} W_{l^\pm} W_{l^\mp}$	0.03
$t\bar{t}W^+W^-$	9.88	$W_{l^\pm} W_{\text{had}} W_{l^\pm} W_{\text{had}}$	0.42
		$W_{l^\pm} W_{l^\mp} W_{l^\pm} W_{\text{had}}$	0.27
		$W_{l^\pm} W_{l^\mp} W_{l^\pm} W_{l^\mp}$	0.03

Nb of events passing the cuts in 2SSL+3L search channels

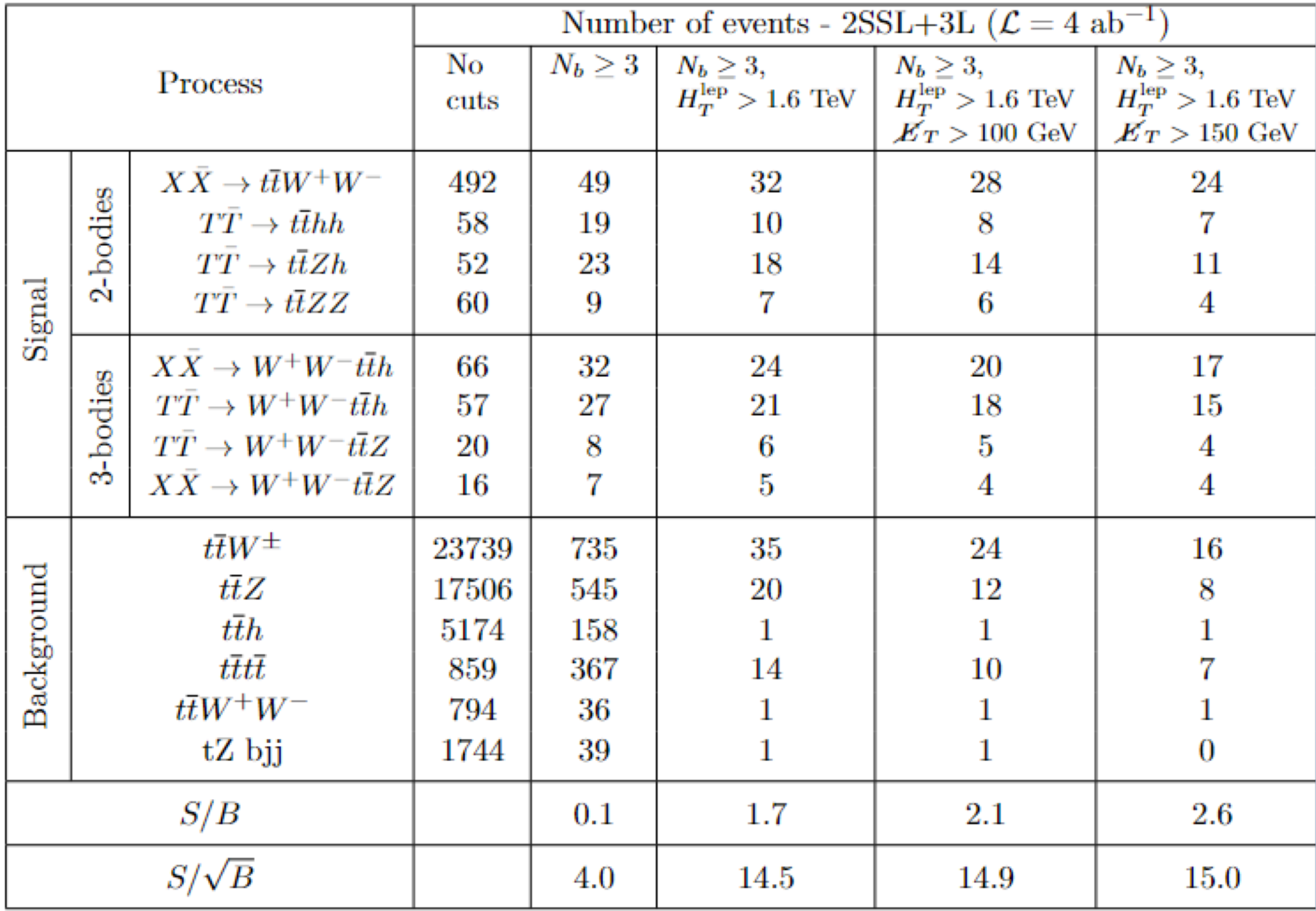

		Process	Number of events - 2SSL+3L ($\mathcal{L} = 4$ ab^{-1})				
			No cuts	$N_b \geq 3$	$N_b \geq 3$, $H_T^{\text{lep}} > 1.6$ TeV	$N_b \geq 3$, $H_T^{\text{lep}} > 1.6$ TeV $\not{E}_T > 100$ GeV	$N_b \geq 3$, $H_T^{\text{lep}} > 1.6$ TeV $\not{E}_T > 150$ GeV
Signal	2-bodies	$X\bar{X} \to t\bar{t}W^+W^-$	492	49	32	28	24
		$T\bar{T} \to t\bar{t}hh$	58	19	10	8	7
		$T\bar{T} \to t\bar{t}Zh$	52	23	18	14	11
		$T\bar{T} \to t\bar{t}ZZ$	60	9	7	6	4
	3-bodies	$X\bar{X} \to W^+W^-t\bar{t}h$	66	32	24	20	17
		$T\bar{T} \to W^+W^-t\bar{t}h$	57	27	21	18	15
		$T\bar{T} \to W^+W^-t\bar{t}Z$	20	8	6	5	4
		$X\bar{X} \to W^+W^-t\bar{t}Z$	16	7	5	4	4
Background		$t\bar{t}W^{\pm}$	23739	735	35	24	16
		$t\bar{t}Z$	17506	545	20	12	8
		$t\bar{t}h$	5174	158	1	1	1
		$t\bar{t}t\bar{t}$	859	367	14	10	7
		$t\bar{t}W^+W^-$	794	36	1	1	1
		tZ bjj	1744	39	1	1	0
		S/B		0.1	1.7	2.1	2.6
		$S/\sqrt{B}$		4.0	14.5	14.9	15.0

NB: In the case of 3-body decays the cross sections are around four times bigger than expected: direct consequence of the off-shell contributions

Concluding remarks and perspectives (for pheno part)

Probing the top Higgs sector with CHM

- Focus on tth & tthh production processes in the context of CHM
- Probed by precision measurements of couplings + resonance searches

$$\boxed{\sigma_{\mathrm{MCHM}}(t\bar{t}h) = \left(\frac{y_t}{y_t^{\mathrm{SM}}}\right)^2 \sigma_{\mathrm{SM}}(t\bar{t}h)}$$

tthh:Sum of Resonant + Non Resonant contributions controlled by:

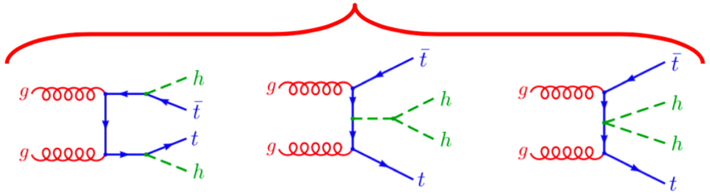

Yukawa vertex Trilinear Self Coupling “Double Higgs” Yukawa vertex

Non Resonant (NR) production can dominate if resonances are heavy

Pheno study with simu (including DELPHES) within the overall MCHM5&14 param scale => stress important features of tth/tthh

Study of couplings & link to EFT (not discussed here)

On the importance of the 3-body decay of VLQ’s

- **Vector-like top partners: ubiquitous in models attempting to address the naturalness puzzle of SM**
- With MCHM_5 as a concrete example of such an extension, we showed:
  - VLQ’s can have sizeable 3-body decays, and
  - taking these decays into account can improve significantly the exclusion limits obtained by previous analyses.
- NOTE: Even if done within MCHM5, the features are generic in any model containing a vector-like doublet.
- **Most experimental studies consider a SM-like doublet (top and bottom partner), with a two-body saturated width.**
- **However, on the contrary, a doublet naturally leads to near degenerate states and sizeable three-body decays.**
- Thus, **simplified models built on this assumption do not capture model independent physics, but instead impose constraints on their possible UV completions, needed to suppress the three-body channel.**
- Furthermore, the narrow spectrum leads to large contributions to the production cross section in the three-body decay channels, coming from one of the states being slightly off- shell.
- The effect can make the cross-section as large as 4 times the naive estimate from cross-section times branching ratio for narrow states
- This makes it difficult to search for one of these states in isolation, hence an **inclusive search can be more profitable.**

From theory to experiment:
Search for and study of the ttHH production process at LHC and beyond

Search for tt(SL)HH(4b) non resonant production at HL-LHC, WP Snowmass 2022

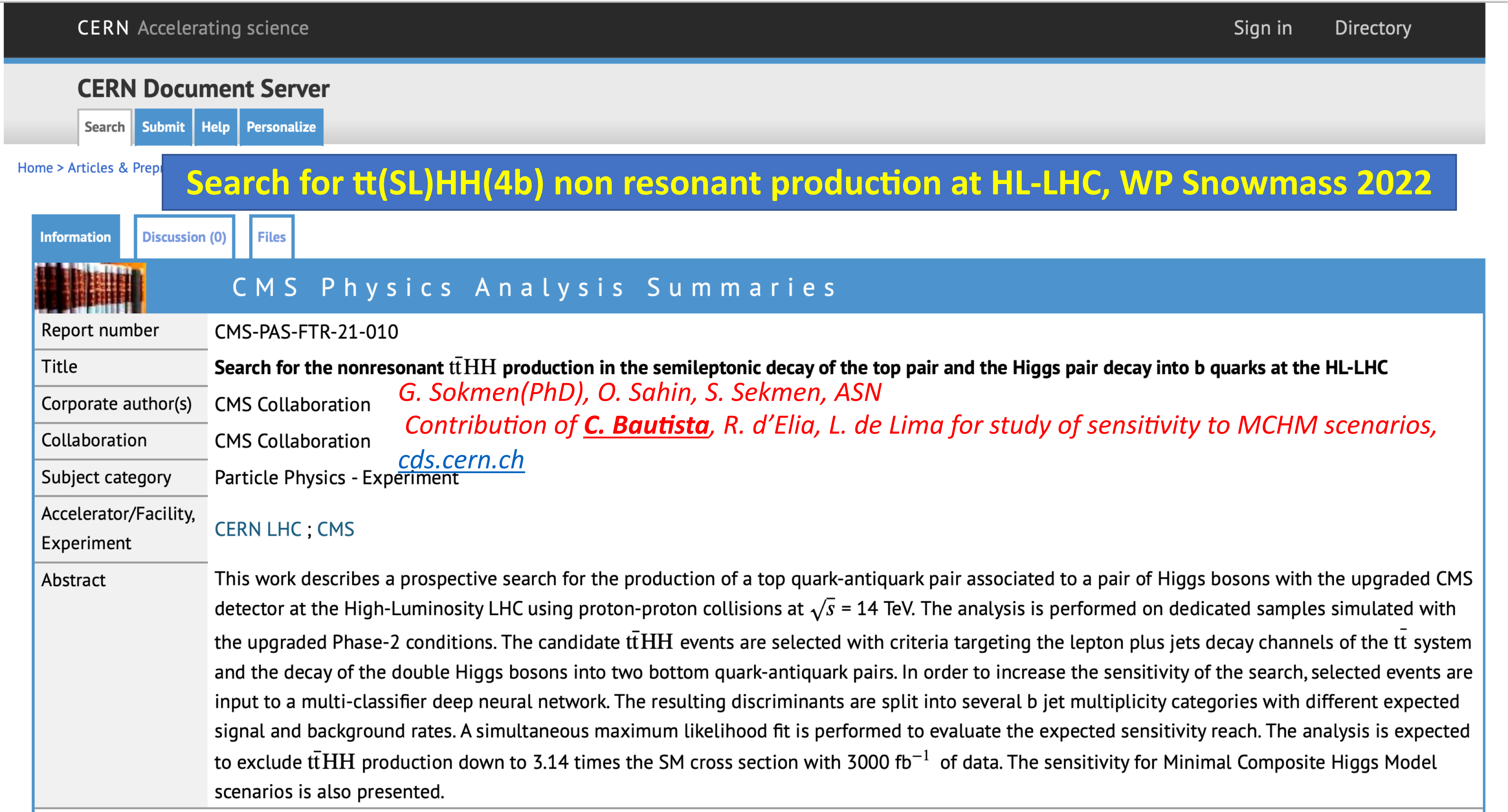

Report number	CMS-PAS-FTR-21-010
Title	**Search for the nonresonant $t\bar{t}HH$ production in the semileptonic decay of the top pair and the Higgs pair decay into b quarks at the HL-LHC**
Corporate author(s)	CMS Collaboration
Collaboration	CMS Collaboration
Subject category	Particle Physics - Experiment
Accelerator/Facility, Experiment	CERN LHC ; CMS
Abstract	This work describes a prospective search for the production of a top quark-antiquark pair associated to a pair of Higgs bosons with the upgraded CMS detector at the High-Luminosity LHC using proton-proton collisions at $\sqrt{s}$ = 14 TeV. The analysis is performed on dedicated samples simulated with the upgraded Phase-2 conditions. The candidate $t\bar{t}HH$ events are selected with criteria targeting the lepton plus jets decay channels of the $t\bar{t}$ system and the decay of the double Higgs bosons into two bottom quark-antiquark pairs. In order to increase the sensitivity of the search, selected events are input to a multi-classifier deep neural network. The resulting discriminants are split into several b jet multiplicity categories with different expected signal and background rates. A simultaneous maximum likelihood fit is performed to evaluate the expected sensitivity reach. The analysis is expected to exclude $t\bar{t}HH$ production down to 3.14 times the SM cross section with 3000 fb^{-1} of data. The sensitivity for Minimal Composite Higgs Model scenarios is also presented.

G. Sokmen(PhD), O. Sahin, S. Sekmen, ASN

*Contribution of **C. Bautista**, R. d'Elia, L. de Lima for study of sensitivity to MCHM scenarios,*

cds.cern.ch

Search for tt(SL)HH(4b) non resonant production at HL-LHC

It is a **dedicated analysis** performed at 14 TeV with 3000 fb^{-1} with DELPHES based simulation and searching for the tt(SL)HH4b signature.
A dedicated BSM study is included in this study: 1st time!

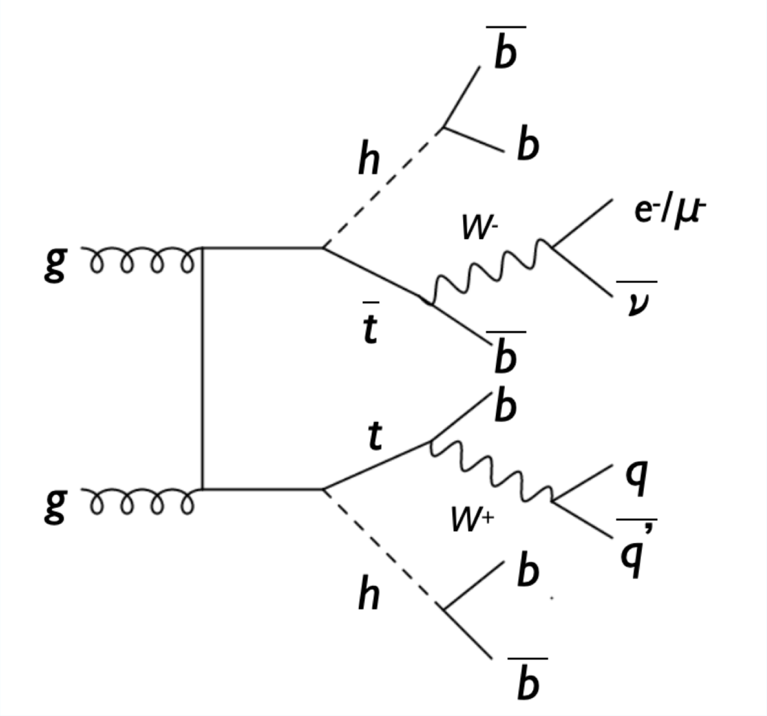

- ✓ Starts from the pioneering ttHH analysis framework performed with 2017 CMS data (L.F. Do Prado's PhD thesis, unpublished),
- ✓ Follows the progress of the ongoing analysis with the full Run 2 data, actively ongoing at CMS; several of the new developments are introduced **within the Delphes HL-LHC framework** to perform this search .

Br(Tot) =11.4%

Analysis strategy: outline

- Object and event selections applied on simulated signal & background samples.
- Events passing the selection are used for training DNNs for signal extraction. Background yields are predicted directly from simulated MC samples.
- The resulting final DNN discriminants are used for
  - obtaining upper limits on the expected signal strength, taking into account various systematic uncertainties reflecting the Phase-2 conditions.
- The same analysis methodology is used for the SM ttHH and MCHM ttHH cases.

Analysis strategy: object and event selection

1) Selection applied to simulated objects:

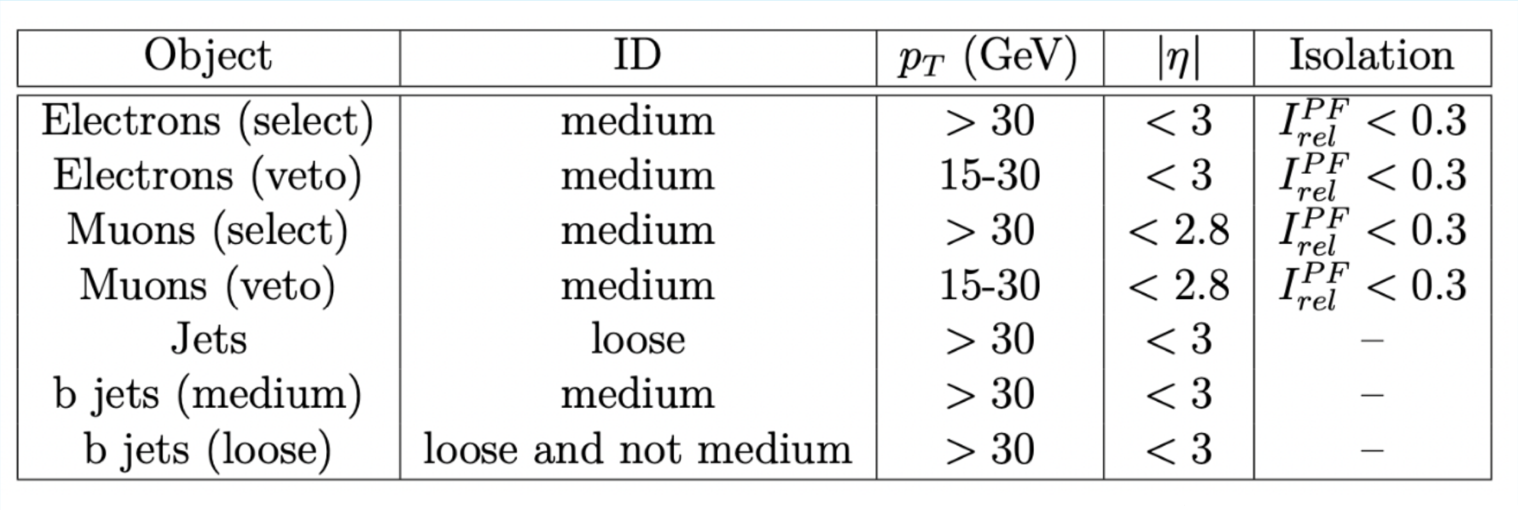

Object	ID	p_T (GeV)	$\lvert\eta\rvert$	Isolation
Electrons (select)	medium	> 30	< 3	$I_{rel}^{PF} < 0.3$
Electrons (veto)	medium	15-30	< 3	$I_{rel}^{PF} < 0.3$
Muons (select)	medium	> 30	< 2.8	$I_{rel}^{PF} < 0.3$
Muons (veto)	medium	15-30	< 2.8	$I_{rel}^{PF} < 0.3$
Jets	loose	> 30	< 3	–
b jets (medium)	medium	> 30	< 3	–
b jets (loose)	loose and not medium	> 30	< 3	–

2) Event baseline selection:

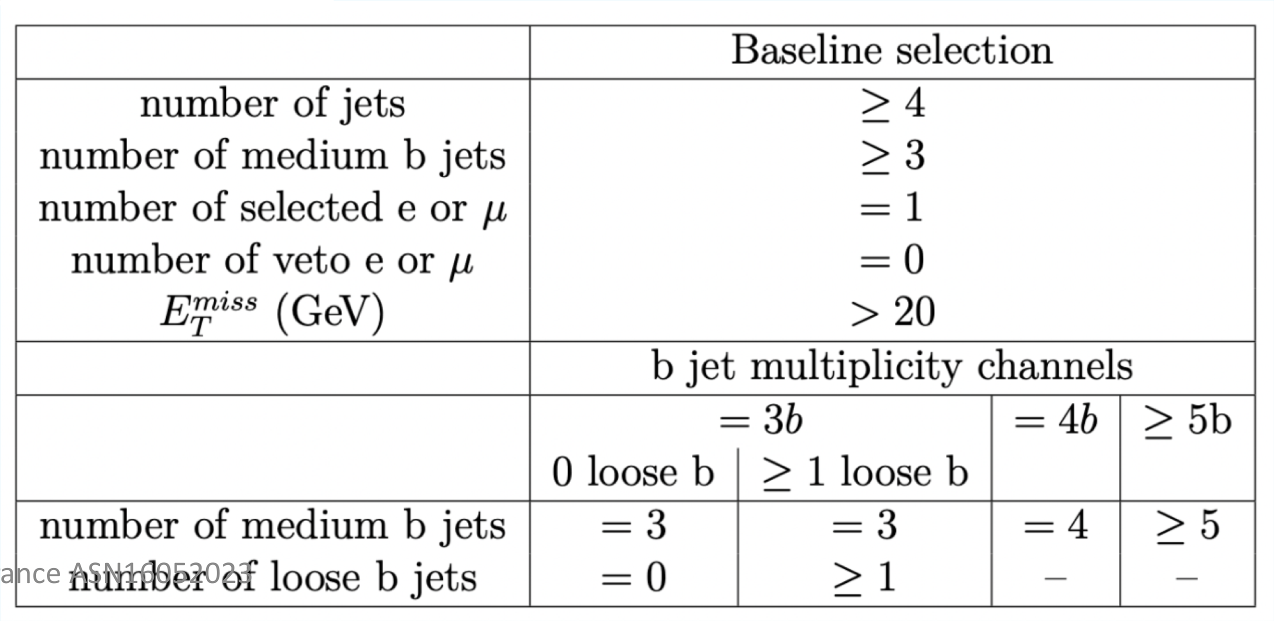

	Baseline selection			
number of jets	≥ 4			
number of medium b jets	≥ 3			
number of selected e or μ	$= 1$			
number of veto e or μ	$= 0$			
E_T^{miss} (GeV)	> 20			
	b jet multiplicity channels			
	$= 3b$		$= 4b$	$\geq 5b$
	0 loose b	≥ 1 loose b		
number of medium b jets	$= 3$	$= 3$	$= 4$	≥ 5
number of loose b jets	$= 0$	≥ 1	–	–

Simulated samples: most are especially produced for this study

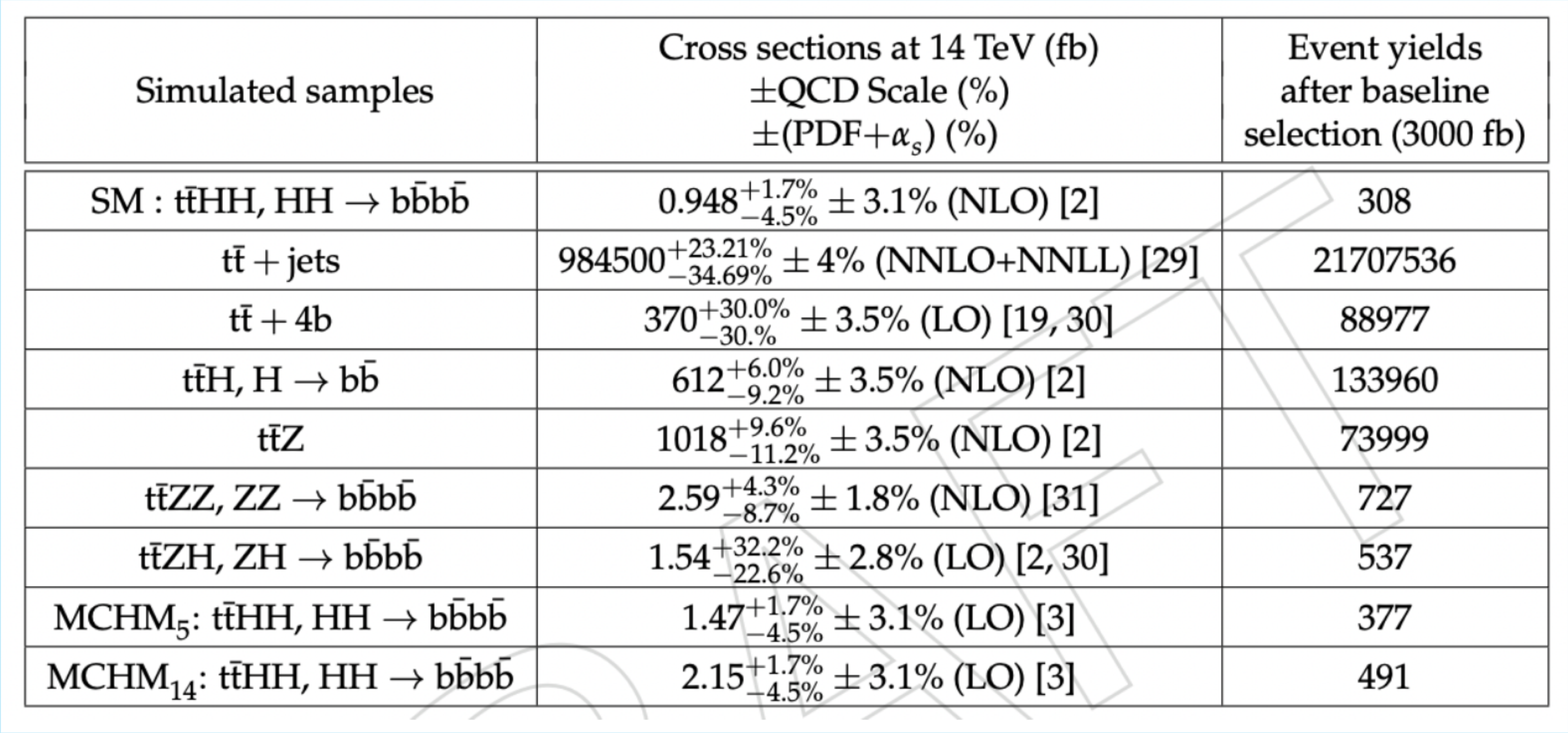

Simulated samples	Cross sections at 14 TeV (fb) ±QCD Scale (%) ±(PDF+α_s) (%)	Event yields after baseline selection (3000 fb)
SM : $t\bar{t}HH$, $HH \to b\bar{b}b\bar{b}$	$0.948^{+1.7\%}_{-4.5\%} \pm 3.1\%$ (NLO) [2]	308
$t\bar{t} + \text{jets}$	$984500^{+23.21\%}_{-34.69\%} \pm 4\%$ (NNLO+NNLL) [29]	21707536
$t\bar{t} + 4b$	$370^{+30.0\%}_{-30.\%} \pm 3.5\%$ (LO) [19, 30]	88977
$t\bar{t}H$, $H \to b\bar{b}$	$612^{+6.0\%}_{-9.2\%} \pm 3.5\%$ (NLO) [2]	133960
$t\bar{t}Z$	$1018^{+9.6\%}_{-11.2\%} \pm 3.5\%$ (NLO) [2]	73999
$t\bar{t}ZZ$, $ZZ \to b\bar{b}b\bar{b}$	$2.59^{+4.3\%}_{-8.7\%} \pm 1.8\%$ (NLO) [31]	727
$t\bar{t}ZH$, $ZH \to b\bar{b}b\bar{b}$	$1.54^{+32.2\%}_{-22.6\%} \pm 2.8\%$ (LO) [2, 30]	537
MCHM_5: $t\bar{t}HH$, $HH \to b\bar{b}b\bar{b}$	$1.47^{+1.7\%}_{-4.5\%} \pm 3.1\%$ (LO) [3]	377
MCHM_{14}: $t\bar{t}HH$, $HH \to b\bar{b}b\bar{b}$	$2.15^{+1.7\%}_{-4.5\%} \pm 3.1\%$ (LO) [3]	491

Special thanks to Carlos Bautista (IFT-UNESP, ICTP-SAIFR, BR) for his collaboration in generating the MCHM samples, preparing the MCHM gridpacks and verifying the generated and simulated MCHM data with dedicated DELPHES samples he produced.

Benchmark points as show cases for MCHM study for Snowmass 2022

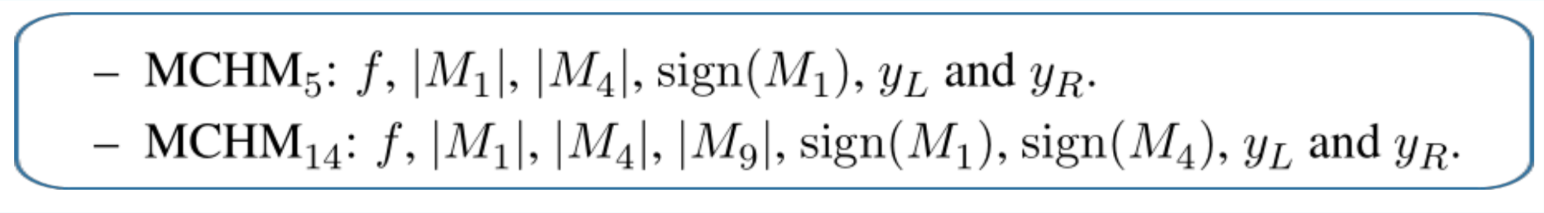

– MCHM_5: f, $|M_1|$, $|M_4|$, $\text{sign}(M_1)$, y_L and y_R.
– MCHM_{14}: f, $|M_1|$, $|M_4|$, $|M_9|$, $\text{sign}(M_1)$, $\text{sign}(M_4)$, y_L and y_R.

- **MCHM_5(C2) benchmark point: main parameters space values:**

f = 1593 GeV;

M_1= -1809 GeV; M_4 = 1479 GeV;

y_L= 1.38; y_R= 0.58

μ(ttH)=0.94;

μ(ttHH)=1.47 NR-ttHH/ttHH= 0.59

3 heavy charge 2/3 top-partner resonances->tH decay:

T^1: mass 1.5 TeV, Br(tH)=45.4%; Γ(T^1)=5,5 GeV

T^2: mass 2.0 TeV, Br(tH)=21.8%; Γ(T^2)=13.6 GeV

T^3: mass 3.9 TeV, Br(tH)=6.2%; Γ(T^3)=163.2 GeV

- **MCHM_{14}(D7) benchmark point: main parameters space values :**

f = 863 GeV;

M_1= -801 GeV; M_4= -1907 GeV; M_9= 1500 GeV

y_L= 1.23; y_R= 1.67

μ(ttH)=0.93;

μ(ttHH)=2.15 NR-ttHH/ttHH= 0.37

6 heavy charge 2/3 top-partner resonances->tH decay:

T^1: mass 1.4 TeV, Br(tH)=28.3%; Γ(T^1)=64.2 GeV

T^2: mass 1.5 TeV, Br(tH)~0%; Γ(T^2)=17.0 GeV

T^3: mass 1.5 TeV, Br(tH)=27.5%; Γ(T^3)=7.8 GeV

T^4: mass 1.5 TeV, Br(tH)=67.9%; Γ(T^4)=43.2 GeV

T^5: mass 2.0 TeV, Br(tH)=8.2%; Γ(T^5)=10.7 GeV

T^6: mass 2.2 TeV, Br(tH)=40.0%; Γ(T^6)=10.8 GeV

Background events:

1)**The top pair+jets backgrounds: some special aspects for this DELPHES based study/CMS data analysis**

- The top pair production in association with 2b jets constitutes a large irreducible background in the ttH where Higgs decays into a b-quark pair [arXiv:1610.07922].
  - It has been the object of a detailed NLO+PS QCD study [arXiv:1912.00068].
- Similarly, the top pair production in association with 4 b jets is an important background for ttHH(4b). Unlike tt+2b, there is no such NLO QCD study and only a LO generated sample is produced.
- Estimation of the QCD scale uncertainty on tt+4b sample is done in the consideration of tt +2b studies showing that the NLO QCD effects reduce scale uncertainties from the 70-80% level to 20-30% at LO.
- Hence, tt+4b QCD scale uncertainty is treated with two scenarios; *70% and 30%*.
- The tt + 2b process also contributes to the background.Though dedicated samples for this process do not exist here, the background is partially taken into account through the tt+jets samples.

2) **The other Physics backgrounds**: Note that as for the full Run 2 data ttHH analysis:

- ttHbb, ttZbb
- ttZH4b and ttZZ4b

are included as additional Physics backgrounds.

Definition and choice of the DNN input variables

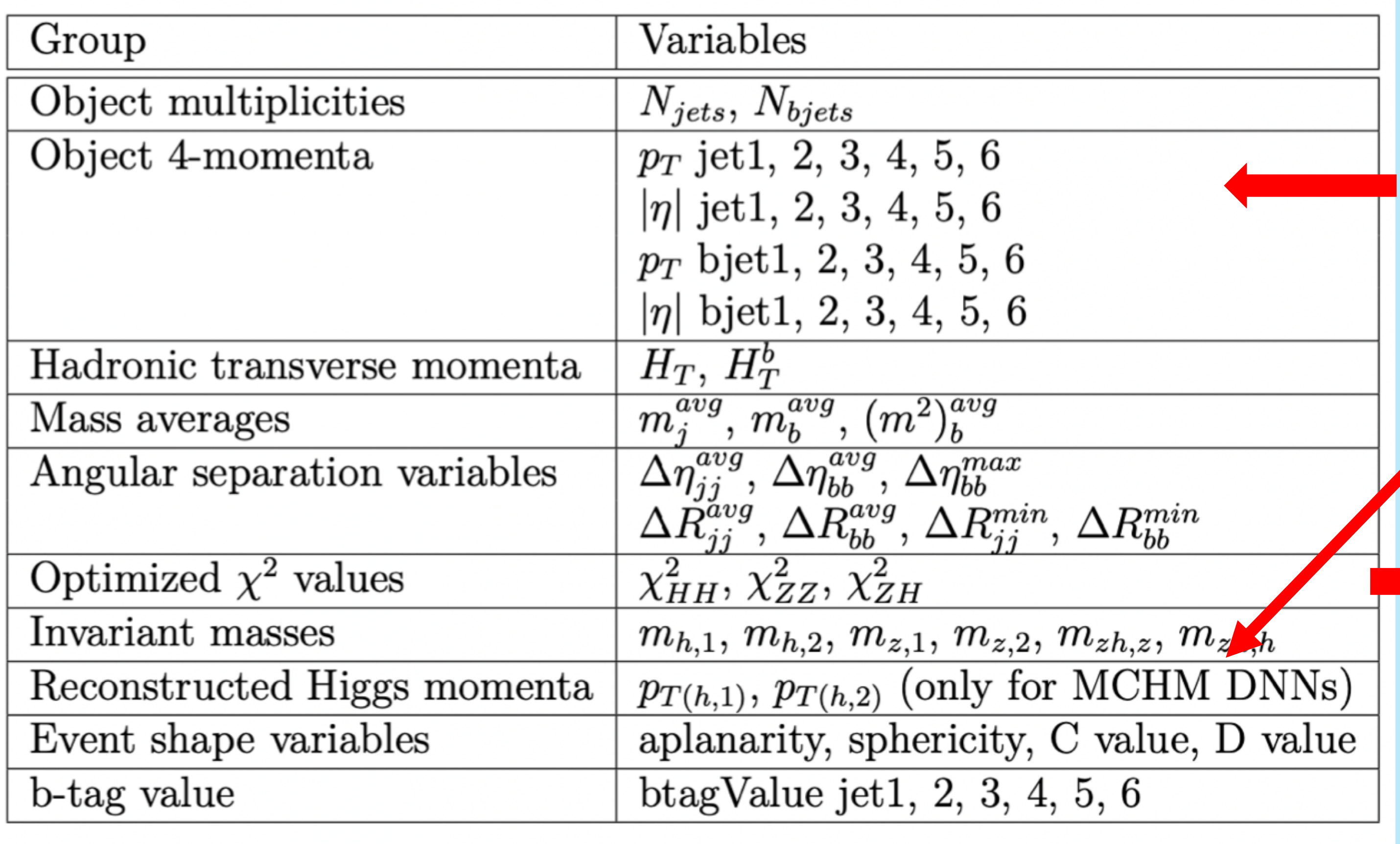

Group	Variables
Object multiplicities	N_{jets}, N_{bjets}
Object 4-momenta	p_T jet1, 2, 3, 4, 5, 6 $\|\eta\|$ jet1, 2, 3, 4, 5, 6 p_T bjet1, 2, 3, 4, 5, 6 $\|\eta\|$ bjet1, 2, 3, 4, 5, 6
Hadronic transverse momenta	H_T, H_T^b
Mass averages	m_j^{avg}, m_b^{avg}, $(m^2)_b^{avg}$
Angular separation variables	$\Delta\eta_{jj}^{avg}$, $\Delta\eta_{bb}^{avg}$, $\Delta\eta_{bb}^{max}$ ΔR_{jj}^{avg}, ΔR_{bb}^{avg}, ΔR_{jj}^{min}, ΔR_{bb}^{min}
Optimized χ^2 values	χ^2_{HH}, χ^2_{ZZ}, χ^2_{ZH}
Invariant masses	$m_{h,1}$, $m_{h,2}$, $m_{z,1}$, $m_{z,2}$, $m_{zh,z}$, $m_{zh,h}$
Reconstructed Higgs momenta	$p_{T(h,1)}$, $p_{T(h,2)}$ (only for MCHM DNNs)
Event shape variables	aplanarity, sphericity, C value, D value
b-tag value	btagValue jet1, 2, 3, 4, 5, 6

- Important to note the restricted number of variables characterizing an event with DELPHES as compared to CMSSW:
  - ''Only'' 57 such variables as inputs to DNN for SM case
  - and 57+2 such variables as inputs to DNN for BSM case

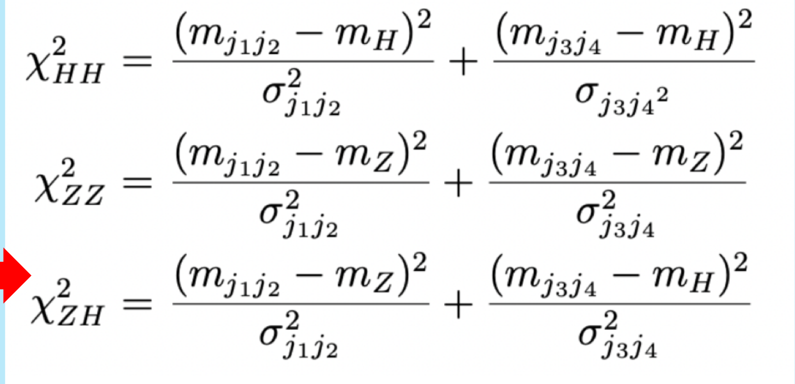

$$\chi^2_{HH} = \frac{(m_{j_1j_2} - m_H)^2}{\sigma^2_{j_1j_2}} + \frac{(m_{j_3j_4} - m_H)^2}{{\sigma_{j_3j_4}}^2}$$

$$\chi^2_{ZZ} = \frac{(m_{j_1j_2} - m_Z)^2}{\sigma^2_{j_1j_2}} + \frac{(m_{j_3j_4} - m_Z)^2}{\sigma^2_{j_3j_4}}$$

$$\chi^2_{ZH} = \frac{(m_{j_1j_2} - m_Z)^2}{\sigma^2_{j_1j_2}} + \frac{(m_{j_3j_4} - m_H)^2}{\sigma^2_{j_3j_4}}$$

Invariant mass and χ^2 calculated for HH, ZH and ZZ diboson case, by:

- Scanning over all b-jets combination to find the minimum χ^2, and
- Using the b-jets corresponding this minimum χ^2 to compute the invariant mass.

Variable Distributions After Baseline Selection

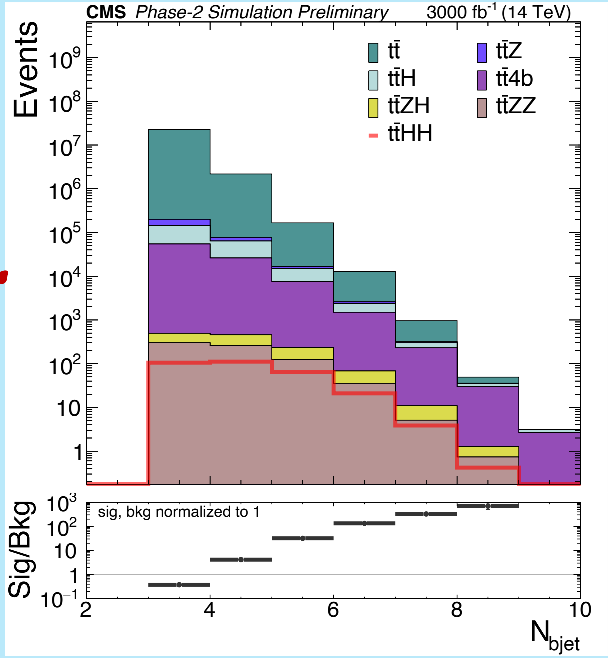

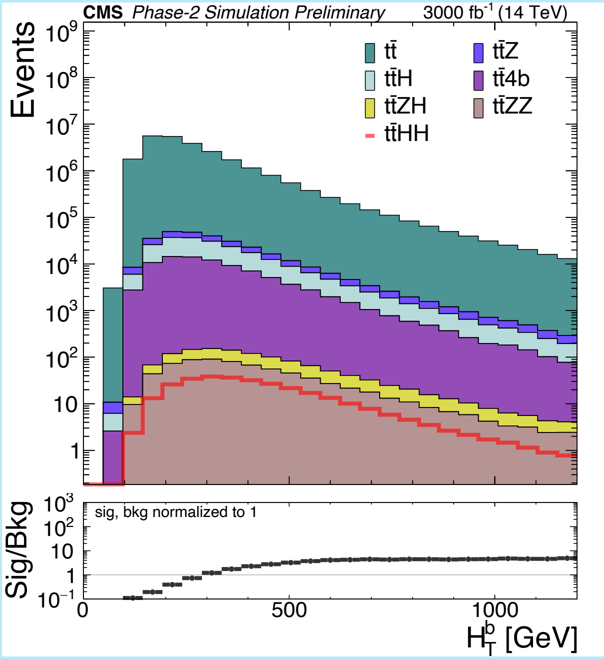

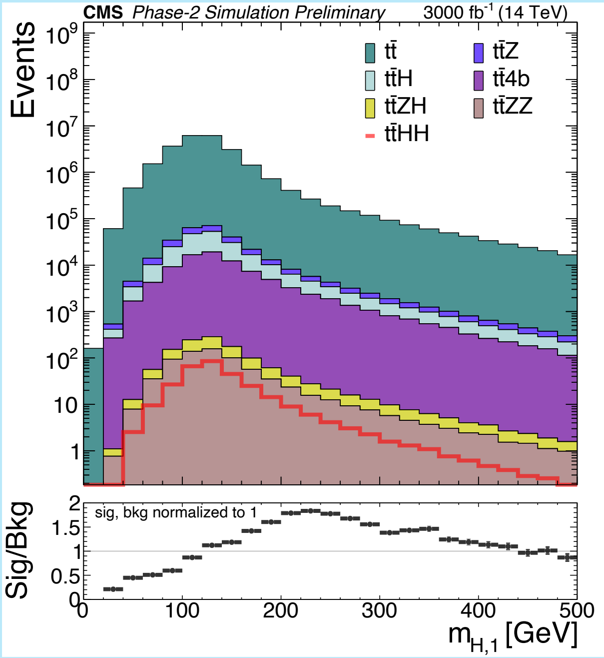

Kinematic variables with particularly high discriminative power for the SM ttHH signal and all SM backgrounds.

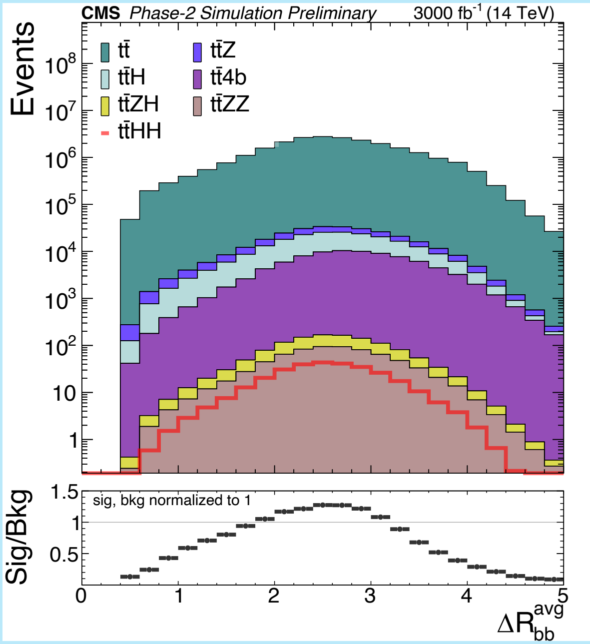

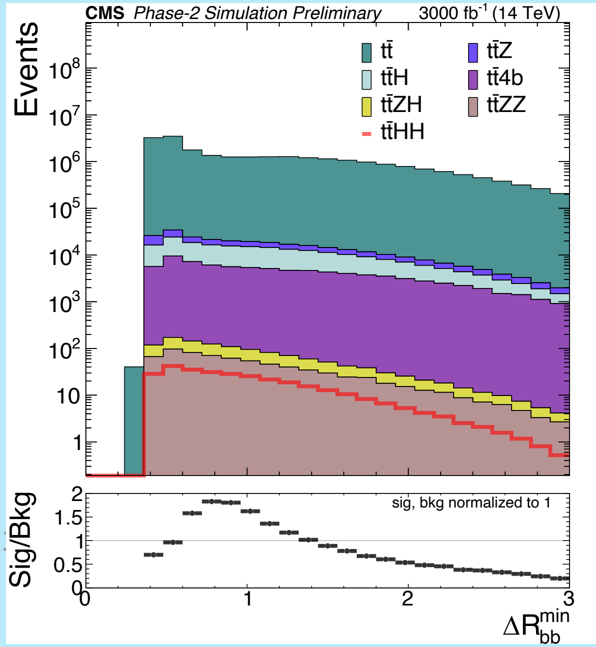

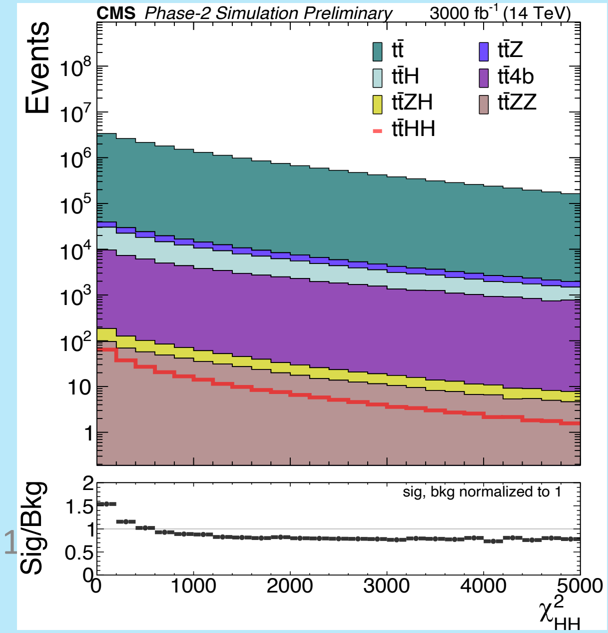

Discriminating between ttHH, ttHZ and ttZH: difficult

See: Shape comparison with kinematic variables with high discriminating power

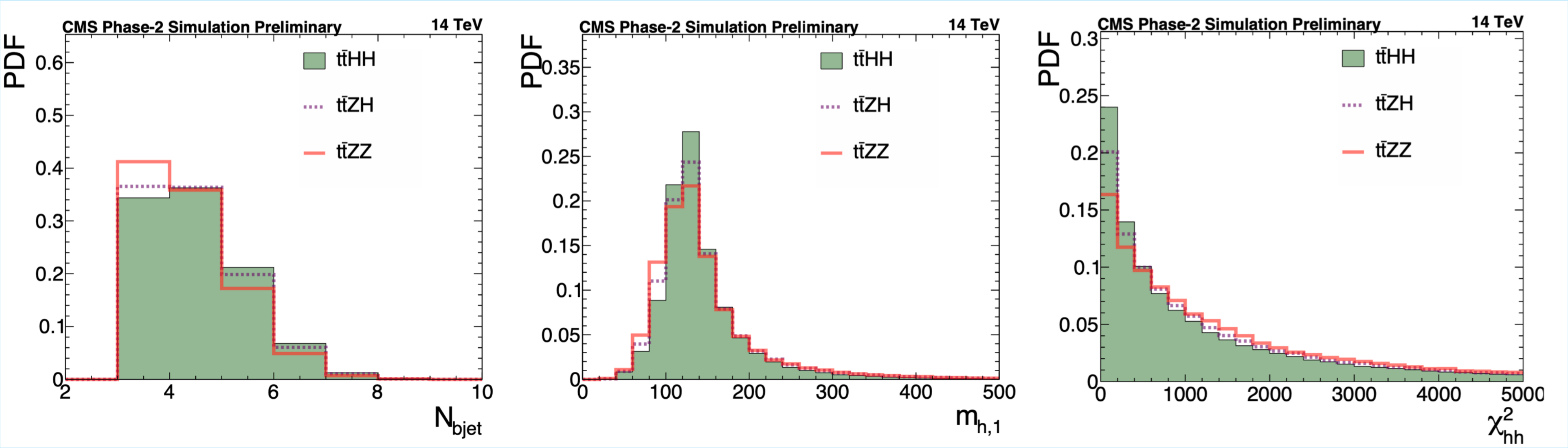

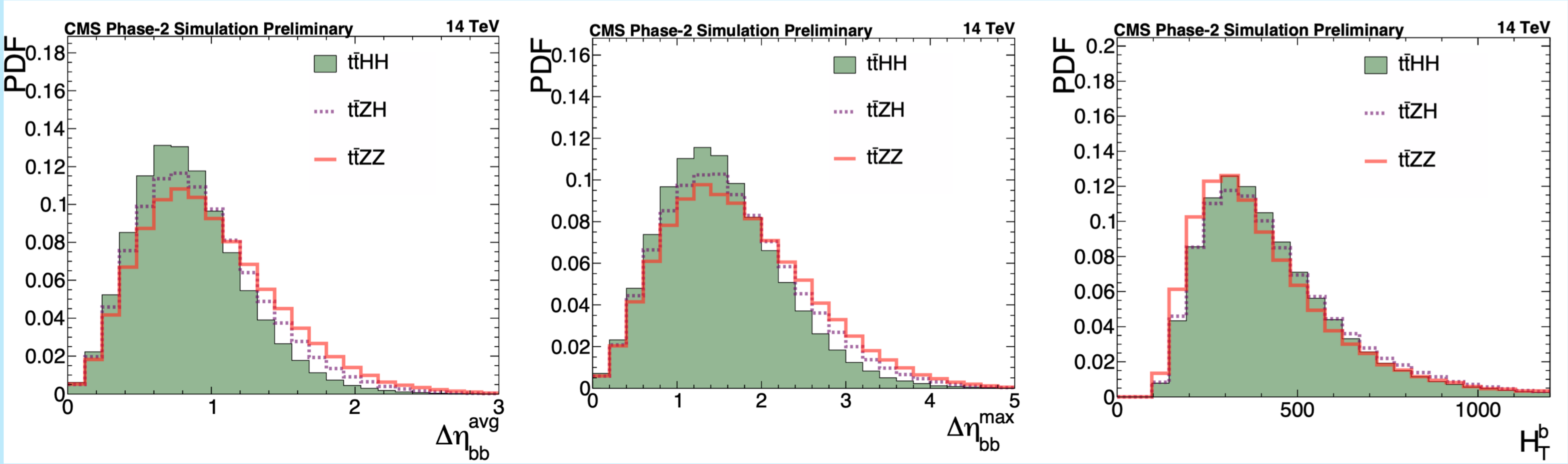

IMPACT of BSM on kinematic variables: effect of resonances

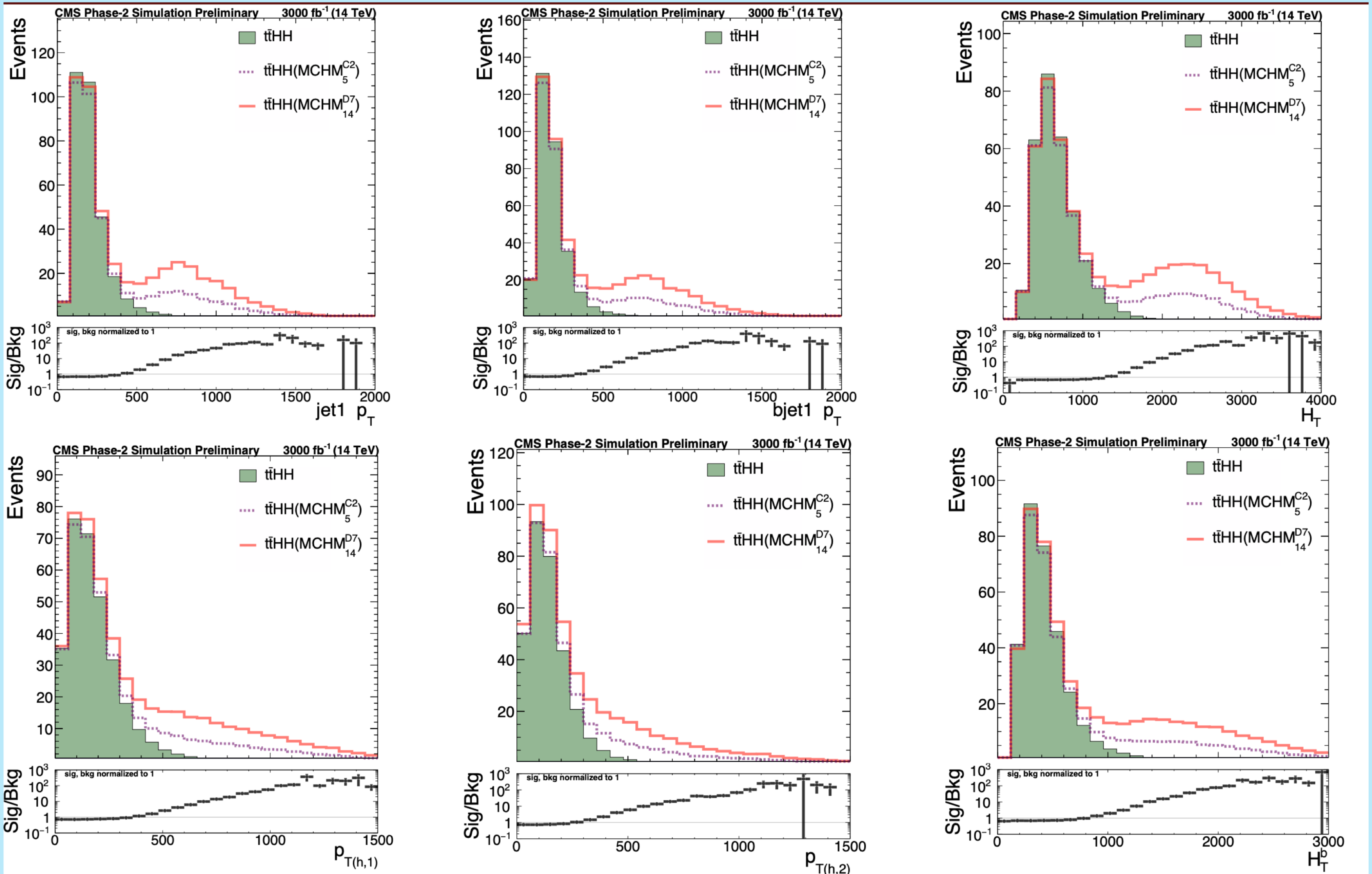

! NEW ! Event Categorization Flowchart: works in two steps

1st step: Binary DNN to extract ttHH /ttHZ and ttZZ implemented with subset of the

2nd step: all observables + DNN binary discriminant

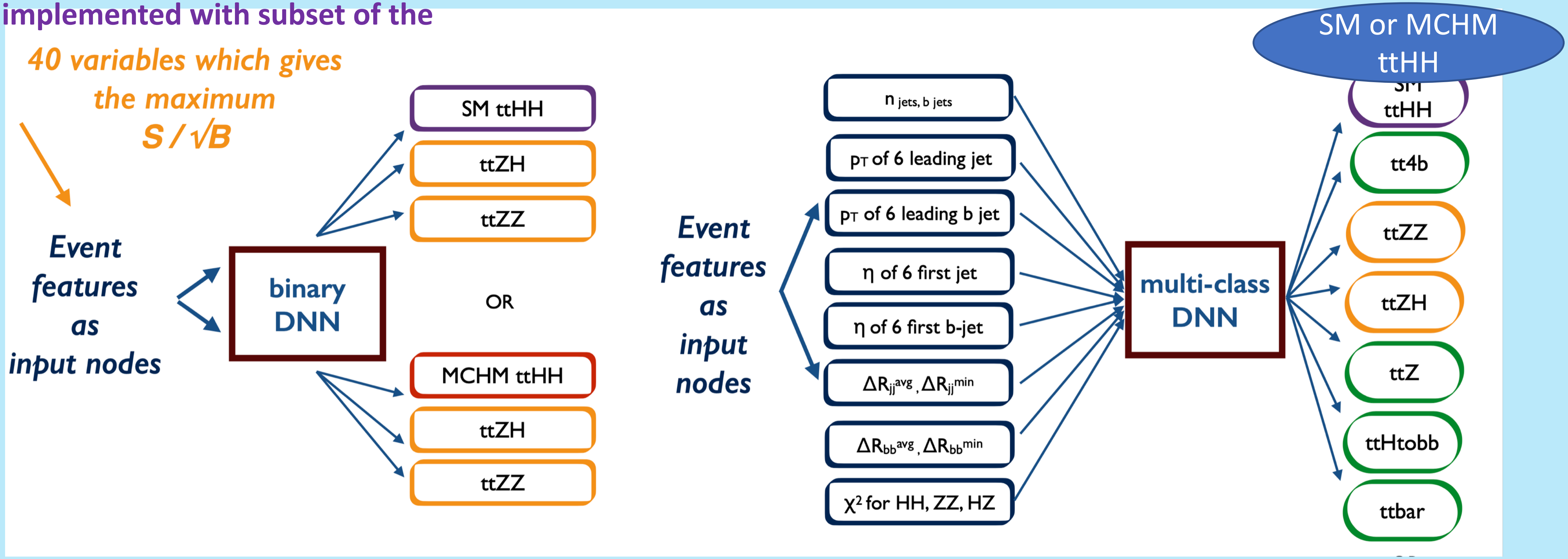

40 variables which gives the maximum ***S / √B***

Event features as input nodes

binary DNN

SM ttHH

ttZH

ttZZ

OR

MCHM ttHH

ttZH

ttZZ

Event features as input nodes

$n_{\text{jets, b jets}}$

p_T of 6 leading jet

p_T of 6 leading b jet

η of 6 first jet

η of 6 first b-jet

$\Delta R_{jj}^{avg}, \Delta R_{jj}^{min}$

$\Delta R_{bb}^{avg}, \Delta R_{bb}^{min}$

χ^2 for HH, ZZ, HZ

multi-class DNN

SM or MCHM ttHH

SM ttHH

tt4b

ttZZ

ttZH

ttZ

ttHtobb

ttbar

Schema of the binary and the multi-classifier DNN network :

Same event categorization strategy applied to both the SM ttHH and MCHM ttHH cases.

N.B. *This 2-stages categorization is a new input in our overall ttHH strategy, as developed so far in the tt(SL)HH4b data analysis. We might extend it to the CMS data case to strengthen the discrimination of ttHH wrt ttZH & ttZZ ("newcomers" in this analysis).*

DNN-based event categorization

- The DNN consists of fully connected neural network nodes for the consecutive layers.
- To prevent a bias (over-training), independent validation and training samples are identified.
- Hyperparameters are optimized on the validation samples, evaluated by same DNN in 3 different number of b jet categories; nbjet = 3, 4, >=5

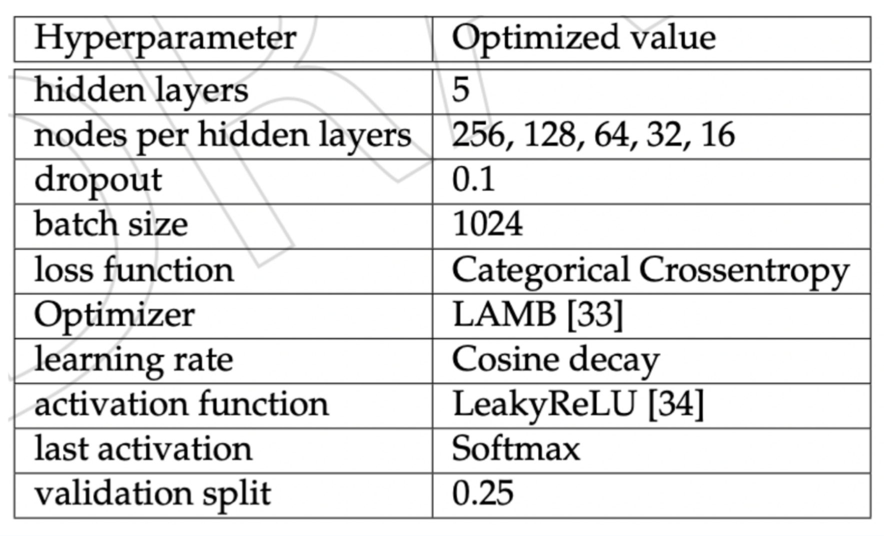

Hyperparameter	Optimized value
hidden layers	5
nodes per hidden layers	256, 128, 64, 32, 16
dropout	0.1
batch size	1024
loss function	Categorical Crossentropy
Optimizer	LAMB [33]
learning rate	Cosine decay
activation function	LeakyReLU [34]
last activation	Softmax
validation split	0.25

Confusion matrix,
ROC-AUC=0.77
Eff(ttHH)=71.4%

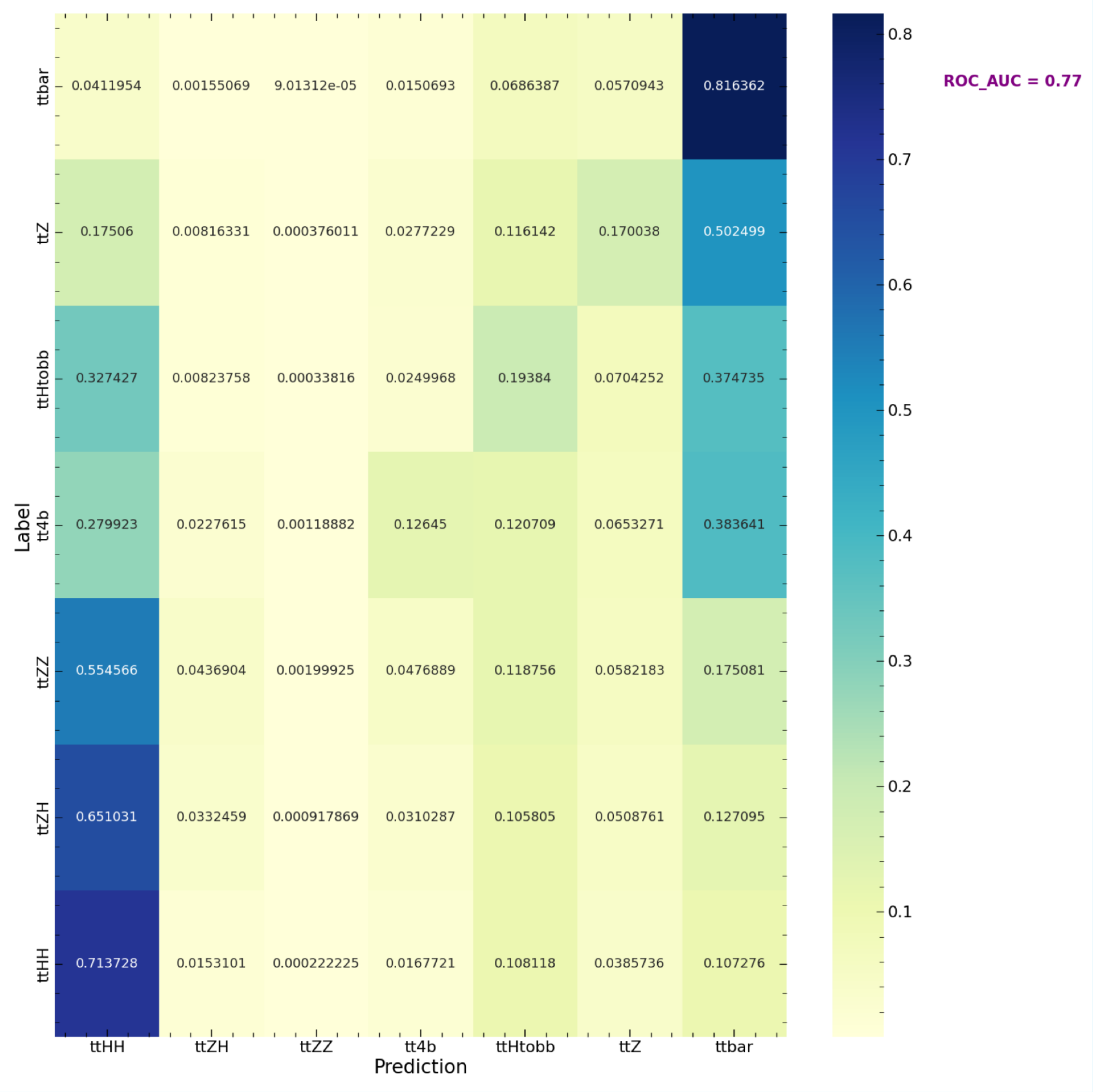

Label	ttHH	ttZH	ttZZ	tt4b	ttHtobb	ttZ	ttbar
ttbar	0.0411954	0.00155069	9.01312e-05	0.0150693	0.0686387	0.0570943	0.816362
ttZ	0.17506	0.00816331	0.000376011	0.0277229	0.116142	0.170038	0.502499
ttHtobb	0.327427	0.00823758	0.00033816	0.0249968	0.19384	0.0704252	0.374735
tt4b	0.279923	0.0227615	0.00118882	0.12645	0.120709	0.0653271	0.383641
ttZZ	0.554566	0.0436904	0.00199925	0.0476889	0.118756	0.0582183	0.175081
ttZH	0.651031	0.0332459	0.000917869	0.0310287	0.105805	0.0508761	0.127095
ttHH	0.713728	0.0153101	0.000222225	0.0167721	0.108118	0.0385736	0.107276

DNN Results: Final discriminants for the SM ttHH training

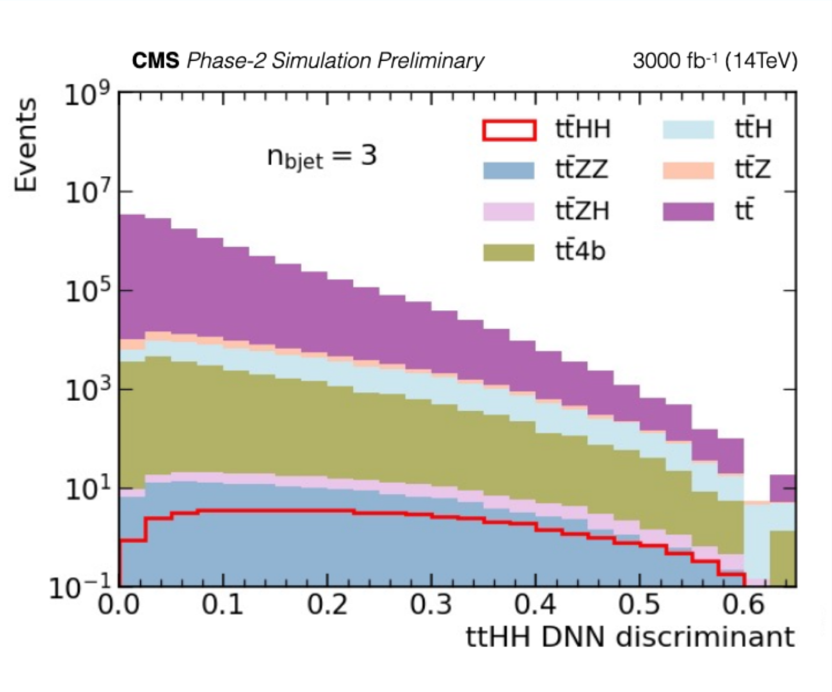

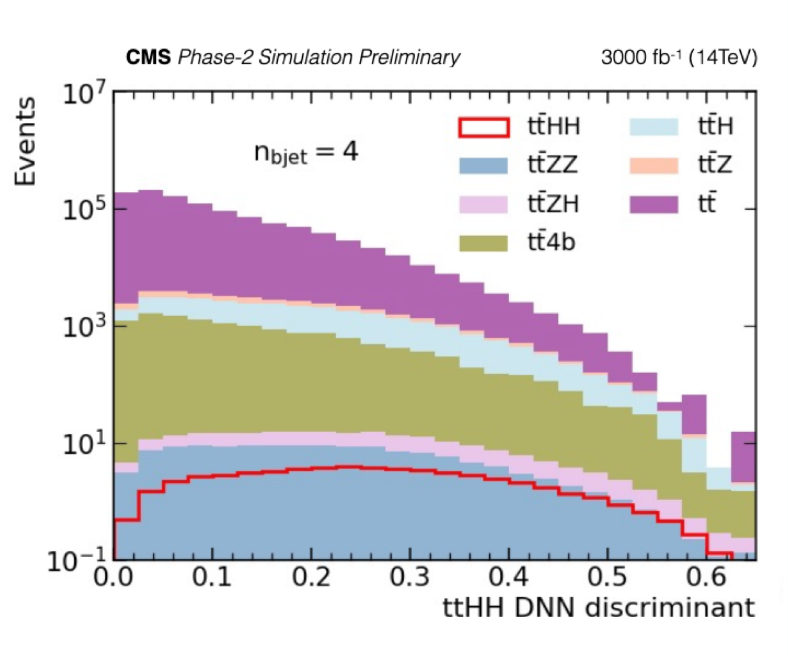

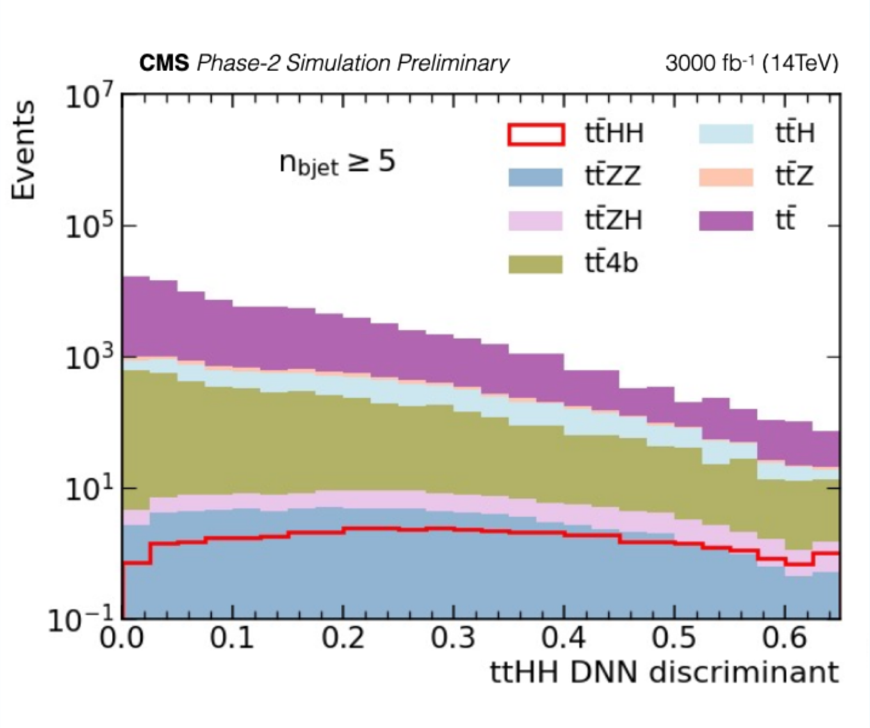

DNN Results: Final discriminants for the MCHM training

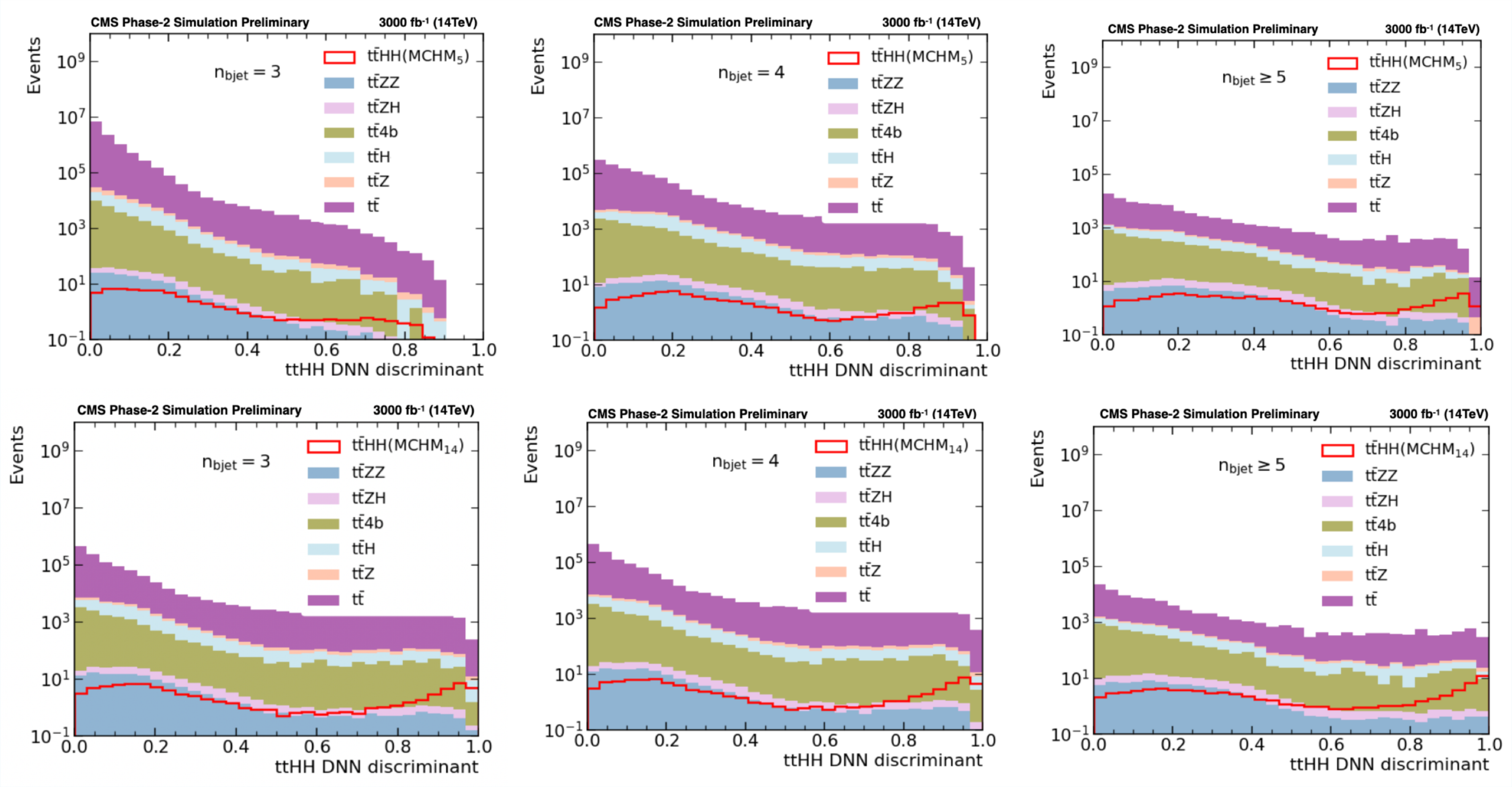

Systematic uncertainties

- Recommended systematics for HL-LHC are applied: https://twiki.cern.ch/twiki/bin/viewauth/CMS/YR2018Systematics Three scenarios for systematic uncertainties are considered
  - “YR18” systematics scenario:This scenario represents the realistic systematic uncertainties assumed for the Phase-2 era. A scale uncertainty of 30% is considered for the tt + 4b background.
  - “YR18 conservative” systematics scenario: Same as above, but a scale uncertainty of 70% is considered for the tt + 4b background.
  - Statistics-only scenario:We only consider statistical uncertainties.

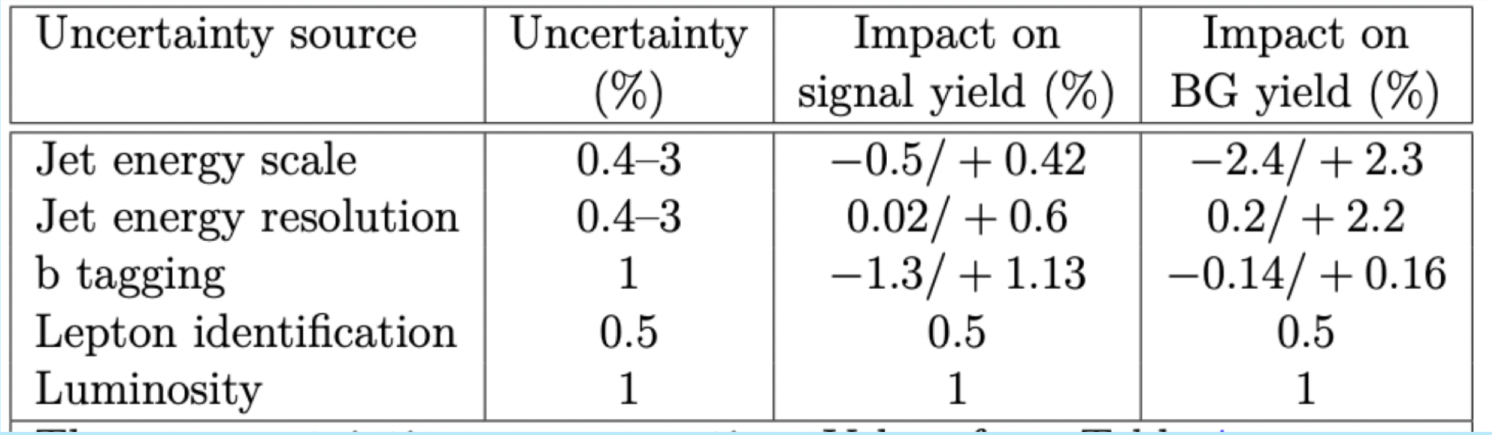

Uncertainty source	Uncertainty (%)	Impact on signal yield (%)	Impact on BG yield (%)
Jet energy scale	0.4–3	$-0.5/+0.42$	$-2.4/+2.3$
Jet energy resolution	0.4–3	$0.02/+0.6$	$0.2/+2.2$
b tagging	1	$-1.3/+1.13$	$-0.14/+0.16$
Lepton identification	0.5	0.5	0.5
Luminosity	1	1	1

Plus Theory uncertainties on cross-section, given in the table of simulated samples

Results: Limits- Combine Tool for SM tt(SL)HH4b

- A log likelihood scan is performed with the shapes of each discriminants.
- Upper limits for 3 different cases are obtained:
  - *ttHH: $3.14_{-0.9}^{+1.27}$ times the SM cross section.*
  - *ttHH and ttZH : $1.31_{-0.37}^{+0.53}$ time the SM cross section.*
  - *ttHH, ttZH & ttZZ: $0.84\text{-}_{0.24}^{+0.34}$ times the SM cross section*

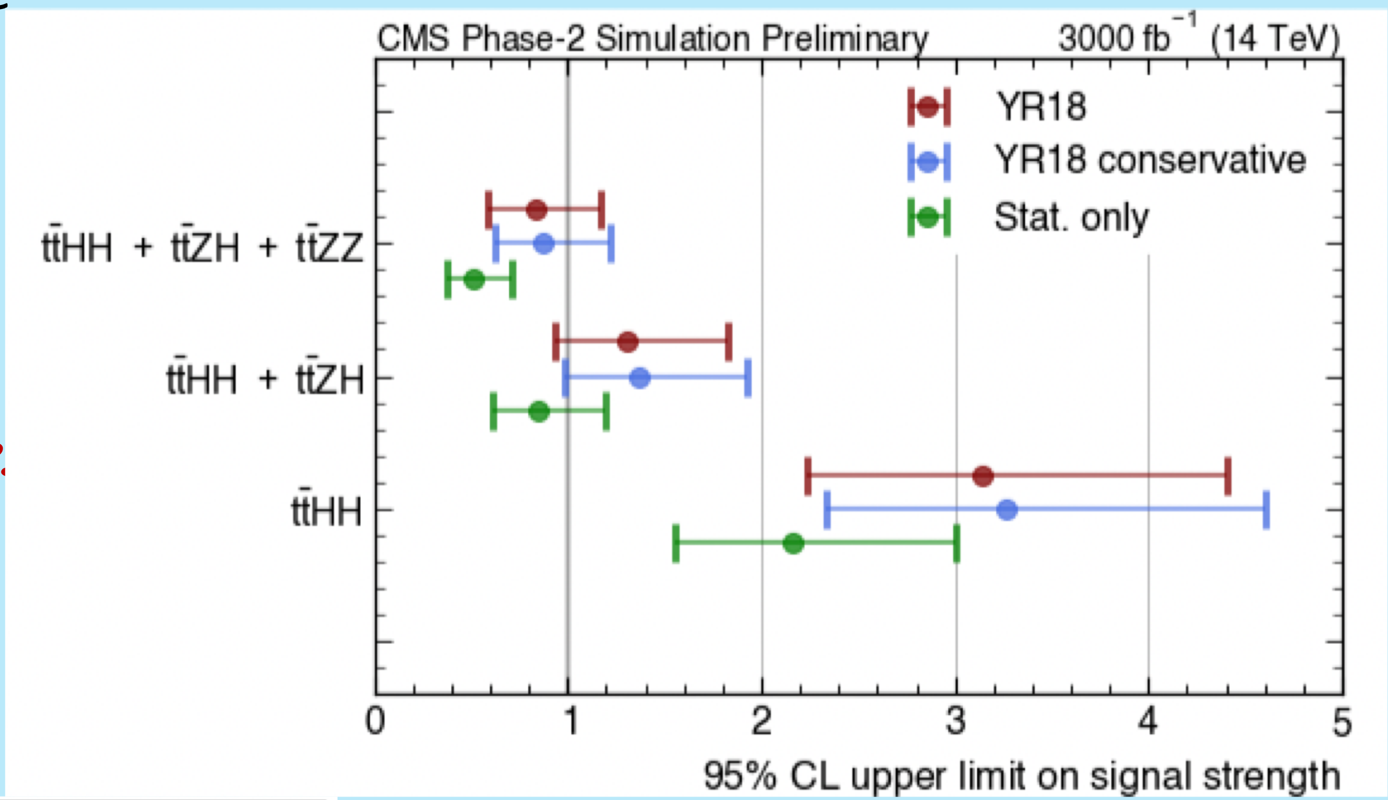

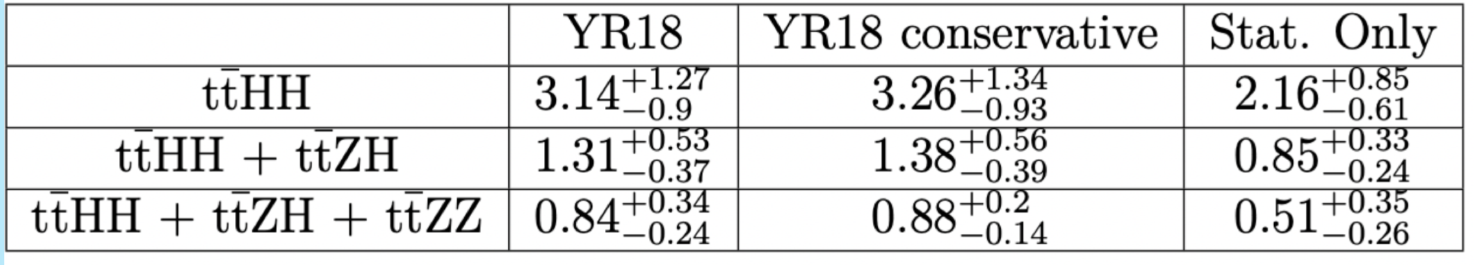

	YR18	YR18 conservative	Stat. Only
$t\bar{t}HH$	$3.14_{-0.9}^{+1.27}$	$3.26_{-0.93}^{+1.34}$	$2.16_{-0.61}^{+0.85}$
$t\bar{t}HH + t\bar{t}ZH$	$1.31_{-0.37}^{+0.53}$	$1.38_{-0.39}^{+0.56}$	$0.85_{-0.24}^{+0.33}$
$t\bar{t}HH + t\bar{t}ZH + t\bar{t}ZZ$	$0.84_{-0.24}^{+0.34}$	$0.88_{-0.14}^{+0.2}$	$0.51_{-0.26}^{+0.35}$

Results: Limits- Combine Tool for 2 considered MCHM cases

- A log likelihood scan is performed with the shapes of each discriminant.
- 95% CL upper limits for the 2 considered

  MCHM ttHH benchmark points are:
- $\mu(ttHH\_MCHM_5^{C2}) = 1.72_{-0.53}^{+0.76}$
- $\mu(ttHH\_MCHM_{14}^{D7}) = 1.08_{-0.30}^{+0.43}$

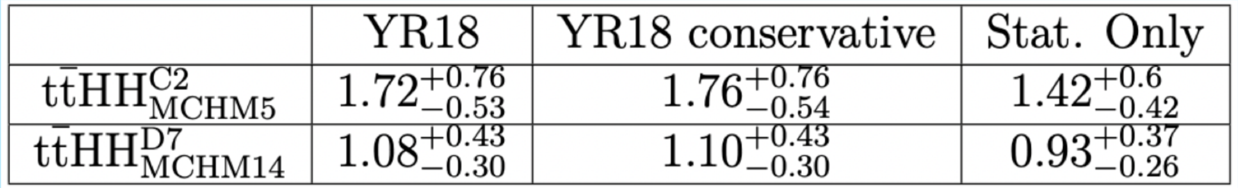

	YR18	YR18 conservative	Stat. Only
$t\bar{t}HH^{C2}_{MCHM5}$	$1.72^{+0.76}_{-0.53}$	$1.76^{+0.76}_{-0.54}$	$1.42^{+0.6}_{-0.42}$
$t\bar{t}HH^{D7}_{MCHM14}$	$1.08^{+0.43}_{-0.30}$	$1.10^{+0.43}_{-0.30}$	$0.93^{+0.37}_{-0.26}$

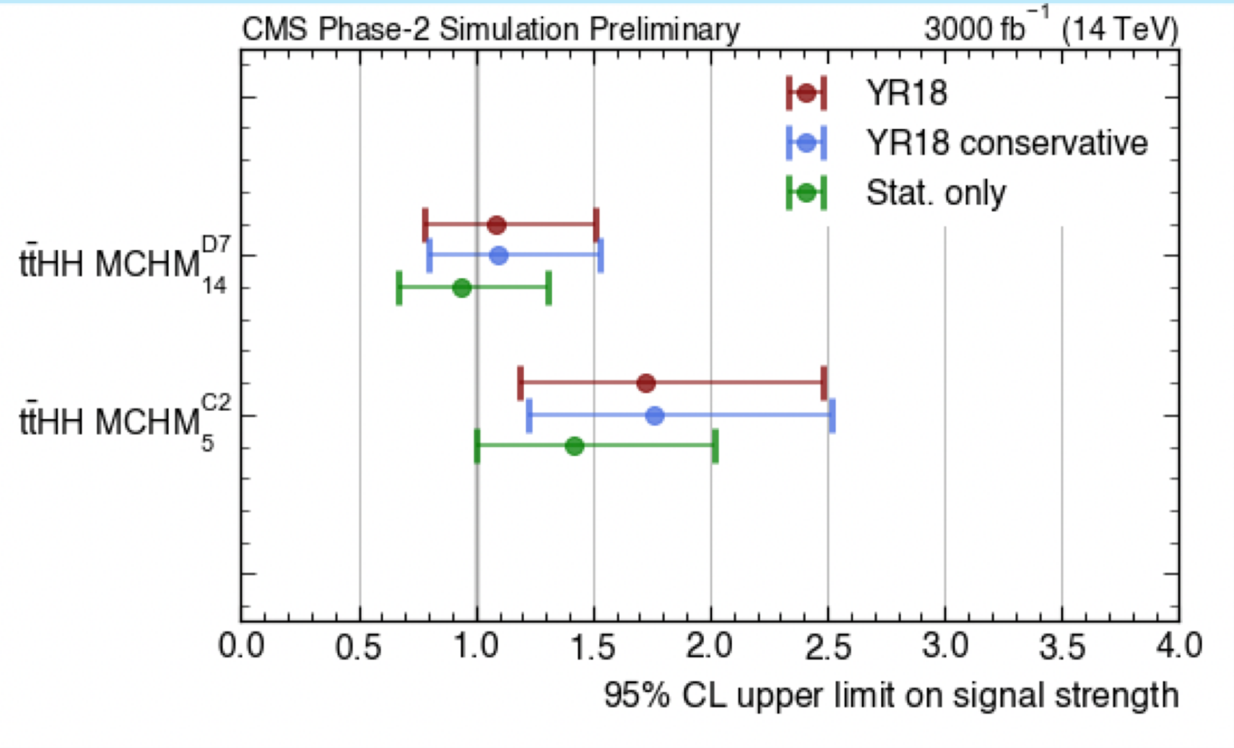

Concluding remarks & perspectives on the experimental side

- ✓ Motivated by the theoretical interest and the phenomenology studies, experimental searches on the tthh non-resonant production at LHC with the current Run 2 data have been launched and results with full Run 2 data expected by end of 2023.
- ✓ Also starting to address the Run 3 data analyses that will double the statistics.
- ✓ In parallel perspectives study with HL-LHC have been performed with a as realistic as possible framework.

- ✓ The 4 top results show: 10 fb-cross section barrier can be overcome => Next step are the fb cross-section processes; especially the tthh multifacted process both in SM and BSM:

- ✓ The search for VLQ's as well in the resonant production of tthh are as well extremely promising in these scenarios and quite complementary.

- ✓ CHM offers an excellent playground to explore BSM with features that are rather generic.
  => STAY TUNED!!

Backup slides

Vector Boson Fusion (VBF) production mechanism

Courtesy Brunella d'Anzi

★ It is a unique mean for probing the VVHH ($V=Z^*,W^{\pm}$) C_{2V} Higgs self-coupling!

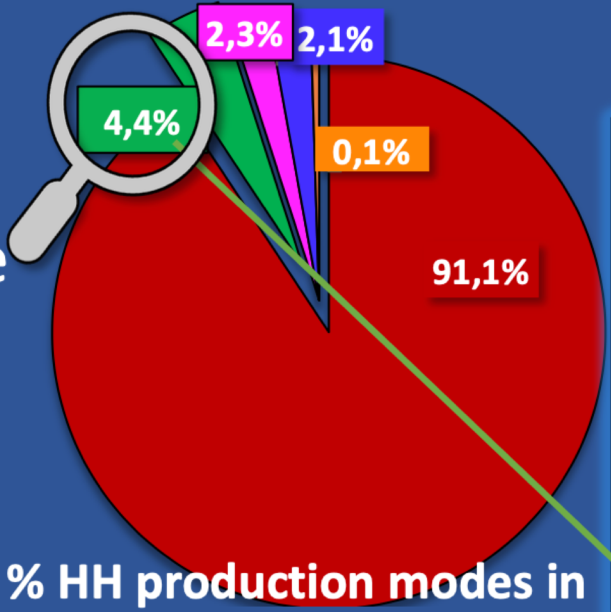

% HH production modes in SM Higgs mass hypothesis

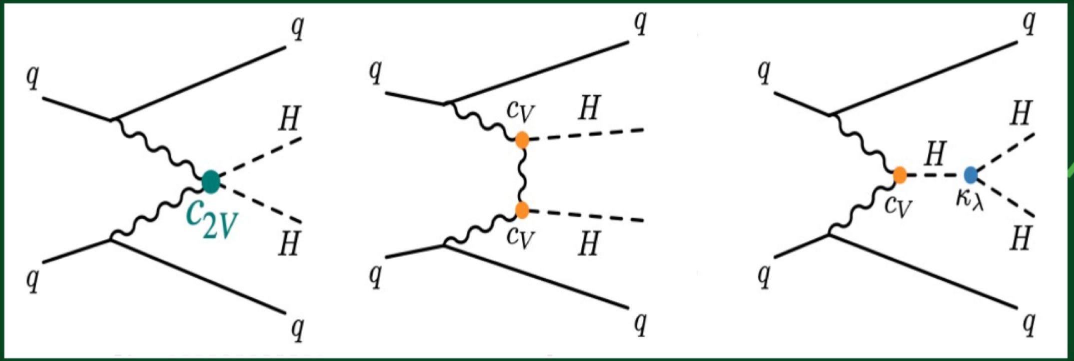

Vector boson fusion (VBF)

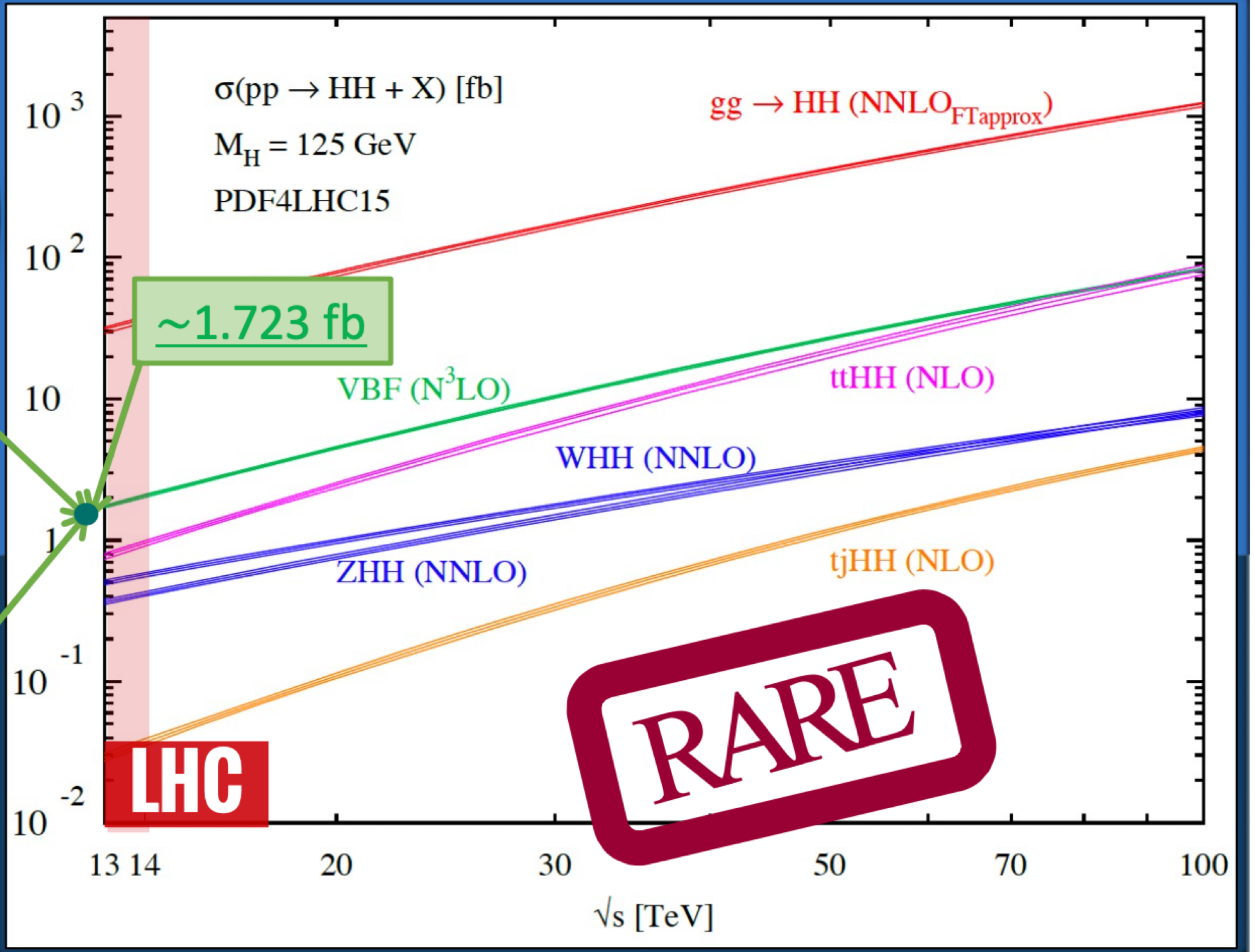

CERN Technical report, 2019

SIGNATURES, BR's & Nb of evts for ≥ Run 2

- Top quark has a very short life-time ~ 10^{-25} sec ⇒ decay before hadronisation
- In SM $|V_{tb}|$~1 ⇒ Br(t→Wb) ~ 100%
- Dileptons:
  - e, μ, τ → e (μ) : ~ 6.5%, low background
  - τ → had + e (μ) : ~ 3.6%, reasonable bckg
- Leptons + jets,
  - e, μ, τ → e (μ) + jets ~ 35%, reasonable bckg
  - τ → had + jets ~ 9.5%, high background
- All jets ~ 46%, high bckg

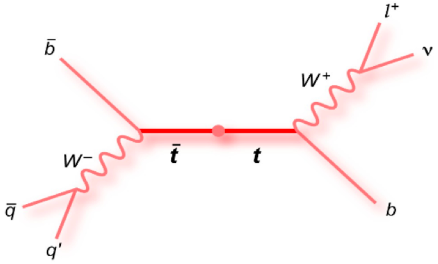

Top Pair Branching Fractions

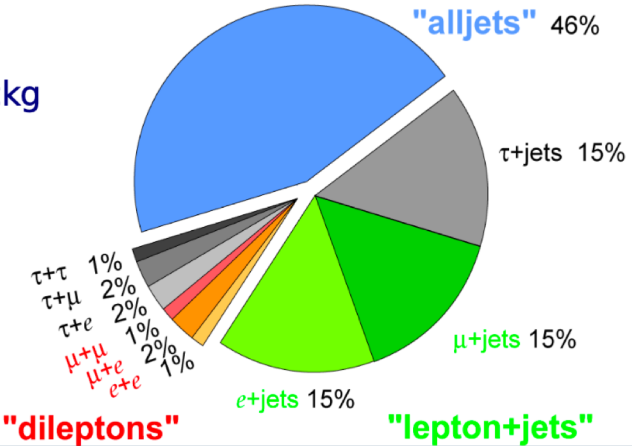

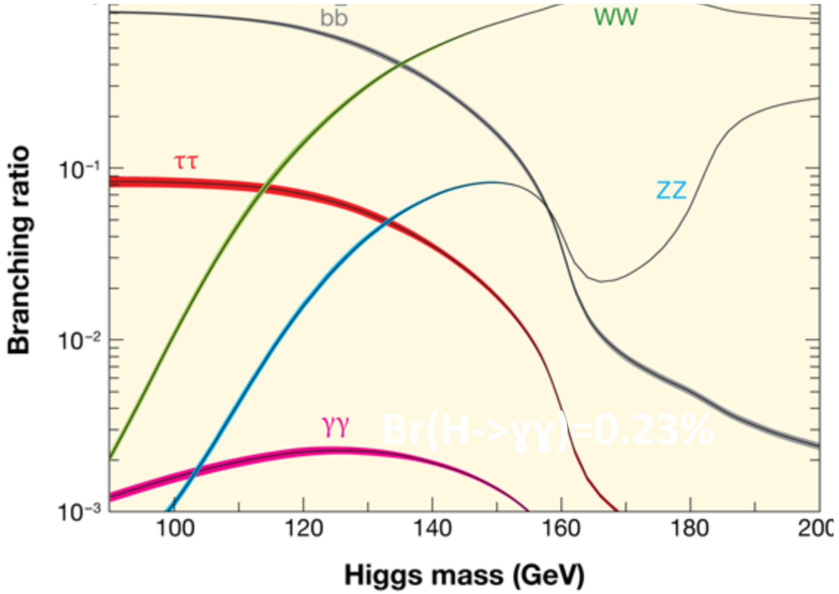

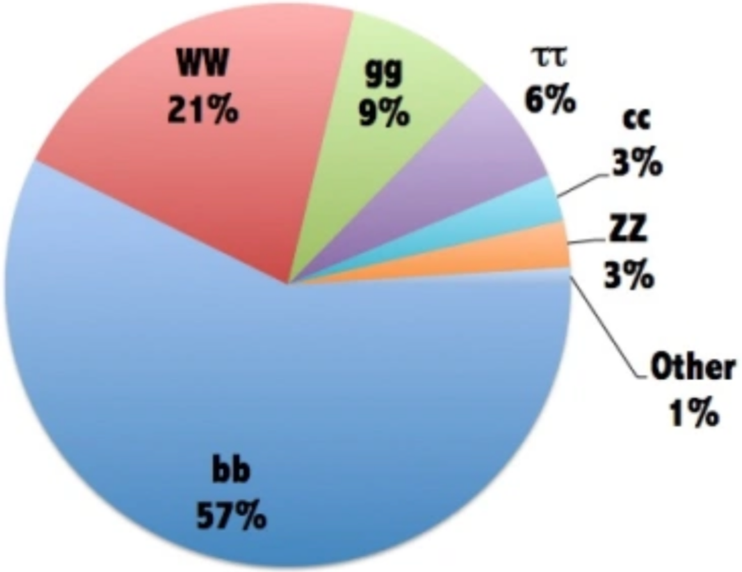

Br[tt(SL)HH(4b)]= 0,35x0,57² => 137,1fb⁻¹ => 11.4% =>12.1 evts
Br(tt(DL)HH(4b)) =0.10x0,57² => 3.2% => 3.4 evts
Br(tt(had)HH(4b))= 0,46x0,57² => 15.0% => 15,9 evts
Br[tt(SL)H(2b)H(2ɣ)]=0.35x0.57x0.0023 =>0,046% => 0.05 evt
Br[tt(SL)H(2b)H(WW)]=0.35x0.57x0.21 => multileptons signature
Br[tt(SL)H(2b)H(**ττ**)]=0.35x0.57x0.06=> 1.6 evt, interesting add. 2**τ**

Three body decays in MCHM$_5$

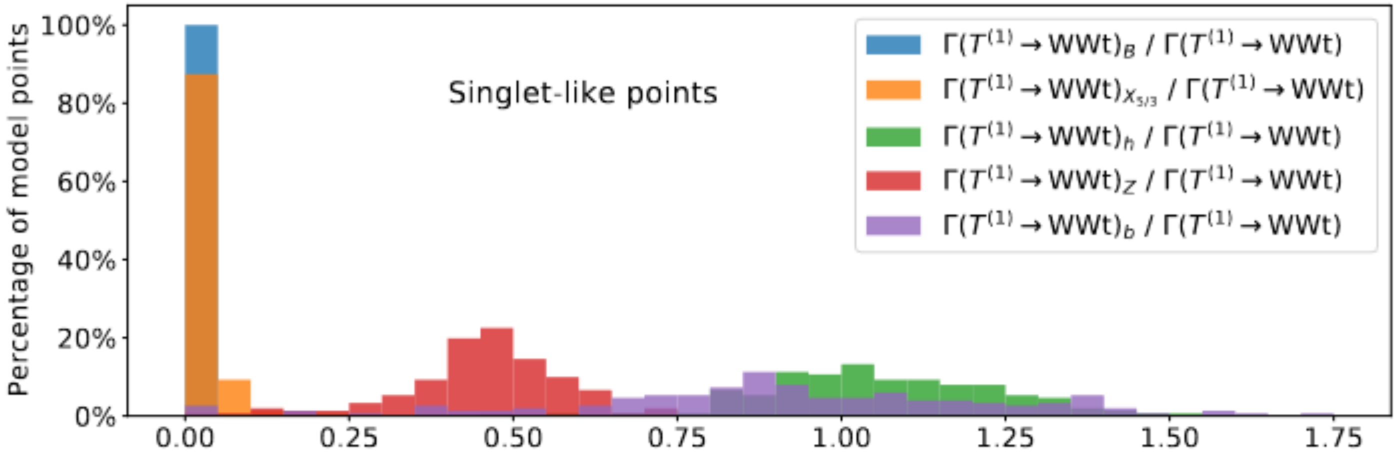

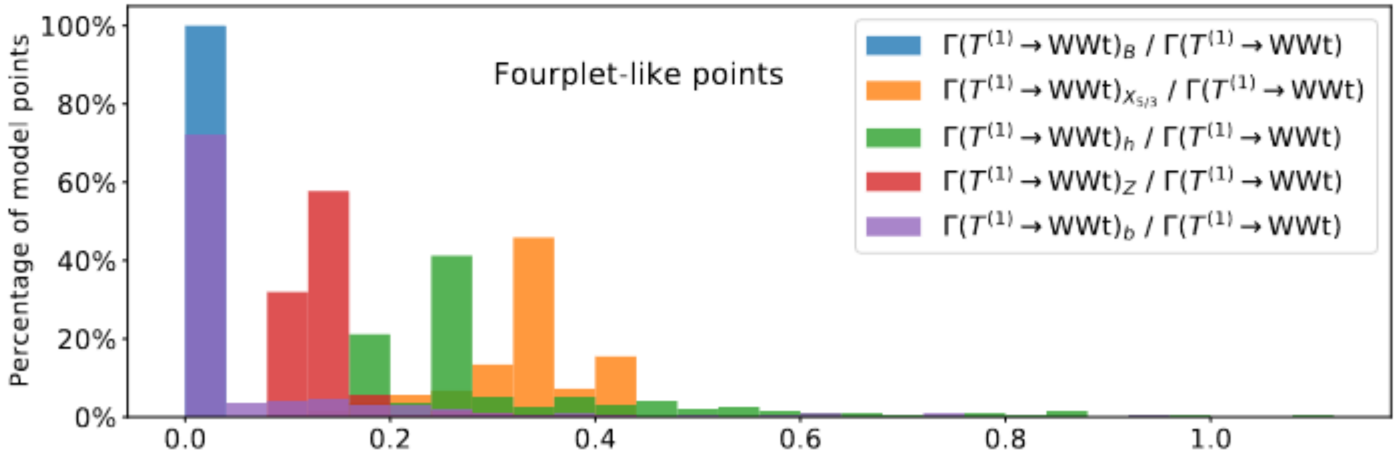

CMS Search (hep-ex: 2209.07327)

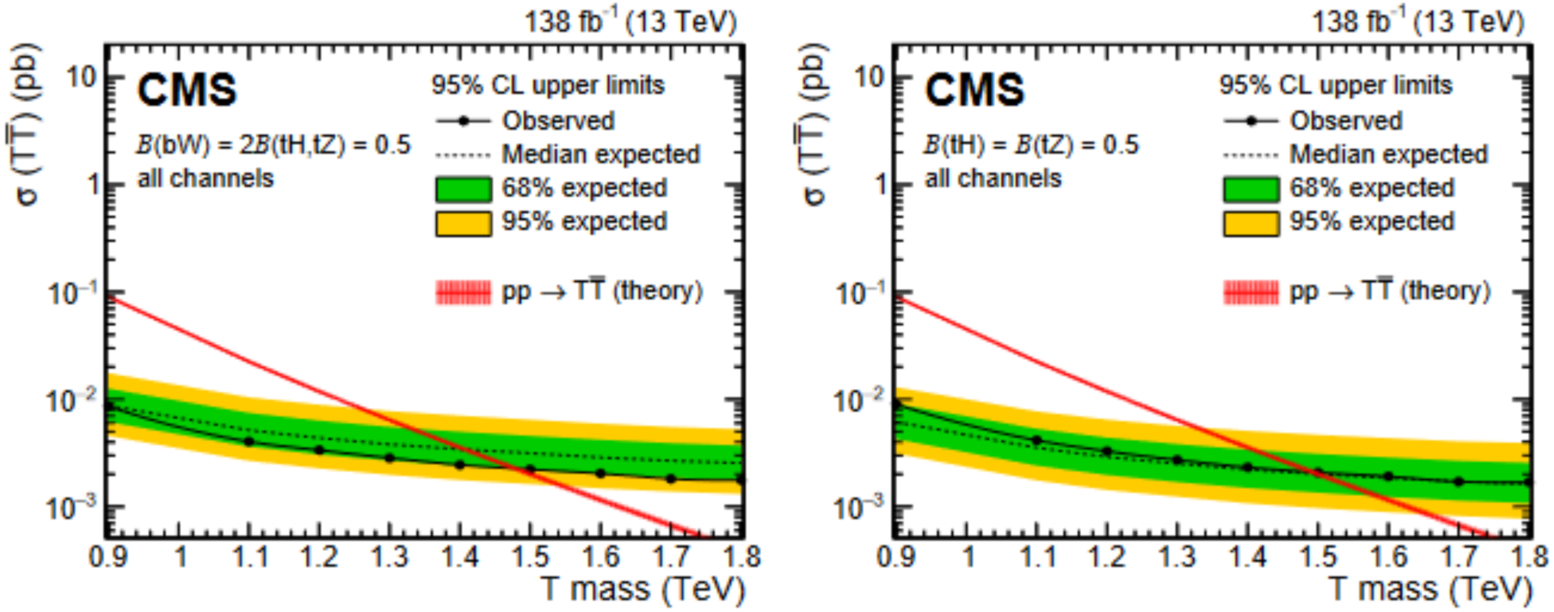

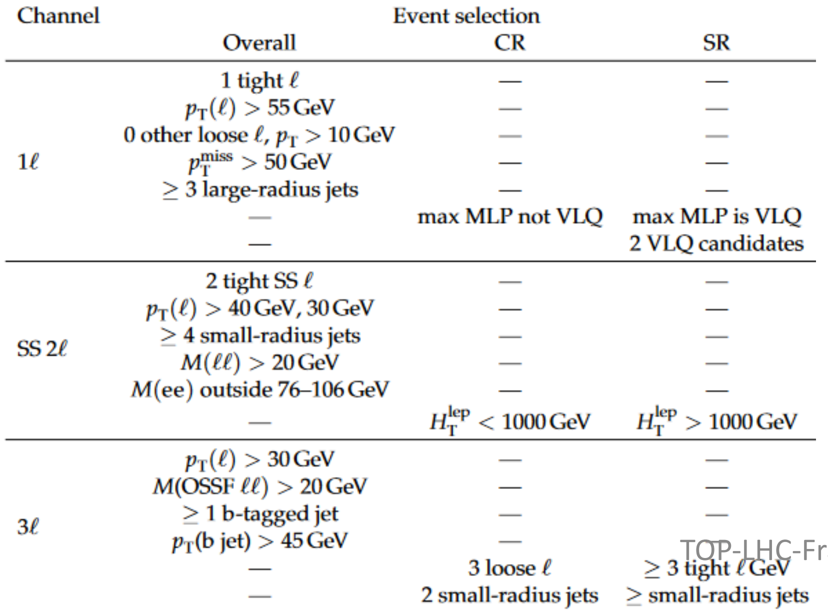

Channel	Event selection		
	Overall	CR	SR
1ℓ	1 tight ℓ	—	—
	$p_T(\ell) > 55$ GeV	—	—
	0 other loose ℓ, $p_T > 10$ GeV	—	—
	$p_T^{miss} > 50$ GeV	—	—
	≥ 3 large-radius jets	—	—
	—	max MLP not VLQ	max MLP is VLQ
	—		2 VLQ candidates
SS 2ℓ	2 tight SS ℓ	—	—
	$p_T(\ell) > 40$ GeV, 30 GeV	—	—
	≥ 4 small-radius jets	—	—
	$M(\ell\ell) > 20$ GeV	—	—
	M(ee) outside 76–106 GeV	—	—
	—	$H_T^{lep} < 1000$ GeV	$H_T^{lep} > 1000$ GeV
3ℓ	$p_T(\ell) > 30$ GeV	—	—
	M(OSSF $\ell\ell$) > 20 GeV	—	—
	≥ 1 b-tagged jet	—	—
	p_T(b jet) > 45 GeV	—	—
	—	3 loose ℓ	≥ 3 tight ℓ GeV
	—	2 small-radius jets	$\geq$ small-radius jets